INVESTIGATING NORTH AMERICAN GRASSLAND BIOGEOGRAPHY THROUGHOUT THE HOLOCENE

by

JULIE L. COMMERFORD

B.S., University of Minnesota, 2008
M.A., Kansas State University, 2010

AN ABSTRACT OF A DISSERTATION

submitted in partial fulfillment of the requirements for the degree

DOCTOR OF PHILOSOPHY

Department of Geography
College of Arts and Sciences

KANSAS STATE UNIVERSITY
Manhattan, Kansas

2016

Abstract

Throughout the Holocene, North American grassland vegetation has shifted in composition and spatial extent. However, it has been difficult to characterize these changes because the drivers—particularly climate, fire, topography, or grazing from large herbivores—operate at different spatial and temporal scales. Long-term archives such as lacustrine sediment cores, and the proxy records they contain, can help illustrate vegetation changes on relevant timescales. Yet, accurate interpretations of grassland vegetation composition from pollen (a common proxy used to infer vegetation of the past) remain limited by the number of calibrations of pollen and the drivers of vegetation change in modern conditions. This research addresses those gaps by evaluating grassland vegetation at different spatial and temporal scales in the context of modern and historical drivers. First, I reconstruct vegetation composition and diversity, fire activity, and erosion activity at a sub-regional scale over the last 9,300 years by analyzing pollen, charcoal, and magnetic data from a sediment core from a grassland lake in southern Minnesota. Second, I quantify the relationships between modern grassland pollen and fire, grazing, and topography at a fine spatial and temporal resolution, using pollen samples collected annually from traps at Konza Prairie Biological Station in the Flint Hills of Kansas. Finally, I synthesize modern pollen assemblages across the Great Plains to create a transfer function that quantitatively links precipitation and temperature with pollen. I apply this function to pollen data from the past to interpret the climate history of three sites across the Great Plains, including the aforementioned site in southern Minnesota. The results from this research suggest that grassland vegetation diversity remained relatively resilient to the climatic fluctuations of the Holocene, including the driest time at 5,000 yr BP. In addition, this work facilitates more

informed interpretations of fossil pollen by effectively calibrating modern grassland pollen assemblages with their abiotic and biotic drivers.

INVESTIGATING NORTH AMERICAN GRASSLAND BIOGEOGRAPHY THROUGHOUT THE HOLOCENE

by

JULIE L. COMMERFORD

B.S., University of Minnesota, 2008
M.A., Kansas State University, 2010

A DISSERTATION

submitted in partial fulfillment of the requirements for the degree

DOCTOR OF PHILOSOPHY

Department of Geography
College of Arts and Sciences

KANSAS STATE UNIVERSITY
Manhattan, Kansas

2016

Approved by:

Major Professor
Kendra K. McLauchlan

Copyright

Abstract

Throughout the Holocene, North American grassland vegetation has shifted in composition and spatial extent. However, it has been difficult to characterize these changes because the drivers—particularly climate, fire, topography, or grazing from large herbivores—operate at different spatial and temporal scales. Long-term archives such as lacustrine sediment cores, and the proxy records they contain, can help illustrate vegetation changes on relevant timescales. Yet, accurate interpretations of grassland vegetation composition from pollen (a common proxy used to infer vegetation of the past) remain limited by the number calibrations of pollen and the drivers of vegetation change in modern conditions. This research addresses those gaps by evaluating grassland vegetation at different spatial and temporal scales in the context of modern and historical drivers. First, I reconstruct vegetation composition and diversity, fire activity, and erosion activity at a sub-regional scale over the last 9,300 years by analyzing pollen, charcoal, and magnetic data from a sediment core from a grassland lake in southern Minnesota. Second, I quantify the relationships between modern grassland pollen and fire, grazing, and topography at a fine spatial and temporal resolution, using pollen samples collected annually from traps at Konza Prairie Biological Station in the Flint Hills of Kansas. Finally, I synthesize modern pollen assemblages across the Great Plains to create a transfer function that quantitatively links precipitation and temperature with pollen. I apply this function to pollen data from the past to interpret the climate history of three sites across the Great Plains, including the aforementioned site in southern Minnesota. The results from this research suggest that grassland vegetation diversity remained relatively resilient to the climatic fluctuations of the Holocene, including the driest time at 5,000 yr BP. In addition, this work facilitates more informed

interpretations of fossil pollen by effectively calibrating modern grassland pollen assemblages with their abiotic and biotic drivers.

Table of Contents

List of Figures

List of Tables

Acknowledgements

This work would not have been possible without the help and guidance of several people. The biggest thanks goes to my advisor, Kendra McLauchlan. She directly taught me many concepts and techniques, but, probably more importantly, demonstrated by example how to be a great scientist. Bérangère Leys, Laci Gerhart-Barley, and Claire Ruffing inspired me with their enthusiasm, grit, and support. My science friends (and real friends, too), Nicole Green, Ben Katz, and Samantha Warnecke spent many hours discussing ideas and embracing the interdisciplinary nature of our work as scientists. Becky Steiger taught me how to communicate my research to different demographics, and I am so grateful for her mentorship. Paleolab members Emily Mellicant, Kyleen Kelly, Bobby Scharping, and Scott McConaghy provided input on numerous draft figures and presentations. Finally, my committee members, Carolyn Ferguson, Dave Haukos, and Shawn Hutchinson deserve special thanks for their suggestions and input on this work.

I am also grateful for all of the financial support I received, including an NSF Career Grant to my advisor (BCS-0955225, PI-McLauchlan), an NSF GK-12 fellowship during my 2014-2015 academic year (DGE-0841414, PI-Ferguson), and an NSF Doctoral Dissertation Research Improvement Award (BCS-1558228, PI-McLauchlan, Co-PI Commerford). The Kansas State University Department of Geography also provided a graduate research grant during the 2015-2016 academic year.

Note: Specific chapter acknowledgements are included at the end of each chapter.

Dedication

This work is dedicated to my family. My dad, Steve, has always encouraged me in my love of science and been willing to discuss my papers, drive around in the field with me, and even read my proposals. My mom, Sue, has taught me that I can do whatever I put my mind to, and that any daunting project can be completed if you do "just a little bit each day" (and sometimes more). My brother, Patrick, has been my longest friend and has taught me to not take myself too seriously. My uncle, Willie, provided humor at just the right times with his jokes and funny comments. Last, but certainly not least, my fiancé, Rhett, has been my biggest supporter and partner throughout this whole process. He has seen me through my highest and lowest moments, and I cannot imagine doing any of this without him by my side. I can't wait to see where life takes us next.

Preface

This dissertation is the outcome of research that I developed in collaboration with my advisor and co-authors. As such, the writing is presented in third person format, and plural where applicable, following traditional peer-review journal guidelines. At the time of this writing, Chapter 2 is published in *The Holocene* with Bérangère Leys, Joshua Mueller, and Kendra K. McLauchlan as co-authors. Chapter 3 has been accepted with minor revisions for *Ecology and Evolution* with Thomas Minckley and Kendra K. McLauchlan as co-authors. Chapter 4 is formatted for submission to the *Journal of Climate* with Christopher J. Morris, Eric C. Grimm, and Kendra K. McLauchlan as co-authors.

Chapter 1 - Introduction

Interpreting past vegetation from lacustrine proxy data has been a central tenet of paleoecology since Von Post's (1916) work connecting pollen preserved in sediment with vegetation changes on the landscape. The long-term perspective provided by lacustrine proxy data has allowed researchers to pinpoint the timing of critical changes in vegetation or climate history at specific locations on Earth, such as the end of the last glaciation in North America (Shuman *et al.* 2002), or the onset of mid-Holocene aridity on the Great Plains (Grimm *et al.* 2011). More importantly, some ecological processes—such as multi-decadal megadroughts, continuous grazing from large herbivores, or vegetation response to changes in fire regimes—operate over long time scales of several decades to millennia, making a long-term perspective not only useful, but necessary. To complicate things further, these processes operate at different spatial scales. While climate tends to operate at a regional scale, there can be local differences in how vegetation and fire respond to climate. In addition, topography and faunal activity also play a role in dictating vegetation structure and function on a local scale (Hartnett *et al.* 1996).

The grassland biome has traditionally experienced extreme spatial and temporal variability in climate, and is predicted to be especially vulnerable to future climate change (IPCC 2014). Modern grassland composition in North America is strongly driven by precipitation, with tallgrass prairie dominating in the higher precipitation areas of the eastern Great Plains, and shortgrass prairie in the lower precipitation areas of the western Great Plains (Lane *et al.* 2000). Throughout the Holocene (12,000 yr BP to present), the vegetation of the Great Plains region has changed in composition and spatial distribution in conjunction with changes in climate and fire regimes. Many of these changes are well documented, including the initial shift from woodland to grassland around 8,000 yr BP (Wright 1968; Bartlein *et al.* 1984; Clark *et al.* 2001). Yet, the

time-transgressive and extreme nature of these events makes it important to characterize vegetation response at a local level (Williams *et al.* 2010). In addition, while grassland vegetation composition in North America has been examined in great detail, grassland vegetation diversity has not been explicitly examined, particularly in the context of the fire and climatic fluctuations of the Holocene. In forested landscapes of North America, vegetation diversity decreased during times of rapid climate change during the Holocene (Blarquez *et al.* 2014). In addition, current models of plant diversity project that the risk of extinction is large for many plants by 2080 CE, even under the less extreme projections of future climate (Thuiller *et al.* 2005). It is critical to assess how grassland vegetation changed not only in composition, but also in diversity, throughout the Holocene in order to facilitate better prediction of grassland response to future climate change.

While pollen is a robust indicator of the types and abundances of vegetation present on a landscape in the distant past, the relationship between pollen and vegetation is not direct or linear. This is primarily because plant species do not produce pollen in proportion to their abundance on the landscape. In recent decades, massive efforts have been directed toward calibrating modern pollen with vegetation and climate to better inform interpretations of fossil pollen (Sugita 1994; Whitmore *et al.* 2005; Brostrom *et al.* 2008). Several different approaches have been taken with these calibration studies. One approach is the pollen productivity modeling approach, which quantifies the amount of pollen produced by a given plant taxon in reference to other plant taxa (Sugita 1994; Brostrom *et al.* 2008). Those estimates are then applied to fossil pollen assemblages to infer vegetation cover on the landscape. Another approach is the modern analog technique (Overpeck *et al.* 1985; Williams and Shuman 2008), which builds a transfer function that quantitatively matches a pollen assemblage from known, modern climate and

vegetation conditions with a pollen assemblage from the past, to infer the climate or vegetation from the past. Other transfer function approaches, such as weighted averaging and pollen response surfaces (Bartlein et al. 1984; ter Braak and Juggins 1993; Birks 1995), are similar to the modern analog technique in that they characterize quantitative relationships between pollen and climate or vegetation, but have an advantage in allowing users to make inferences outside of the climate or vegetation space covered by the modern samples.

However, there are limits to all of the above-mentioned approaches. One of the biggest limits is the number and quality of modern pollen samples available for a given biome. For grasslands, this has posed a huge challenge because pollen assemblages from grasslands have been undersampled compared to forested biomes. Additionally, the finest level to which pollen can typically be identified is the family or genus level. The relationship between pollen and vegetation can vary within a taxon, making it even more important to obtain calibrations that are specific to an individual biome. In the grassland biome, the grass family (Poaceae) dominates the vegetation cover but varies enormously in ecological function. Furthermore, vegetation reconstructions are of little use without a broader context of the climatic changes that occurred in the region. Fortunately, the relationship between pollen assemblages and climate variables such as mean annual precipitation or mean annual temperature can be modeled at present day and applied to the past (Seppa *et al.* 2004; Li *et al.* 2007; Klemm *et al.* 2013), although these relationships are best modeled at the regional level to minimize within-taxon variation.

Much progress has been made quantifying the relationships between pollen and vegetation, and pollen and climate, but less attention has been directed toward evaluating the relationships between pollen and other drivers of vegetation structure. In North American grasslands, three drivers that have strongly influenced vegetation structure throughout the

Holocene and at present are fire, herbivory, and topography (Knapp et al. 1999a; Craine and McLauchlan 2004; Brown et al. 2005). Fire has been critical in allowing grasslands to remain grasslands by constraining woody vegetation, and has historically occurred with greater frequency in grassland ecosystems than forested ecosystems (Whelan 1995). Macroscopic charcoal found in lacustrine sediment has been the key proxy for reconstructing this information about fire history (Whitlock and Larsen 2001; Umbanhowar *et al.* 2006; Umbanhowar *et al.* 2009; Grimm *et al.* 2011). One recent study calibrated modern charcoal with local and regional burning patterns and found that charcoal concentrations were a direct indicator of the amount of area burned on the landscape (Leys *et al.* 2015). Yet, no studies have evaluated the influence of modern grassland fires on pollen assemblages, which is necessary to examine given the known role that fire plays in structuring vegetation (Hely and Alleaume 2006).

Large herbivores have been another driver of vegetation structure in North American grasslands. The population of American bison (*Bison bison*) has dramatically declined in recent centuries, but they foraged across much of the Great Plains throughout the Holocene (Hill *et al.* 2008). These animals have been found to increase vegetation diversity by preferentially grazing grasses, thereby promoting the growth of forbs (Knapp et al. 1999a). One study has found an indication of bison grazing behavior in modern pollen, manifested through increased ragweed (*Ambrosia sp.)* pollen in areas currently grazed by bison (Gill *et al.* 2013). However, pollen data are most informative when examined holistically as an entire assemblage instead of as individual pollen types. It is critical that effort be directed toward detecting a grazing signal in overall pollen assemblages at present day, so that we can interpret its presence through pollen assemblages from the past.

Topography also influences grassland vegetation structure and diversity, particularly at a fine spatial scale. Evidence of this influence is exhibited in modern grasslands like the Flint Hills ecoregion, where greater abundances of woody plant species are found in the lower elevation riparian areas (Veach *et al.* 2014). Furthermore, previous work in this region has found that plant species diversity is greater in uplands given the high richness of grasses and forbs compared to lowlands (Collins and Calabrese 2012; Gibson and Hulbert 1987). Although pollen diversity is not a direct reflection of vegetation diversity, they are closely linked (Goring *et al.* 2013; Birks *et al.* 2016), and so the influence of topography on vegetation should be discernible in pollen assemblages. This has been studied in detail in forested regions in Europe (Birks and Bjune 2010; Bjune 2014), but not in North American grasslands.

This dissertation seeks to advance our understanding of North American grassland vegetation composition throughout the Holocene and at present, in the context of biotic and abiotic drivers such as fire, erosion, herbivory, and topography. Because pollen is a key proxy for reconstructing vegetation, I also focus on quantifying the drivers of pollen assemblage composition and diversity at modern spatial and temporal scales. In Chapter 2, I evaluate changes in vegetation, fire, and erosion over the last 9,300 years by analyzing the paleorecord from Fox Lake, a grassland lake in southern Minnesota. I use pollen, charcoal, magnetic susceptibility, and other elemental proxies to assess the timing and drivers behind these changes at a sub-regional spatial scale. In Chapter 3, I quantify relationships between pollen assemblages and topography, fire, and herbivory over a very fine spatial and temporal scale by identifying modern pollen from a set of 28 traps placed at the Konza Prairie Biological Station in northeast Kansas. Pollen in these traps was collected annually during 2011-2014. I also calculate overall pollen assemblage dissimilarity to assess whether the assemblages are more similar at a given

trap between years, or in a given year across traps. In Chapter 4, I synthesize a set of modern pollen data from the surficial sediments of 141 small ponds across the Great Plains to develop transfer functions for pollen and mean annual precipitation, mean annual temperature, and mean July temperature. I apply these functions to the fossil pollen records from Fox Lake and two other lakes on the Great Plains to reconstruct climate throughout the Holocene. In Chapter 5, I summarize the findings of these chapters. At the time of this writing, Chapter 2 has been published in *The Holocene*, Chapter 3 has been accepted with minor revisions to *Ecology and Evolution*, and Chapter 4 is formatted for submission to the *Journal of Climate*.

References

Bartlein, P. J., T. Webb, and E. Fleri, 1984: Holocene climatic-change in the northern Midwest - pollen-derived estimates. *Quat. Res.*, **22**, 361–374.

Birks, H. H., and A. E. Bjune, 2010: Can we detect a west Norwegian tree line from modern samples of plant remains and pollen? Results from the DOORMAT project. *Veg. Hist. Archaeobot.*, **19**, 325–340.

Birks, H. J. B., 1995: No Title. *Statistical modeling of Quaternary science data.*, D. Edwards, D. Maddy, and J.S. Brew, Eds., Quaternary Research Association, 161–254.

Birks, H. J. B., V. A. Felde, A. E. Bjune, J.-A. Grytnes, H. Seppä, and T. Giesecke, 2016: Does pollen-assemblage richness reflect floristic richness? A review of recent developments and future challenges. *Rev. Palaeobot. Palynol.*, doi:10.1016/j.revpalbo.2015.12.011.

Bjune, A. E., 2014: After 8 years of annual pollen trapping across the tree line in western Norway: are the data still anomalous? *Veg. Hist. Archaeobot.*, **23**, 299–308.

Blarquez, O., C. Carcaillet, T. Frejaville, and Y. Bergeron, 2014: Disentangling the trajectories of alpha, beta and gamma plant diversity of North American boreal ecoregions since 15,500 years. *Front. Ecol. Evol.*, **2**, 1–8.

Brostrom, A., and Coauthors, 2008: Pollen productivity estimates of key European plant taxa for quantitative reconstruction of past vegetation: a review. *Veg. Hist. Archaeobot.*, **17**, 461–478.

Brown, K. J., J. S. Clark, E. C. Grimm, J. J. Donovan, P. G. Mueller, B. C. S. Hansen, and I. Stefanova, 2005: Fire cycles in North American interior grasslands and their relation to prairie drought. *Proc. Natl. Acad. Sci. U. S. A.*, **102**, 8865–8870.

Clark, J. S., E. C. Grimm, J. Lynch, and P. G. Mueller, 2001: Effects of Holocene climate change

on the C4 grassland/ woodland boundary in the Northern Plains, USA. *Ecology*, **82**, 620–636.

Collins, S. L., and L. B. Calabrese, 2012: Effects of fire, grazing and topographic variation on vegetation structure in tallgrass prairie. *J. Veg. Sci.*, **23**, 563–575.

Craine, J. M., and K. K. McLauchlan, 2004: The influence of biotic drivers on North American palaeorecords: alternatives to climate. *Holocene*, **14**, 787–791.

Gibson, D. J., and L. C. Hulbert, 1987: Effects of fire, topography and year-to-year climate variation on species composition in tallgrass prairie. *Vegetatio*, **72**, 175–185.

Gill, J. L., K. K. McLauchlan, A. M. Skibbe, S. Goring, C. R. Zirbel, and J. W. Williams, 2013: Linking abundances of the dung fungus Sporormiella to the density of bison: implications for assessing grazing by megaherbivores in palaeorecords. *J. Ecol.*, **101**, 1125–1136.

Goring, S., T. Lacourse, M. G. Pellatt, and R. W. Mathewes, 2013: Pollen assemblage richness does not reflect regional plant species richness: a cautionary tale. *J. Ecol.*, **101**, 1137–1145.

Grimm, E. C., J. J. Donovan, and K. J. Brown, 2011: A high-resolution record of climate variability and landscape response from Kettle Lake, northern Great Plains, North America. *Quat. Sci. Rev.*, **30**, 2626–2650.

Hartnett, D. C., K. R. Hickman, and L. E. F. Walter, 1996: Effects of bison grazing, fire, and topography on floristic diversity in tallgrass prairie. *J. Range Manag.*, **49**, 413–420.

Hely, C., and S. Alleaume, 2006: Dryland Ecohydrology. P. D'Odorico and A. Porporato, Eds., Springer Netherlands, Dordrecht, 283–301.

Hill, M. E., M. G. Hill, and C. C. Widga, 2008: Late Quaternary Bison diminution on the Great Plains of North America: evaluating the role of human hunting versus climate change. *Quat. Sci. Rev.*, **27**, 1752–1771.

IPCC, 2014: *Climate Change 2014: Impacts, Adaptation, and Vulnerability. Part A: Global and Sectoral Aspects. Contribution of Working Group II to the Fifth Assessment Report of the Intergovernmental Panel on Climate Change [Field, C.B., V.R. Barros, D.J. Dokken, K.J.* Cambridge University Press, Cambridge, United Kingdom and New York, NY, USA.

Klemm, J., U. Herzschuh, M. F. J. Pisaric, R. J. Telford, B. Heim, and L. A. Pestryakova, 2013: A pollen-climate transfer function from the tundra and taiga vegetation in Arctic Siberia and its applicability to a Holocene record. *Palaeogeogr. Palaeoclimatol. Palaeoecol.*, **386**, 702–713.

Knapp, A. K., J. M. Blair, J. M. Briggs, S. L. Collins, D. C. Hartnett, L. C. Johnson, and E. G. Towne, 1999: The Keystone Role of Bison in North American Tallgrass Prairie. *Bioscience*, **49**, 39.

Lane, D., D. Coffin, and W. Lauenroth, 2000: Changes in grassland canopy structure across a precipitation gradient. *J. Veg. Sci.*, **11**, 359–368.

Leys, B., S. C. Brewer, S. McConaghy, J. R. Mueller, and K. K. McLauchlan, 2015: Fire history reconstruction in grassland ecosystems: amount of charcoal reflects local area burned. *Environ. Res. Lett.*, **10**, 114009.

Li, Y., Q. Xu, J. Liu, X. Yang, and T. Nakagawa, 2007: A transfer-function model developed from an extensive surface-pollen data set in northern China and its potential for paleoclimate reconstructions. *The Holocene*, **17**, 897–905.

Overpeck, J. T., T. Webb, and I. C. Prentice, 1985: Quantitative Interpretation of Fossil Pollen Spectra - Dissimilarity Coefficients and the Method of Modern Analogs. *Quat. Res.*, **23**, 87–108.

Seppa, H., H. J. B. Birks, A. Odland, A. Poska, and S. Veski, 2004: A modern pollen-climate

calibration set from northern Europe: Developing and testing a tool for palaeoclimatological reconstructions. *J. Biogeogr.*, **31**, 251–267.

Shuman, B., P. Bartlein, N. Logar, P. Newby, and T. Webb, 2002: Parallel climate and vegetation responses to the early Holocene collapse of the Laurentide Ice Sheet. *Quat. Sci. Rev.*, **21**, 1793–1805.

Sugita, S., 1994: Pollen representation of vegetation in quaternary sediments: theory and method in patchy vegetation. *J. Ecol.*, **82**, 881–897.

Ter Braak, C. J. F., and S. Juggins, 1993: Weighted averaging partial least squares regression (WA-PLS): an improved method for reconstructing environmental variables from species assemblages. *Hydrobiologia*, **269**, 485–502.

Thuiller, W., S. Lavorel, M. B. Araujo, M. T. Sykes, and I. C. Prentice, 2005: Climate change threats to plant diversity in Europe. *Proc. Natl. Acad. Sci.*, **102**, 8245–8250.

Umbanhowar, C. E., P. Camill, C. E. Geiss, and R. Teed, 2006: Asymmetric vegetation responses to mid-Holocene aridity at the prairie–forest ecotone in south-central Minnesota. *Quat. Res.*, **66**, 53–66.

Umbanhowar , C. E., and Coauthors, 2009: Regional fire history based on charcoal analysis of sediments from nine lakes in western Mongolia. *Holocene*, **19**, 611–624.

Veach, A. M., W. A. Dodds, and A. Skibbe, 2014: Fire and grazing influences on rates of riparian woody plant expansion along grassland streams. *PLoS One*, **9**, e106922.

Von Post, L., 1916: Forest tree pollen in south Swedish peat bog deposits. *Pollen et Spores*, **9**, 375–401.

Whelan, R. J., 1995: *The ecology of fire*. Cambridge University Press.

Whitlock, C., and C. Larsen, 2001: Charcoal as a fire proxy. *Track. Environ. Chang. using lake*

sediments Vol 3 Terr. algal siliceous Indic., **3**, 75–97.

Whitmore, J., and Coauthors, 2005: Modern pollen data from North America and Greenland for multi-scale paleoenvironmental applications. *Quat. Sci. Rev.*, **24**, 1828–1848.

Williams, J. W., and B. Shuman, 2008: Obtaining accurate and precise environmental reconstructions from the modern analog technique and North American surface pollen dataset. *Quat. Sci. Rev.*, **27**, 669–687.

Williams, J. W., B. Shuman, P. J. Bartlein, N. S. Diffenbaugh, and T. Webb, 2010: Rapid, time-transgressive, and variable responses to early Holocene midcontinental drying in North America. *Geology*, **38**, 135–138.

Wright, H. E., 1968: Roles of Pine and Spruce in Forest History of Minnesota and Adjacent Areas. *Ecology*, **49**, 937–955.

Chapter 2 - Great Plains vegetation dynamics in response to fire and climatic fluctuations during the Holocene at Fox Lake, Minnesota (USA)

Abstract

Vegetation composition and fire frequency are tightly linked in North American grasslands, and have varied considerably throughout the Holocene in response to different drivers. Yet, detailed records of both long-term changes in grassland vegetation composition and diversity, coupled with fire history are still relatively sparse. In this study, we examine a sediment core from Fox Lake, Minnesota, using pollen, charcoal, magnetic susceptibility, organic carbon (%C) and silica (%Si) records with the aim of understanding grassland structure and function during the Holocene, particularly in the context of vegetation composition and diversity, erosion, and fire activity. Non-arboreal pollen comprises between 37% and 86% of the assemblage throughout the record with the largest percentages occurring during the mid-Holocene (~8000 – 4000 yr BP). The pollen record also suggests that at 8200 yr BP, there was an abrupt shift from oak-elm woodland to a more open landscape of grassland or savanna, which remained throughout the mid-Holocene. Additionally, the pollen data suggest that vegetation composition exhibited little change in diversity through time despite recurring fire. Charcoal concentrations varied from 30 particles·cm^{-3} to nearly 1200 particles·cm^{-3}, indicating changes in relative amount of biomass burned, but the morphotypes of charcoal pieces indicate that woody fuels persisted during the mid-Holocene despite the apparent grassland-dominated landscape. Magnetic susceptibility in the sediment ranges from -0.9 to 22.4 (x 10^{-5} SI) throughout the record, with the biggest increase occurring as the vegetation shifted from woodland to grassland

entering the mid Holocene. Organic carbon ranges from 4.6% to 20.0% and exhibits a slow but steady increase after the 8200 yr BP event. Silica decreases slightly but remains generally high between 20.4% and 22.5%.

Introduction

North American grasslands have experienced extreme climate variability with respect to temperature and moisture throughout the Holocene: multi-decadal megadroughts (Laird *et al.* 1996a; Booth *et al.* 2005; Cook *et al.* 2010), as well as shorter-duration droughts (Borchert 1950). In the Great Plains region of the U.S., the mid-Holocene (approximately 8000 – 4000 yr BP) was generally characterized by warmer temperatures, less moisture, and extreme fluctuations between moist and arid phases (Grimm *et al.* 2011; Schmieder *et al.* 2013) compared to the early or late Holocene. Current projections of climate change indicate that extreme phases like these are expected to increase in frequency and intensity in the future (IPCC 2014). However, prediction of possible responses of grassland vegetation and fire to future climate change scenarios requires an understanding of responses of vegetation and fire to climate changes throughout the past. While climate is a regional driver of vegetation and fire, local differences exist in how vegetation and fire respond (Camill and Clark 2000; Power *et al.* 2008). Additionally, previous work suggests that climate may affect fire regimes indirectly through vegetation composition and productivity, rather than through a direct link (Clark *et al.* 2001; Camill *et al.* 2003), making it critical to understand these systems in the context of each other.

In the Northern Great Plains, substantial climatic and vegetation changes occurred during the Holocene and have been noted in many records across the region, including the vegetation shift from deciduous woodland to grassland entering the mid-Holocene due to an

increase in regional aridity (Van Zant 1979; Baker *et al.* 1992; Laird *et al.* 1996b; Baker *et al.* 2002; Grimm *et al.* 2011). However, vegetation changes throughout the Holocene have often been asymmetrical with climate change through time. For example, the shift from woodland to grassland at the onset of the mid-Holocene was quite abrupt in most records, while the increased presence of woody species during the late-Holocene was relatively gradual (Umbanhowar *et al.* 2006). It is well-established that grassland ecosystems dominated much of the Northern Great Plains throughout the mid-Holocene and into the late-Holocene (Watts and Bright 1968; Van Zant 1979; Baker *et al.* 2002; Camill *et al.* 2003), however, their composition and floristic diversity relative to forested times has not been investigated. Furthermore, examination of grassland composition and diversity in the context of the rapid climate fluctuations of the Holocene can provide insight into the functions and processes involved in grassland ecosystems on a broad temporal scale.

Grassland fire regimes have generally been interpreted to consist of high frequency, low intensity events, and seem to produce high charcoal concentrations in lake sediments (Umbanhowar *et al.* 2009; Grimm *et al.* 2011). However, the fuel sources for grassland fires as interpreted through charcoal morphology (Lynch *et al.* 2006; Jensen *et al.* 2007) are likely mixtures of arboreal and non-arboreal sources. Fire has been a major component of grassland ecosystems of North America, and regular fire activity has been shown to be crucial in maintaining grasslands by inhibiting the invasion of woody plants, such as *Quercus sp.* (Danner and Knapp 2001; Briggs *et al.* 2005). Nevertheless, understanding the relationship between fire and vegetation in grasslands, particularly during the Holocene, is complex. Fire frequency can increase during arid times if fuel condition is ideal, or decrease during arid times if fuel quantity is limited (Nelson *et al.* 2012). At Kettle Lake, North Dakota, fire activity increased during the

intermittent humid phases of mid-Holocene due to higher fuel loads, and decreased during the predominant arid phases as a result of discontinuous and decreased vegetation cover (Grimm *et al.* 2011), suggesting that fuel quantity was the limiting factor rather than fuel quality.

Additionally, extremely arid phases with discontinuous vegetation and bare ground have been found to prompt soil mobilization at some locations across the Great Plains (Miao *et al.* 2007; Schmieder *et al.* 2013) which could have destabilized the landscape and further complicated the relationships between grassland vegetation and fire. In lacustrine sediments, magnetic susceptibility has become an increasingly utilized proxy for interpreting erosion activity during different phases of wet and dry conditions, although interpretation is not always straightforward (Geiss *et al.* 2003; Geiss *et al.* 2004; Schwalb *et al.* 2010, Lascu *et al.* 2012). Magnetic susceptibility values can vary greatly depending on the severity of drought, from high levels during severe droughts, to low levels in moderate droughts (Lascu *et al.* 2012). Geiss *et al.* (2003) found high magnetic susceptibility levels in sediment at lakes near the prairie-forest ecotone in Minnesota resulting from increased clastic deposition during mid-Holocene droughts. Given the longstanding history of droughts in the region (Laird *et al.* 1996a; Booth *et al.* 2005; Cook *et al.* 2010), a holistic understanding of these processes achieved through a multi-proxy study using both magnetic and non-magnetic proxies is needed.

In this study, we present a high-resolution multi-proxy reconstruction of the paleoecological history at Fox Lake, Minnesota, with the aim of understanding grassland structure and function during the Holocene, particularly in the context of vegetation composition and diversity, erosion, and fire activity. We use pollen, charcoal, magnetic susceptibility, organic carbon, and silica proxies from lake sediment to achieve four main objectives: 1) identify the major transitions in vegetation cover, fire and erosion at Fox Lake throughout the Holocene

during periods of rapid climate change; 2) understand grassland composition and diversity at this site; 3) assess changes in fire activity and fuel sources for those fire; and 4) examine the variation in erosion from the landscape as a function of vegetation cover. By doing so, we provide greater insight into the interactions between grassland vegetation and some of their characterizing factors that function on broad temporal scales, such as recurring drought and fire.

Study Area

Fox Lake (43°40'35"N, 94°41'14"W) is located in southern Minnesota (Figure 2.1), and formed during the retreat of the Des Moines Lobe at the end of the Wisconsin glaciation about 12,000 years ago. The surface area of the lake is approximately 385 ha and has approximate dimensions of 5.5 km from west to east and 0.75 km north to south. At its deepest, Fox Lake has a water depth of 6 m (Minnesota Department of Natural Resources 2014). The catchment of the lake is fairly flat with little topographic relief aside from a few small wetlands and kettle lakes to the north. Current land use near the lake primarily consists of row crop agriculture, but also contains some mixed deciduous trees (*Quercus macrocarpa, Salix nigra, Fraxinus pennsylvanica*), grasses, and forbs at the lake edges. The modern climate at Fox Lake is humid continental (Dfa), with hot summers, great seasonal temperature differences and year-round precipitation (Köppen and Geiger 1930). July and January mean monthly temperatures average 22°C and -9°C, respectively (PRISM Climate Group 2015). Average total annual precipitation is around 800 mm (PRISM Climate Group 2015). The lake was chosen for this study because: 1) Its location in the prairie biome of the northern Great Plains makes it an ideal place to study changes in grassland vegetation composition throughout the Holocene, 2) It is sufficiently deep to have contained water throughout the duration of the Holocene, thereby providing a good

depositional and preservational environment for our target proxies, and 3) It is a grassland lake in the wettest current climate conditions for this biome, thus, its climate history is linked with well-documented changes in the position of the prairie-forest border during the mid-Holocene (Williams *et al.* 2010).

Methods

Field and Chronology

In January 2012, 9.3 meters of sediment taken in nine overlapping drives were extracted from the near-deepest part of the lake (Figure 2.1) using a combination of piston corers including a modified Livingstone corer (Wright 1967). The core was transported to the National Lacustrine Core Facility (LacCore) at the University of Minnesota, where it was split into archive and working halves. 1-cm^3 subsamples of sediment spaced throughout the entire core at measured depths were extracted for pollen and charcoal analysis. Ninety-six 1-cm^3 subsamples were taken every 10 cm or less (approximately every 50-120 cal yr) for pollen analysis and 233 1-cm^3 subsamples were taken every 4 cm (approximately every 15-40 cal yr) for charcoal analysis. Plant macrofossils and charcoal were taken from the core for AMS 14C dating, and their position within the core was recorded (Table 2.1). The five uncalibrated 14C dates of the macrofossils and charcoal were calibrated to calendar years before present (hereafter yr BP, with present as 1950 AD) using IntCal13 (Reimer *et al.*, 2013) in CLAM 2.2 (Blaauw, 2010). Calibrated dates were plotted against depth to produce the age-depth model (Figure 2.2) using a smoothed spline at a smoothing level of 0.3 as the interpolation method. A bootstrap method of 1,000 iterations was performed to assess a 95% confidence interval around the curve.

Magnetic Susceptibility

Volume-normalized magnetic susceptibility was measured at LacCore on the archive half of the core at 0.5-cm resolution using a point sensor attached to a multi-section standard Geotek multi-sensor core logger. Magnetic susceptibility measures the abundance of ferromagnetic minerals, such as (titano)magnetite or maghemite, and has been interpreted as a proxy for clastic content within the sediment, delivered through erosion (Geiss *et al.* 2003). High values tend to indicate more magnetic minerals in the sediment and less organic material, as described by Lascu *et al.* (2010).

Magnetic susceptibility was chosen as the basis for zone delineation in this study because it provides unified information about multiple aspects of the ecosystem and integrates both the catchment and the lake. To delineate zones within the magnetic susceptibility data, a broken-stick model was created and a constrained hierarchical cluster analysis was conducted in R statistical software (R Core Team 2013) using the rioja package (Juggins 2014) with Euclidean distance and constrained cluster analysis by the incremental sum of squares (CONISS) as the clustering method. The broken stick model was created through a segmented univariate regression on the magnetic susceptibility data, which separates the data into intervals and fits a separate line segment to each interval. The best number of cluster groups is the point at which the sum of squares approaches 0. Six initial cluster groups were identified as the best fit. Next, the constrained hierarchical cluster analysis defined the cluster boundaries based on the number of groups entered (six, in this case) and by minimizing the sum of variances within the data. A Kruskal-Wallis ANOVA test was conducted on the six cluster groups at the 0.01 significance level to determine whether the means of the groups were statistically different overall. A Kruskal-Wallis post-hoc pairwise comparison tested for significant differences between the mean of each cluster group to the other groups. Because the pairwise comparison identified cluster

group 2 and cluster group 3 as being not statistically different at p=0.01, we combined those two groups to arrive at a total of five cluster groups or zones.

To determine whether any cross-relationships existed with other proxies, Pearson Product-Moment correlation coefficients of magnetic susceptibility with charcoal concentration, total pollen influx, arboreal pollen influx, non-arboreal pollen influx, and %C were calculated using VassarStats and significance was assessed at p=0.05 (Lowry 2015).

Organic carbon and silica

Organic carbon and silica were used to understand the degree to which sediment deposition originated from organic sources. We measured carbon concentrations (%C), which are closely correlated with organic matter concentrations, on dried bulk sediment samples via combustion at the Kansas State University Stable Isotope Mass Spectrometry Laboratory (SIMSL) following established procedures with a Carlo Erba 1110 elemental analyzer with a Conflo II interface. Inorganic carbon concentrations were tested by application of HCl to dried sediments throughout the core, and were negligible.

Silica (Si) was measured using a Cox Analytical Itrax X-Ray Fluorescence core scanner at the Large Lakes Observatory at the University of Minnesota Duluth. The Si data was standardized in a three-step process that corrects for lab error (Si:MoCoh), for erosion (Si:Ti), and then transformed using NIST standards (to percent concentration). The transformed %Si values and %C values have been used as indicators of in-lake productivity.

Pollen analysis and data treatment

Pollen was isolated from each of the 1-cm^3 subsamples (96 total) using standard techniques (Faegri and Iverson 1989), spiked with a known concentration of microspheres, and mounted in silicone oil. Each sample was examined under a light microscope and counted to a

sum of at least 300 terrestrial grains. Each pollen grain was classified to the finest taxonomic resolution possible, generally following McAndrews *et al.* (1973). The raw counts were then converted to percentages using the sum of upland pollen types, and the results were graphed using Tilia (Grimm 1993). In addition, pollen influx (grains·cm^{-2}·$year^{-1}$) was calculated using the raw counts, microsphere totals, and sedimentation rates. Pollen diversity was estimated two ways: first, by calculating the taxonomic richness of the pollen assemblages, and second, by inferring the compositional turnover of the pollen assemblages. Taxonomic richness was evaluated using the total number of pollen taxa present in each sample, plotted against age. This was conducted in R statistical software (R Core Team 2013) using the vegan package and the decostand function (Oksanen *et al.* 2015). To infer the compositional turnover of the pollen assemblages based on the β-diversity (Hill and Gauch 1980), an age constrained detrended canonical correspondence analysis (DCCA) was used (Ter Braak 1986). This was conducted with square-root transformed pollen percentages, detrending by segments, and non-linear rescaling, following Birks (2007). Downweighting and no downweighting of rare taxa options were both tried initially; downweighting has traditionally been used for pollen turnover analysis (see Birks 2007), however, no downweighting was selected in this study because of the many rare pollen taxa present in our data, and results were fairly similar between the downweighting and no downweighting options. A value ≥ 4 SD units would imply complete turnover—a given pollen assemblage shares no taxa with the previous assemblage (Hill and Gauch 1980). All aspects of the DCCA were conducted in Canoco 5 (Ter Braak and Smilauer 2012).

Charcoal analysis

Macroscopic charcoal analysis was conducted on the 1-cm3 subsamples (233 total) following the methods of Long *et al.* (1998). All samples were soaked in a 10% H2O2 solution

for 48-72 hours before being passed through 125 and 250 µm sieves. The sieved charcoal pieces were then placed in gridded petri dishes and identified under a dissection microscope according to the following morphotypes: 1) cellular (thin, rectangular, porous, visible cell wall separations), 2) fibrous (thin, clumped bundles of filamentous charcoal), 3) dark (geometric in shape, thick, opaque, with straight edges), 4) latticed (cross-hatched, rectangular), and 5) branched (dendroidal with jutting arms), generally following Jensen *et al.* (2007) and Mueller *et al.* (2014). Cellular and fibrous morphotypes correspond to grass and shrub (non-arboreal) fuel sources while dark, branched, porous, and spongy morphotypes correspond to woody (arboreal) fuel sources. The total charcoal concentration (particles·cm-3), the charcoal concentration for particles larger than 250 µm, the charcoal concentration for particles larger than 125 µm but smaller than 250 µm, and the non-arboreal:total ratio of all counted particles were each plotted against age to examine the fire history and fuel sources. Charcoal particles larger than 250 µm were used to interpret local fire activity, while charcoal particles larger than 125 µm but smaller than 250 µm were used to interpret regional fire activity, following the findings of Whitlock and Millspaugh (1996). Various ways of distinguishing regional versus local fire exist with charcoal, yet most generally depend on the size of the charcoal particles (Duffin *et al.* 2008; Aleman *et al.* 2013). Charcoal influx was calculated by multiplying the total charcoal concentration and the sedimentation rate.

Our charcoal sampling plan focused on examining one sample every four cm, and was designed because grasslands are known for experiencing annual or near-annual fire activity. This approach is different from other approaches that aim to reconstruct specific fire events, primarily those designed for forested ecosystems, which therefore typically utilize a continuous sampling plan. Our aim was not to reconstruct specific fire events, but rather focus on trends in the amount

biomass burned and the fuel sources of those fires. Each 1-cm3 section of sediment contained between 5-13 calibrated years of deposition, with 15-40 calibrated years of sediment between samples, depending on the sedimentation rate at the given position within the core. Similar discontinuous sampling plans have been used with success in other grassland work in this region (Umbanhowar *et al.* 2006).

Results

Magnetic Susceptibility

Five statistically-derived zones were delineated based on the magnetic susceptibility data (Figure 2.3). The approximate dates of each zone are: Zone 1 from 9300 to 7500 yr BP, Zone 2 from 7500 to 5500 yr BP, Zone 3 from 5500 to 3850 yr BP, Zone 4 from 3850 to 1400 yr BP, and Zone 5 from 1400 yr BP to present. As a whole, magnetic susceptibility is moderately inversely correlated with %C, but exhibits no correlative relationship to pollen or charcoal (Table 2.2). The magnetic susceptibility values throughout the record range from -0.9 to 22.4 (SI x 10^{-5}), indicating a large range in the levels of ferrimagnetic minerals in the sediment throughout the Holocene. The largest range of values for any zone are exhibited in Zone 1, when values increase from -0.3 to 22.4 (SI x 10^{-5}). The greatest amount of intersample variability is in Zone 2, between 7500 and 5500 yr BP, when values vary repeatedly between 5.6 and 22.3 (SI x 10^{-5}). Immediately following that period, from 5500 to 1400 yr BP, values remain steadily low between 0 and 2 (SI x 10^{-5}), indicating very low levels of ferrimagnetic minerals in the sediment during this time.

Zone 1 is characterized by steadily increasing magnetic susceptibility values until approximately 8000 yr BP when the values drop to around 6 (SI x 10^{-5}) and begin to rise at 7850 yr BP (Figure 2.3). Zone 2 exhibits the highest amount of repeated variability in magnetic

susceptibility values compared to the other zones, as the values increase and decrease many times (ranging between 5.6 and 22.3 (SI x 10^{-5})) throughout the zone. Zone 3 begins at 5500 yr BP and exhibits an initial decrease in values which stay relatively low (around 2.5 (SI x 10^{-5})) for the remainder of the zone with little variability. Zone 4 begins at 3850 yr BP and magnetic susceptibility values remains consistently low (between 0 and 2.5 (SI x 10^{-5})) throughout the duration of the zone. Zone 5, the most recent zone, begins at 1400 yr BP with an increase in values that peak at 11 (SI x 10^{-5}) approximately 700 yr BP before steadily decreasing until the present. This zone displays a higher amount of temporal variability in magnetic susceptibility values than the previous two zones.

Organic Carbon and Silica

Carbon concentrations vary between 4.6% and 20.0% throughout the record (Figure 2.3). The lowest values occur at the end of Zone 1 at approximately 8200 yr BP. Conversely, a generally increasing trend is exhibited after 8200 yr BP. As a whole, %C exhibits a moderate negative relationship with magnetic susceptibility ($r = -0.53$) (Table 2.2), but relatively weak relationships with other proxies. %Si concentrations vary minimally (from 20% to 23.5%) throughout the record (Figure 2.3). The highest concentrations occur around 8300 yr BP, and then steadily decrease throughout the duration of the record, although the lowest values are still relatively high at 20%.

Pollen

There is one major stratigraphic change (Figure 2.4), which encompasses a shift from dominant arboreal pollen to non-arboreal pollen at 8200 yr BP. After 8200 yr BP until present, when non-arboreal pollen dominated, arboreal pollen type generally consisted of less than 40% of the total pollen. The lowest values of arboreal pollen in the record were 14% at 7550 yr BP,

and the highest values of arboreal pollen were 63% at 9160 yr BP. Overall, the most common pollen types in the record are *Ambrosia sp., Artemisia sp.,* Undifferentiated Asteraceae, Chenopodiaceae, Poaceae, *Pinus sp., Quercus sp.,* and *Ulmus sp.*, comprising between 82% and 97% of the total assemblage. Total pollen influx is highest at the bottom (around 8500 yr BP) and the top (around 215 yr BP) of the record, with the lowest values occurring toward the middle of the record from approximately 7000 to 5000 yr BP.

The compositional shift at 8200 yr BP is characterized by a sharp peak in *Ambrosia* pollen (from 10% to nearly 60%) (Figure 2.4). The increase in *Ambrosia* is preceded by a more gradual increase in *Artemisia* (from 5% to 10%) and is shortly followed by an increase in *Iva* (from near 0 to 5%). Poaceae initially decreases at 8200 yr BP (from approximately 17% to 12%), then increases to 30% and remains generally unchanged for much of the record. From 8200 to 5500 yr BP Poaceae and *Ambrosia* are the most abundant taxa, with *Ambrosia* exhibiting more temporal variability and a greater range in relative abundance (between 15% and 45% of the total pollen sum) compared to Poaceae (between 15% and 30%) (Figure 2.4).

From 5500 to 1400 yr BP, non-arboreal taxa continue to be the most abundant overall, generally comprising between 50% and 80% of the total pollen sum), but there is a gradual increase in arboreal taxa (Figure 2.4). The highest value of *Pinus* pollen abundance (20%) occurs around 2300 yr BP, and is shortly followed by a peak in *Quercus* (25%) around 2000 yr BP. Another significant feature during this time is the sharp peak in *Ambrosia* (60%) at 3850 yr BP that decreases immediately thereafter.

At approximately 300 yr BP, several indicators of increasing disturbance on the landscape are recorded in the pollen assemblages. *Ambrosia* pollen increases dramatically to nearly 60% following an increase in *Artemisia* to 15%, similar to the event at 8200 yr BP (Figure

2.4). *Xanthium* and Chenopodiaceae pollen both increase at this time, to approximately 3% and 12%, respectively. In addition, *Zea mays* pollen appears for the first time in the record.

Neither pollen-type richness nor turnover changes when the pollen abundance shifts from predominantly arboreal to predominantly non-arboreal at 8200 yr BP (Figure 2.5a and 2.5b). Furthermore, neither richness nor turnover varies with age throughout the entire record. Richness (pollen taxa·sample^{-1}) ranges between 13 and 30 throughout the record, with an average of 20 and standard deviation of 3.6. However, the range of richness values is generally largest during the middle Holocene and beginning of the late Holocene (Zones 3 and 4), although in Zone 4 this could be attributed to the greater number of samples in the zone because it covers the largest amount of time (3850 to 1400 yr BP) than any of the other zones. The range of taxonomic richness values for each zone are: 17-26 taxa per sample in Zone 1, 15-25 taxa in Zone 2, 13-27 taxa in Zone 3, 16-30 taxa in Zone 4, 16-28 taxa – Zone 5. Throughout the record, the majority of samples have a turnover of less than 1 standard deviation unit (4 SD-units would be full turnover). This suggests that the pollen assemblage composition was not drastically changing throughout time, despite the changes in abundances of arboreal and non-arboreal taxa. Two samples have a turnover value higher than 2 SD-units: 2.2 at 5845 yr BP and 2.4 at 50 yr BP; and seven samples have a turnover value higher than 1.5 SD-units, however, turnover values repeatedly return to 1.0 or lower, suggesting that community composition stabilized after each of these instances.

Charcoal

The charcoal data are highly variable throughout the record with regard to both the amount and type of charcoal (Figure 2.6a-c). Total charcoal concentrations (Figure 2.6a) generally stay below 500 particles per cm^3 from 9200 to 7500 yr BP, with the exception of one

peak (600 particles·cm^{-3}) at 9000 yr BP and another peak (about 700 particles·cm^{-3}) at 7950 yr BP. Between 7500 and 5500 yr BP, there is a gradual increase from 250 particles per cm^3 to 600 particles per cm^3 at 6900 yr BP, then a general decline to 250 particles per cm^3 by 6000 yr BP. Total concentrations then begin to increase, and continue to increase through the next zone (5500 to 3850 yr BP). As a whole, total charcoal concentration exhibits a moderate inverse correlation with total pollen influx and non-arboreal pollen influx, but no relationship with arboreal pollen influx (Table 2.2).

From 3850 to 1400 yr BP, total charcoal concentrations fluctuate around 500 particles·cm^{-3} but exhibit a larger amount temporal variability (standard deviation of 122.4 particles·cm^{-3}) relative to the previous zone (standard deviation of 96.8 particles·cm^{-3}) (Figure 2.6a). One sample in this zone at approximately 2200 yr BP has 1100 charcoal particles, the largest number of particles relative to any earlier time in the record. From 1400 yr BP to present, the charcoal data exhibit the greatest amount of temporal variability in the record (standard deviation of 249.9 particles·cm^{-3}). In addition, three samples have concentrations higher than 900 particles·cm^{-3}: 1187 particles·cm^{-3} at 560 yr BP, 1027 particles·cm^{-3} at 690 yr BP, and 991 particles·cm^{-3} at 710 yr BP.

Low concentrations of the local charcoal (larger than 250 μm in size) (Figure 2.6a) are exhibited in the early part of the record from 9200 to 7500 yr BP. This signal is not distinguishable in the regional charcoal (larger than 125 μm but smaller than 250 μm in size) (Figure 2.6a). From 7500 to 1400 yr BP, the local charcoal concentrations exhibit greater temporal variability (standard deviation of 45.2 particles·cm^{-3}) and are higher on average than the early part of the record (Figure 2.6a). From 1400 yr BP to present, they exhibit the highest temporal variability than during any other zone (standard deviation of 76.8 particles·cm^{-3})

(Figure 2.6a). The highest (384 particles·cm^{-3}) and lowest (2 particles·cm^{-3}) concentrations of local charcoal particles throughout the entire record also occur between 1400 yr BP and the present.

Charcoal influx ranges between 5 and 190 particles·cm^{-2}·year^{-1} throughout the record (Figure 2.6b), and shows steadily increasing values from the early part of the record toward present, similar to the charcoal concentration data. The lowest temporal variability in charcoal influx occurs in Zones 1 and 2 (standard deviation of 9.8 and 9.1 particles·cm^{-2}·year^{-1}, respectively). Zone 5 exhibits the highest temporal variability in influx (standard deviation of 38.2 particles·cm^{-2}·year^{-1}), and also contains the lowest and highest influx values of the entire record (5 and 190 particles·cm^{-2}·year^{-1}).

The type of charcoal (based on morphotype) (Figure 2.6c) exhibits high intersample variability, particularly from 9200 to 1800 yr BP. During this time, the ratio of non-arboreal to total charcoal varies between 0.02 and 0.4, with three samples higher than 0.3. This indicates that fuel consisted of both non-arboreal (2% to 40% of total charcoal) and arboreal (60% to 98% of total charcoal) sources during this time, but more strongly arboreal sources. From 1800 yr BP to present, the non-arboreal to total charcoal ratio is generally much lower than earlier in the record and varies between 0.01 and 0.17 (1% to 17% of total charcoal is non-arboreal; 83% to 99% of total charcoal is arboreal), indicating that fuel sources contained a higher proportion of arboreal material than earlier in the record.

Discussion

8200 yr BP transition

The shift in vegetation from deciduous woodland to grassland in the northern Great Plains at the beginning of the mid-Holocene is noted in many records across the region (Grimm

et al. 2011; Schwalb and Dean 2002; Baker *et al.* 1992; Van Zant 1979), although the timing and magnitude of shifts vary. At Fox Lake, this transition occurs at approximately 8200 yr BP, and corresponds with the final collapse of the Laurentide ice sheet (Shuman *et al.* 2002) as well as the documented 8200 yr BP event noted originally in the Greenland ice core records (Alley and Ágústsdóttir 2005). In much of eastern North America, climate transitioned from being partially controlled by ice sheets to being completely controlled by insolation at this time (Shuman *et al.* 2002). At Clear Lake (Baker *et al.* 1992), approximately 100 km east-southeast of Fox Lake, the transition occurred at approximately the same time as at Fox Lake. In the context of prevailing air masses, Baker *et al.* (1992) described this decline in deciduous woodland as corresponding with an increasing presence of dry, warm Pacific air in the region as identified by Bryson (1966). At Lake West Okoboji (Van Zant 1979), approximately 50 km southwest of Fox Lake, the transition occurred slightly earlier (around 9000 yr BP), possibly due to Lake West Okoboji's more western position allowing it to be exposed to the dry, warm Pacific air earlier. However, the dates reported at Lake West Okoboji are uncorrected, as the record precedes current standard age-modeling techniques that include calibration of raw radiocarbon dates, so that could be a reason for the seemingly earlier transition. At Kettle Lake, approximately 850 km northwest of Fox Lake, the 8200 yr BP event is not strongly expressed, as a significant shift toward aridity had already occurred at 9250 yr BP (Grimm *et al.* 2011) (Figure 2.3). Given the timing of the transition at these other sites in the region, Fox Lake is likely one of the most westernmost lakes of current calibrated records in North America exhibiting the 8200 yr BP event.

The large spike in *Ambrosia* pollen that occurred at approximately 8200 yr BP and followed the decline in *Ulmus* and *Quercus* pollen is indicative of an increase in disturbance events. This disturbance likely began as a drought or a series of drought events and was followed

by a fire that consumed the dry biomass, as noted by the spike in total charcoal concentrations, regional charcoal concentrations (125-250 μm), and to a lesser degree local charcoal concentrations (>250 μm) that occurs shortly after 8000 yr BP. In the pollen, classic post-disturbance taxa such as *Iva* and *Xanthium* increase after the initial spike in *Ambrosia*. This supports previous assertions that the transition from the early to mid-Holocene was relatively abrupt compared to transition from mid- to late-Holocene (Nelson *et al.* 2004; Umbanhowar *et al.* 2006). At Fox Lake, *Ambrosia* percentages remain generally higher during the mid-Holocene than the early or late-Holocene, although they exhibit a great amount of intersample variability. These overall higher levels of *Ambrosia* are somewhat counter-intuitive given that *Ambrosia* is not very drought-tolerant (Grimm 2001; Craine and McLauchlan 2004) and the mid-Holocene has been well-established as being an arid time in the Great Plains. However, similar trends in *Ambrosia* at Kettle Lake during the mid-Holocene were attributed to intermittent humid years overlain on a background of drought conditions (Grimm *et al.* 2011). This could have been the case at Fox Lake as well.

Relationship between vegetation diversity and fire

Vegetation Diversity

Diversity in the pollen data remained generally unchanged with fire activity or vegetation community type at Fox Lake throughout the record, as exhibited in both the pollen richness and pollen turnover indices (Figure 2.5a and 2.5b). Present-day grasslands in North America have been known to be floristically species-rich due to their regular exposure to natural disturbances such as grazing and fire which reduce abundance of dominant species and promote growth of rare species (Hartnett *et al.* 1996). However, intense and frequent disturbances, particularly caused by droughts or frequent fire have been found to reduce species diversity in grasslands

(Tilman and Elhaddi 1992; Collins *et al.* 1998). This could explain the large spread and intersample variability in richness of the pollen assemblages throughout the record (range of 13-30 pollen taxa per sample and a standard deviation of 3.6), despite the lack of overall change in average richness. Drought and frequent fire could have prohibited growth of rare species on a frequent temporal basis, causing the vegetation community to be less diverse (the samples with lower total richness) than it could have been if subjected to less frequent or no drought or fire (the samples with higher total richness). This particularly makes sense in the context of recurring megadroughts throughout the Holocene being interspersed by humid periods (Laird *et al.* 1996a; Cook *et al.* 2010), allowing rare species to flourish during the time between large disturbances. Nevertheless, lack of change in average richness or turnover values throughout the record suggest that on a long-term basis, disturbances were not significantly altering the composition of the vegetation at Fox Lake. This remains true even during the mid-Holocene, when total pollen influx levels were lowest, and patches of bare ground were more likely to be present than at any other time during the record.

The low levels of taxonomic turnover throughout the record seem to indicate that the same types of plants were generally present during all temporal zones, albeit in varying amounts. *Quercus* is a good example of this because it was present in relatively large amounts early in the pollen record when it was a main component in the deciduous woodland at the site. During the mid-Holocene, it became much less abundant although still maintained a small presence in the assemblage. In the late-Holocene, *Quercus* was present in a more savanna-like environment as it began to gradually increase in abundance along with other tree taxa. *Quercus* pollen concentrations have also demonstrated high sensitivity to changes in available moisture ranging from savanna to forest conditions in pollen records in Wisconsin, to the east of Fox Lake

(Mueller *et al.* 2014). Additionally, it is possible that turnover could have been occurring within a taxon and remained undetected in the pollen data, for example a shift from C3 to C4 grasses. It is typically not possible to distinguish between C3 and C4 grasses based on pollen alone, but this is an inherent limitation of all pollen proxy data, and is not exclusive to this study. Future effort should be directed toward understanding turnover rates in pollen data from grassland regions in order to provide more opportunity for direct comparison among sites.

Given the relatively large surface of the lake (385 ha) (Figure 2.1), the pollen data from Fox Lake can be interpreted as an indicator of regional vegetation. Generally speaking, larger basins represent regional vegetation while smaller basins represent local vegetation (Sugita 2007a; Sugita 2007b). It should be noted that other pollen records collected from grassland lakes in North America cover a wide range of surface areas, including some that are much larger in size than Fox Lake, such as nearby Lake West Okoboji (1,500 ha) (Van Zant 1979) or Clear Lake (1,500 ha) (Baker *et al.* 1992; Baker *et al.* 2002), and some that are much smaller, such as Amber Lake (72 ha) (Umbanhowar *et al.* 2006), or Kettle Lake (2.2 ha) (Grimm *et al.* 2011). In essence, Fox Lake falls in the middle of this range, but lake size should be taken into consideration when interpreting the context with other work in this region.

Fire and fuel sources

Despite the clear indications from pollen that Fox Lake was in a prairie biome, dominated by herbaceous plants from at least 8000 to 2500 yr BP, the charcoal morphotypes demonstrate persistence of woody fuels throughout the Holocene. In landscapes with both grass and trees, fire plays an important role in determining vegetation structure (Staver *et al.* 2009). Fluctuations in the non-arboreal:total ratio of charcoal have been observed at oak-savanna sites in Wisconsin during times in the Holocene when no change in vegetation occurred (Mueller *et al.* 2014). In

addition, woody plants in a frequently-burned grassland may be overrepresented in charcoal morphotype production (Leys *et al.* 2015).

The charcoal morphotype data at Fox Lake do indicate an increased presence of arboreal fuel sources in the most recent part of the record— 1800 yr BP to present (low non-arboreal:total ratio during that time) (Figure 2.6c). This could be explained by the increasing presence of trees resulting from late-Holocene moisture increases, but this increased presence could take several forms, including shrub growth in wet prairies, trees on the perimeter of the lake, or even woody patches within the region. Indeed, large woody areas and fertile prairies were noted near Fox Lake in 1838 CE, in addition to heavily timbered riparian areas in the region (Geyer 1838 transcribed by Umbanhowar and Kreuger 2012). Given the relatively large size of Fox Lake, arboreal charcoal could have originated from these areas even if the sources were not within the immediate vicinity of the lake. Another possible source could be *Salix sp.* or *Cornus sp.;* woody taxa that were likely common in wet prairies during that time and are still present around the lake today. Also at 1800 yr BP, a higher degree of intersample variability begins to appear in the local charcoal concentrations and influx. This suggests a change in the fire regime, such as changes in intensity or area being burned. Further study of grassland fires and their signature in sedimentary charcoal would be helpful to determine if herbaceous plants were truly less abundant on the landscape during this time relative to other times, or if their charcoal is simply underrepresented.

The charcoal concentrations at Fox Lake are generally higher during grassland times than during the woodland part of the record (Figure 2.3). This difference is more distinct in the local charcoal (>250 microns) than the regional charcoal (125-250 microns) (Figure 2.6). The higher concentrations of charcoal exhibited during grassland times could be due to combustion dynamics, with low temperature fires producing incomplete combustion of both woody and

herbaceous fuel sources (Skikkink and Keane 2012), and therefore a high quantity of charcoal pieces. Alternatively, high charcoal counts could reflect local area burned, which seems to be the case for grasslands in the southern Great Plains region (Leys *et al.* 2015).

It is not completely clear whether fire responded to mid-Holocene aridity, but fluctuations in charcoal concentrations during the mid-Holocene could indicate that fuel quantity or quality varied quite a bit throughout that time, despite the lack of change in vegetation composition or diversity. In addition, charcoal concentration exhibits a moderate inverse relationship with both total pollen influx and non-arboreal influx (Table 2.2) seeming to indicate that fire activity was greater during times of less vegetation. If the lower levels of pollen influx actually do equal less biomass present on the landscape than in the earlier, forest part of the record, grassland fuel quality must have been very high (ie: highly flammable) compared to earlier times. This matches well with known regional climate conditions being more arid during the mid-Holocene (Grimm *et al.* 2011) (Figure 2.3). Alternatively, given the size of the lake and the likely regional vegetation signal represented by the pollen (Sugita 2007a), it is possible that biomass quantity could have been limited in other areas of the pollen source area but not limited locally. Still another possible explanation is that the low pollen influx values could be a result of in-lake dilution from increased aquatic productivity, given that %C increased (albeit very slightly) (Figure 2.3) during the mid-Holocene and %Si remained relatively high (around 20.5% to 21.5%).

From 8000 to 4000 yr BP local charcoal concentrations are generally higher than during the early Holocene, possibly indicating that fires in the catchment were not fuel-limited overall (by fuel quality or possibly fuel quantity). However, local, regional, and total charcoal concentrations all increase from 7800 to 7000 yr BP, but then decrease until approximately 6000

yr BP, so fuel availability could have diminished during that time. The gradual increase in local, regional, and total charcoal concentrations after 6000 yr BP seems to indicate that fuel availability gradually increased again, and matches well with the pollen influx data. The local charcoal concentrations exhibit an obvious increase until 3600 yr BP which is not shown in the regional charcoal, supporting the idea that fire activity in the region probably varied significantly at the local level (Camill *et al.* 2003; Umbanhowar *et al.* 2006).

Variation in magnetic susceptibility

Magnetic susceptibility can be complicated to interpret in the context of climate, vegetation, or fire as it is not a direct proxy of any of these things. At Fox Lake, magnetic susceptibility increases in Zone 1 as arboreal pollen begins to decrease and the vegetation transitions from a deciduous forest to a grassland. A similar trend was also exhibited at nearby Kimble Pond and Sharkey Lake as the vegetation shifted from oak savanna to grassland and led to an increase in magnetic minerals either from eolian input or soil erosion (Geiss *et al.* 2003).

The generally high, yet quite variable magnetic susceptibility values continue into Zone 2 at Fox Lake, although the source (whether from eolian input or soil erosion) of this increased input of magnetic minerals still remains unclear. At Kimble Pond and Sharkey Lake, the high and variable susceptibility values during the mid-Holocene are all attributed to eolian deposition (Geiss *et al.* 2003). Additionally, across the Great Plains, the mid-Holocene has been well-demonstrated to have been the driest time during the Holocene with persistent, recurring megadroughts and/or low effective moisture at several sites, including in Nebraska (Schmieder *et al.* 2013), North Dakota (Laird *et al.* 1996b; Grimm *et al.* 2011) and Minnesota (Bartlein & Whitlock 1993). Given these regional trends in aridity, it seems unlikely that the high levels of magnetic minerals in Fox Lake during this time would be attributed to alluvial transport, and

much more likely that they would have resulted from eolian deposition. In addition, severe droughts can destabilize the landscape by hindering the growth of vegetation and enabling greater influx of sedimentary material into lakes (Lascu *et al.* 2012). However, Geiss *et al.* (2004) found that the magnetic signal of drought can be rather complicated, so it is difficult to say with certainty whether the high values in magnetic susceptibility at Fox Lake were due to eolian or alluvial transport during this time.

The most puzzling part of the magnetic susceptibility record at Fox Lake begins at approximately 5500 yr BP and continues throughout Zone 3 and Zone 4, where values drop very low (near 0 SI x 10^{-5}) and remain low until approximately 1750 yr BP. These low values could be attributed to a number of factors, including a change in effective moisture, changes in eolian activity, or in-lake dilution from aquatic productivity. No dramatic changes are noted in the pollen or charcoal records at the time of the change in magnetic susceptibility around 5500 yr BP. However, as a whole, magnetic susceptibility is moderately inversely correlated with %C ($r = -0.53$) (Table 2.2), and sediment deposition rates gradually increased during this time (Figure 2.2), suggesting a potential shift from clastic to more organic sources of deposition possibly resulting from increasing in-lake productivity. A very similar inversely correlative relationship ($r = -0.603$) was found between magnetic susceptibility and organic carbon at Pickerel Lake (Schwalb *et al.* 2010). They suggested that the periods of increased productivity occurred during calmer and wetter periods, while high magnetic susceptibility values occurred during periods of increased eolian activity. This could be what was occurring at Fox Lake as well.

Additionally, although fire has been found to increase magnetic susceptibility in soil (Gedye *et al.* 2000), fire does not appear to be related to the magnetic susceptibility values at Fox Lake. No significant correlation was found between these two proxies. Fire activity increased

(Figure 2.6) at Fox Lake during Zone 3 and seemingly decreased during Zone 4, but the fires were insufficient in intensity to cause increases in magnetic susceptibility, which is typical of low-intensity grassland fires due to low amounts of biomass (Roman *et al.* 2013).

Conclusion

Aside from the abrupt shift in vegetation composition around 8200 yr BP, little change in vegetation composition occurred at Fox Lake throughout the mid- and late-Holocene. Pollen diversity remained relatively unchanged throughout the record, despite persistent fire activity and changes in total pollen influx. The persistence of woody charcoal during the mid-Holocene despite the indication in the pollen data that the landscape was a grassland supports the clear need for more charcoal records in this region to better understand the mechanisms involved in sedimentary charcoal deposition in grasslands. Additionally, an increase in magnetic susceptibility in the early part of the record occurs as vegetation shifts from woodland to grassland, while low values later in the mid-Holocene are more difficult to interpret and could be attributed to multiple mechanisms. Further multi-proxy analyses combining both magnetic and non-magnetic proxies in this region are essential in order to better establish grassland vegetation, fire, and erosion dynamics in the context of Holocene climate.

Acknowledgements

We gratefully acknowledge support by the National Science Foundation CAREER grant (NSF BCS-0955225) to K.M. LacCore (NSF IF-0949962) provided logistical support. A GK-12 fellowship (NSF DGE-0841414, PI Ferguson) supported J.C. during the 2014-2015 academic year. We thank Amy Myrbo, Kristina Brady, and Joe Williams for coring assistance, and Scott McConaghy, Aaron Lingwall, and Troy Ocheltree for lab assistance. We also thank Christoph

Geiss, Charles Umbanhowar, and an anonymous reviewer for helpful comments on this manuscript.

References

Aleman J. C., Blarquez O., Bentaleb I. *et al.,* 2013: Tracking land-cover changes with sedimentary charcoal in the afrotropics. *Holocene,* **23**, 1853-1862.

Alley R. B. and A. M Ágústsdóttir, 2005: The 8k event: Cause and consequences of a major Holocene abrupt climate change. *Quaternary Science Reviews,* **24**, 1123-1149.

Baker R. G., Bettis E. A., Denniston R.F. *et al.,* 2002: Holocene paleoenvironments in southeastern Minnesota - chasing the prairie-forest ecotone. *Palaeogeography Palaeoclimatology Palaeoecology,* **177,** 103-122.

Baker R. G., Maher L. J., Chumbley C. A. *et al.,* 1992: Patterns of Holocene environmental-change in the Midwestern United States. *Quaternary Research,* **37**, 379-389.

Bartlein, P. J. and C. Whitlock, 1993: In Elk Lake, Minnesota: Evidence for Rapid Climate Change in the North-Central United States, Bradbury, J. P. & Dean, W. E., Eds., Geol. Soc. Am., Boulder, CO.

Birks, H. J. B., 2007: Estimating the amount of compositional change in late-quaternary pollen-stratigraphical data. *Vegetation History and Archaeobotany,* **16**, 197-202.

Blaauw, M., 2010: Methods and code for 'classical' age-modelling of radiocarbon sequences. *Quaternary Geochronology,* **5**, 512-518.

Borchert J. R. 1950: The climate of the central North American grassland. *Annals of the Association of American Geographers,* **40**, 1-39.

Briggs J. M., Knapp A. K., Blair J. M. *et al.,* 2005: An ecosystem in transition: causes and consequences of the conversion of mesic grassland to shrubland. *Bioscience,* **55**, 243-254.

Bryson R. A., 1966: Air masses, streamlines, and the boreal forest. *Geographical Bulletin,* **1**, 228-269.

Camill P. and J. Clark, 2000: Long-term perspectives on lagged ecosystem responses to climate change: Permafrost in boreal peatlands and the Grassland/Woodland boundary. *Ecosystems,* **3**, 534-544.

Camill P., Umbanhowar C. E., Teed R. *et al.,* 2003: Late-glacial and Holocene climatic effects on fire and vegetation dynamics at the prairie-forest ecotone in south-central Minnesota. *Journal of Ecology,* **91**, 822-836.

Clark J. S., Grimm E. C., Lynch J. *et al.,* 2001: Effects of Holocene climate change on the C4 grassland/woodland boundary in the northern plains, USA. *Ecology,* **82**, 620-636.

Collins S. L., Knapp A. K., Briggs J. M. *et al.,* 1998: Modulation of diversity by grazing and mowing in native tallgrass prairie. *Science,* **280**, 745-747.

Cook E. R., Seager R., Heim R. R. Jr *et al.,* 2010: Megadroughts in North America: Placing IPCC projections of hydroclimatic change in a long-term palaeoclimate context. *Journal of Quaternary Science,* **25**, 48-61.

Craine J. M. and K. K. McLauchlan, 2004: The influence of biotic drivers on North American palaeorecords: Alternatives to climate. *Holocene,* **14**, 787-791.

Danner B. T. and A. K. Knapp, 2001: Growth dynamics of oak seedlings (*Quercus macrocarpa michx.* and *Quercus muhlenbergii engelm*.) from gallery forests: Implications for forest expansion into grasslands. *Trees-Structure and Function,* **15**, 271-277.

Duffin, K. I., Gillson L., and K. J. Willis 2008: Testing the sensitivity of charcoal as an indicator of fire events in savanna environments: Quantitative predictions of fire proximity, area and intensity. *Holocene,* **18**, 279-291.

Faegri K. and J. Iversen, 1989: Textbook of pollen analysis. Chichester, UK: Wiley.

Gedye S. J., Jones R. T., Tinner W. *et al.,* 2000: The use of mineral magnetism in the reconstruction of fire history: A case study from Lago di Origlio, Swiss Alps. *Palaeogeography, Palaeoclimatology, Palaeoecology*, **164**, 101-110.

Geiss C. E., Umbanhowar C. E., Camill P. *et al.*, 2003: Sediment magnetic properties reveal Holocene climate change along the Minnesota prairie-forest ecotone. *Journal of Paleolimnology,* **30**, 151-166.

Geiss C. E., Banerjee S. K., Camill P. *et al.,* 2004: Sediment-magnetic signature of land-use and drought as recorded in lake sediment from south-central Minnesota, USA. *Quaternary Research,* **62**, 117-125.

Geyer, C. A., Report of an agricultural botanical survey, as an addition to a general report of a geographical survey of the country between the Mississippi and the Missouri rivers. Accomplished in the years 1838 and 39 under the guidance of J.N. Nicollet. Transcribed by C.E. Umbanhowar Jr. and M. Kreuger. 2012. St. Olaf College, Northfield, MN.

Grimm E. C., 1993: *TILIA: A pollen program for analysis and display*. Springfield, IL: Illinois State Museum.

Grimm E. C., 2001: Trends and palaeoecological problems in the vegetation and climate history of the northern Great Plains, U.S.A. *Biology and Environment,* **101B**, 47-64.

Grimm E. C., Donovan J. J. and K. J. Brown, 2011: A high-resolution record of climate variability and landscape response from Kettle Lake, northern Great Plains, North America. *Quaternary Science Reviews,* **30,** 2626-2650.

Hartnett D. C., Hickman K. R. and L. E. F. Walter, 1996: Effects of bison grazing, fire, and topography on floristic diversity in tallgrass prairie. *Journal of Range Management,* **49**, 413-420.

Hill M. O. and H. Gauch, 1980: Detrended correspondence analysis: An improved ordination technique. *Plant Ecology*, **42**, 47-58.

Intergovernmental Panel on Climate Change, 2014: *Climate change 2014: Impacts, adaptation, and vulnerability. Part A: Global and sectoral aspects. Contribution of working group II to the fifth assessment report of the intergovernmental panel on climate change [Field, C.B., V.R. Barros, D.J. Dokken, K.J. Mach, M.D. Mastrandrea, T.E. Bilir, M. Chatterjee, K.L. Ebi, Y.O. Estrada, R.C. Genova, B. Girma, E.S. Kissel, A.N. Levy, S. MacCracken, P.R. Mastrandrea, and L.L. White (eds.)]*. Cambridge, United Kingdom and New York, NY, USA: Cambridge University Press.

Jensen K., Lynch E. A. *et al.,* 2007: Interpretation of charcoal morphotypes in sediments from Ferry Lake, Wisconsin, USA: Do different plant fuel sources produce distinctive charcoal morphotypes? *Holocene*, **17,** 907-915.

Juggins S., 2014: rioja: Analysis of Quaternary Science Data, R package version (0.9-3). (http://cran.r-project.org/package=rioja).

Köppen W. and R. Geiger, 1930: *Handbuch der klimatologie, vol. 3, no. 1*. Berlin, Germany: Gebrüder Borntraeger.

Laird K., Fritz S., Maasch K. *et al.,* 1996a: Greater drought intensity and frequency before AD 1200 in the northern Great Plains, USA. *Nature,* **384,** 552-554.

Laird K., Fritz S., Grimm E. *et al.*, 1996b: Century-scale paleoclimatic reconstruction from Moon Lake, a closed-basin lake in the northern Great Plains. *Limnology and Oceanography*, **41**, 890-902.

Lascu I., Banerjee S.K. and T. S. Berquo TS, 2010: Quantifying the concentration of ferrimagnetic particles in sediments using rock magnetic methods. *Geochemistry Geophysics Geosystems*, **11**, Q08Z19.

Lascu I., McLauchlan K.K., Myrbo A. *et al.*, 2012: Sediment-magnetic evidence for last millennium drought conditions at the prairie-forest ecotone of northern United States. *Palaeogeography Palaeoclimatology Palaeoecology*, **337**, 99-107.

Leys B., Finsinger W. and C. Carcaillet, 2014: Historical range of fire frequency is not the Achilles' heel of the Corsican black pine ecosystem. *Journal of Ecology*, **102**, 381-395.

Leys B., Brewer S., Mueller J. *et al.*, 2015: Fire history reconstruction in grassland ecosystems: charcoal amount reflects the local area burned. *Environmental Research Letters, **10**, 114009.*

Long C. J., Power M. J. and B. McDonald, 2011: Millennial-scale fire and vegetation history from a mesic hardwood forest of southeastern Wisconsin, USA. *Journal of Quaternary Science*, **26,** 318-325.

Long C. J., Whitlock C., Bartlein P. J. *et al.*, 1998: A 9000-year fire history from the Oregon coast range, based on a high-resolution charcoal study. *Canadian Journal of Forest Research-Revue Canadienne De Recherche Forestiere*, **28,** 774-787.

Lowry R., 2015: *VassarStats: Website for statistical computation.* Retrieved 15 June, 2015, from http://vassarstats.net/

Lynch E., Calcote R. and S. Hotchkiss, 2006: Late-Holocene vegetation and fire history from ferry lake, northwestern Wisconsin, USA. *Holocene,* **16**, 495-504.

McAndrews J., Berti A. and G. Norris, 1973: *Key to the quaternary pollen and spores of the Great Lakes region*. Toronto, Ontario: Royal Ontario Museum.

Miao X., Mason J. A., Swinehart J. B. *et al.*, 2007: A 10,000 year record of dune activity, dust storms, and severe drought in the central Great Plains. *Geology,* **35,** 119-122.

Minnesota Department of Natural Resources, 2014: *Fisheries lake survey: Fox Lake Minnesota.* Retrieved 13 October 2014, from http://www.dnr.state.mn.us/lakefind/showreport.html?downum=46010900

Mueller J. R., Long C. J., Williams J. J. *et al.,* 2014: The relative controls on forest fires and fuel source fluctuations in the Holocene deciduous forests of southern Wisconsin, USA. *Journal of Quaternary Science*, **29**, 561-569.

Nelson D. M., Hu F. S., Tian J. *et al.,* 2004: Response of C(3) and C(4) plants to middle-Holocene climatic variation near the prairie-forest ecotone of Minnesota. *Proceedings of the National Academy of Sciences of the United States of America*, **101**, 562-567.

Nelson D. M., Verschuren D. *et al.,* 2012: Long-term variability and rainfall control of savanna fire regimes in equatorial east Africa. *Global Change Biology,* **18**, 3160-3170.

Oksanen J. F., Blanchet G., Kindt R. *et al.,* 2015: vegan: Community Ecology Package. R package version 2.2-1. http://CRAN.R-project.org/package=vegan

Power M. J., Marlon J., Ortiz N. *et al.,* 2008: Changes in fire regimes since the last glacial maximum: An assessment based on a global synthesis and analysis of charcoal data. *Climate Dynamics,* **30**, 887-907.

PRISM Climate Group, Oregon State University, 2015: 30-Year Normals of Precipitation and Mean Temperature. Retrieved 30 March 2015 from: http://prism.oregonstate.edu

R Core Team, 2013: R: A language and environment for statistical computing. R Foundation for Statistical Computing, Vienna, Austria. http://www.R-project.org/

Reimer P. J., Bard E., Bayliss A. *et al.*, 2013: IntCal13 and Marine13 radiocarbon age calibration curves 0-50,000 years cal bp. *Radiocarbon*, **55**, 1869-1887.

Roman S. A., Johnson W. C. and C. E. Geiss, 2013: Grass fires-an unlikely process to explain the magnetic properties of prairie soils. *Geophysical Journal International*, **195**, 1566-1575.

Schmieder J., Fritz S.C., Grimm E.C. *et al.,* 2013: Holocene variability in hydrology, vegetation, fire, and eolian activity in the Nebraska Sand Hills, USA. *Holocene,* **23**, 515-527.

Schwalb A. and W. E. Dean, 2002: Reconstruction of hydrological changes and response to effective moisture variations from north-central USA lake sediments. *Quaternary Science Reviews*, **21**, 1541-1554.

Schwalb A., Dean W. E., Fritz S. C. *et al.,* 2010: Centennial eolian cyclicity in the great plains, USA: A dominant climate pattern of wind transport over the past 4000 years? *Quaternary Science Reviews, **29**,* 2325-2339.

Shuman B., Bartlein P., Logar N. *et al.,* 2002 Parallel climate and vegetation responses to the early Holocene collapse of the Laurentide ice sheet. *Quaternary Science Reviews*, **21,** 1793-1805.

Sikkink P. G. and R. E. Keane, 2012: Predicting fire severity using surface fuels and moisture. RMRS-RP-96. Fort Collins, CO: U.S. Department of Agriculture, Forest Service, Rocky Mountain Research Station. 37 p.

Staver A. C., Bond W. J., Stock W. D. *et al.*, 2009: Browsing and fire interact to suppress tree density in an African savanna. *Ecological Applications,* **19**, 1909-1919.

Sugita S., 2007a: Theory of Quantitative Reconstruction of Vegetation I: Pollen from Large Sites Reveals Regional Vegetation Composition. *Holocene,* **17**, 229-241.

Sugita S., 2007b: Theory of Quantitative Reconstruction of Vegetation II: All You Need Is Love. *Holocene,* **17**, 243-257.

Ter Braak C. J. F., 1986: Canonical correspondence analysis a new eigenvector technique for multivariate direct gradient analysis. *Ecology, **67***, 1167-1179.

Ter Braak C. J. F. and P. Smilauer, 2012: *Canoco reference manual and user's guide: software for ordination, version 5.0*. Ithaca, NY: Microcomputer Power.

Tilman D. and A. Elhaddi, 1992: Drought and biodiversity in grasslands. *Oecologia,* **89**, 257-264.

Umbanhowar C. E., Shinneman A. L. C., Tserenkhand G. *et al.*, 2009: Regional fire history based on charcoal analysis of sediments from nine lakes in western Mongolia. *Holocene,* **19**, 611-624.

Umbanhowar C. E., Camill P., Geiss C. E. *et al.*, 2006: Asymmetric vegetation responses to mid-Holocene aridity at the prairie-forest ecotone in south-central Minnesota. *Quaternary Research,* **66**, 53-66.

Van Zant K., 1979: Late glacial and post glacial pollen and plant macro fossils from Lake West Okoboji, northwestern Iowa, USA. *Quaternary Research*, **12**, 358-380.

Watts W. A. and R. C. Bright, 1968: Pollen, seed and mollusk analysis of a sediment core from Pickerel Lake, northeastern South Dakota. *Geological Society of America Bulletin,* **79**, 855-876.

Whitlock C. and S. H. Millspaugh, 1996: Testing the assumptions of fire history studies: An examination of modern charcoal accumulation in Yellowstone National Park, USA. *Holocene,* **6**, 7-15.

Williams J. W., Shuman B., Bartlein P. J. *et al.*, 2010: Rapid, time-transgressive, and variable responses to early Holocene midcontinental drying in North America. *Geology*, **38**, 135-138.

Wright H. E. J. 1967: A square-rod piston sampler for lake sediments. *Journal of Sedimentary Petrology,* **37**, 975-976.

Table 2.1: Radiocarbon ages and calibrated age equivalents used in determining the age model for Fox Lake. Calibration was conducted using IntCal13 (Reimer *et al.*, 2013) in CLAM 2.2 (Blaauw, 2010).

CAMS #	Depth (cm)	Material Dated	Uncalibrated 14C yr BP ± 1σ	Calibrated range (yr BP)
160884	85	Stem macrofossil	345 ± 30	370-471
160883	265	Stem macrofossil	1775 ± 30	1629-1788
160882	633	Charcoal particles	4770 ± 40	5400-4480
160881	726	Charcoal particles	5860 ± 40	6600-6738
160880	916	Charcoal particles	8220 ± 130	8880-9378

Table 2.2: Pearson Product-Moment correlations of magnetic susceptibility, pollen, charcoal and %C proxies. Bolded results are significant at $p < 0.05$. Degrees of freedom = 92 for all comparisons.

	Magnetic Susceptibility	Total Pollen Influx	Non-arboreal Pollen Influx	Arboreal Pollen Influx	Charcoal Concentration	%C
Magnetic Susceptibility	---	-0.02	0.07	-0.18	-0.19	**-0.53**
Charcoal Concentration	-0.19	**-0.31**	**-0.41**	-0.06	---	0.20
%C	**-0.53**	0.01	-0.11	0.21	0.20	---

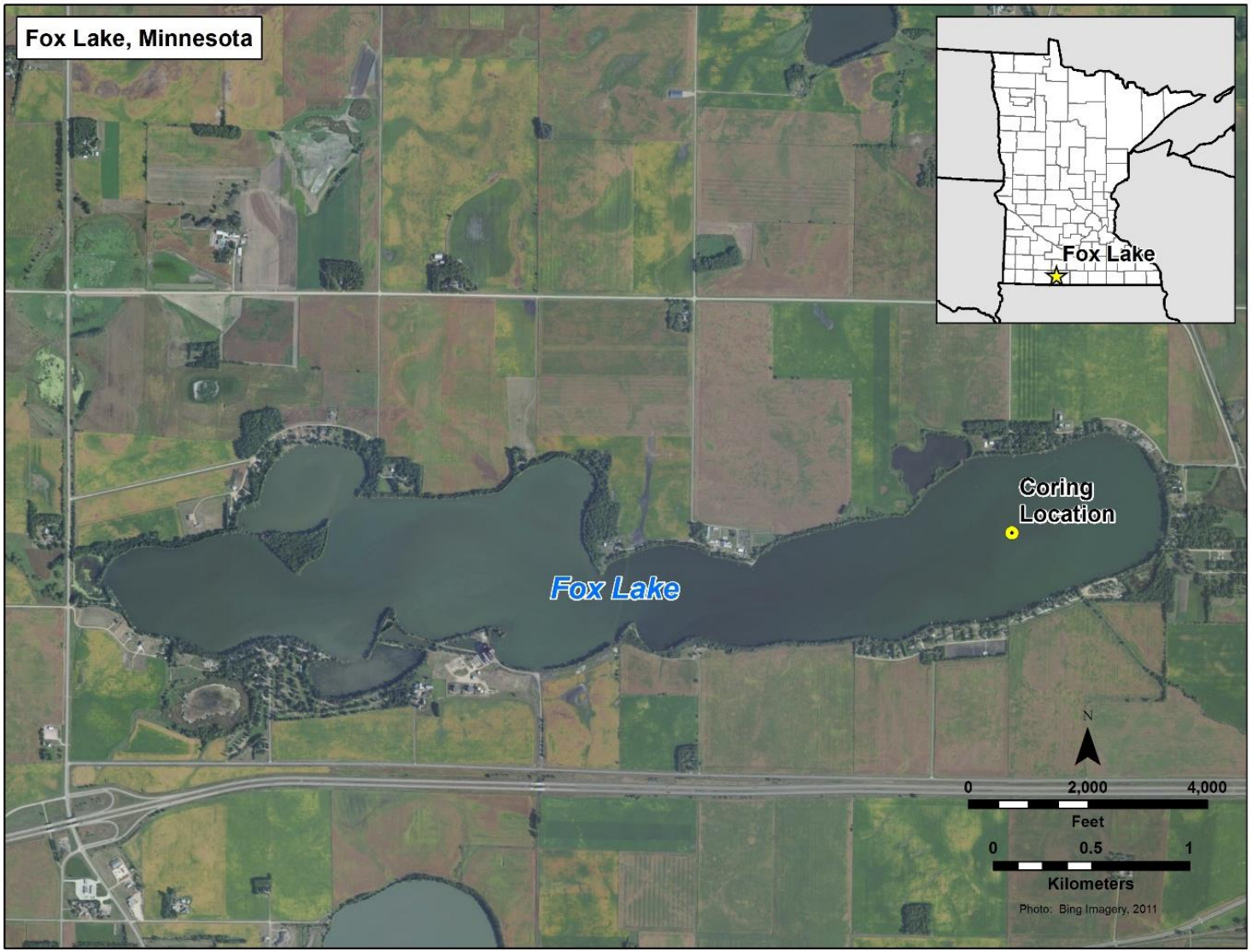

Figure 2.1: Fox Lake, Minnesota. Coring location is shown by the dot on the main figure. Inset figure shows the location of Fox Lake within Minnesota.

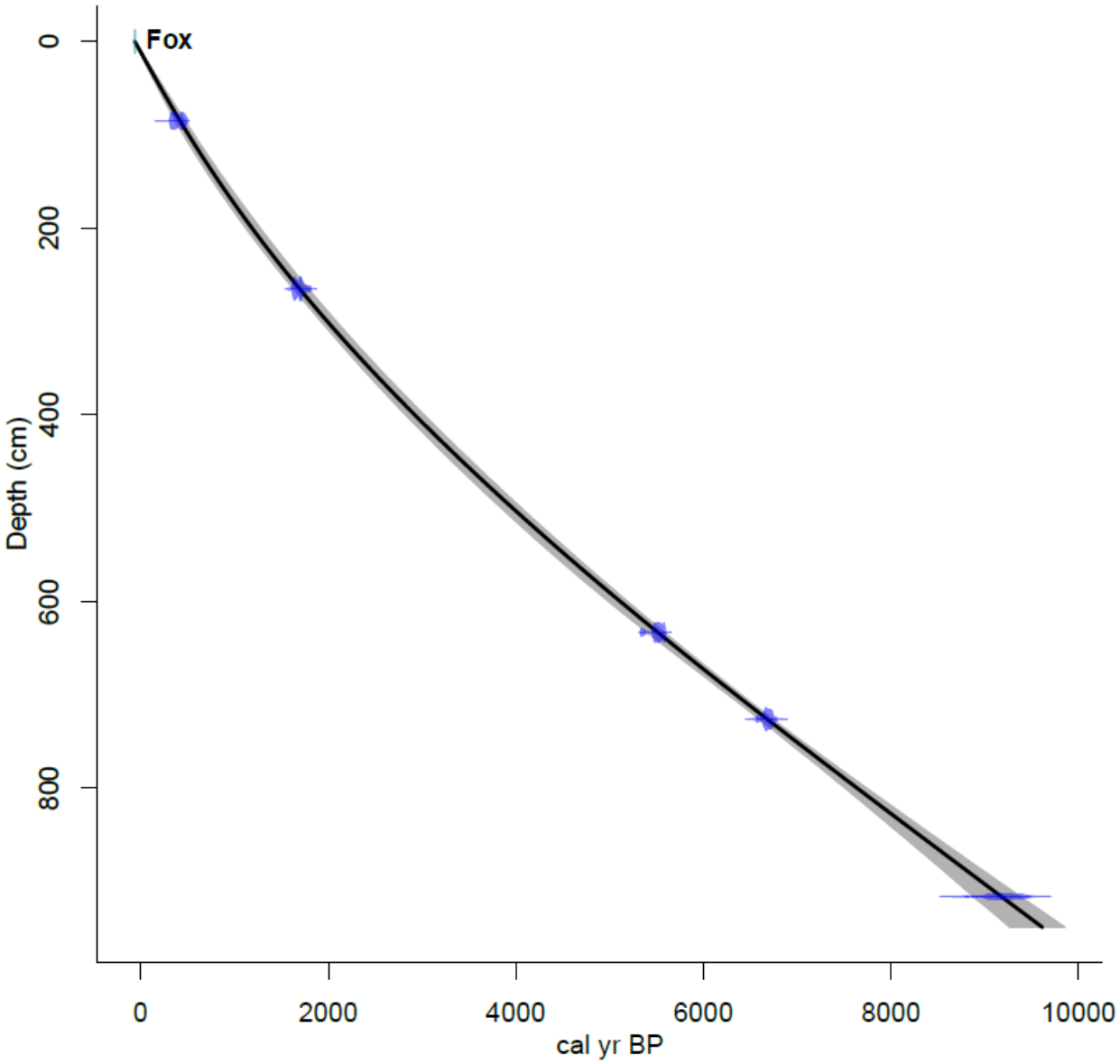

Figure 2.2: Age-Depth Model for Fox Lake, generated in CLAM (Blaauw, 2010).

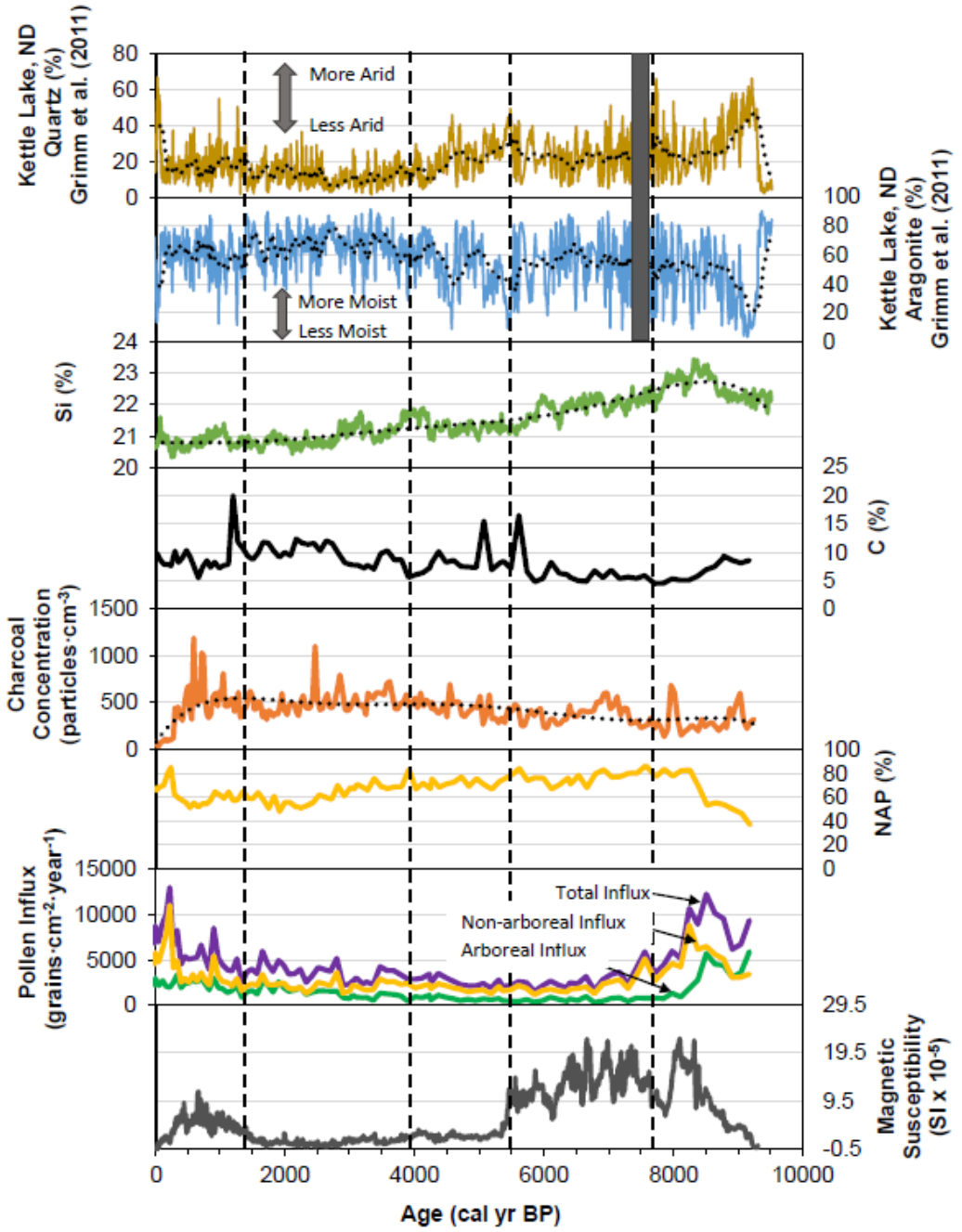

Figure 2.3: Summary of main proxies for Fox Lake, MN (this paper), in addition to quartz and aragonite from Kettle Lake, ND (Grimm *et al.*, 2011), all plotted against age. From top to bottom: Kettle Lake %Quartz, Kettle Lake %Aragonite, Fox Lake %Si, Fox Lake %C, Fox Lake charcoal concentrations (particles·cm-3), Fox Lake %Non-arboreal pollen, Fox Lake pollen influx (grains·cm-2·yr-1), Fox Lake magnetic susceptibility (SI x 10-5). Dashed vertical lines indicate zones defined from constrained hierarchical cluster analysis on magnetic susceptibility data. Trendlines shown on Kettle Lake data (%Quartz and %Aragonite) were defined by a 25-period moving average fit. Trendlines shown on Fox Lake data (%Si and charcoal concentrations) were defined by 6th order polynomial fit.

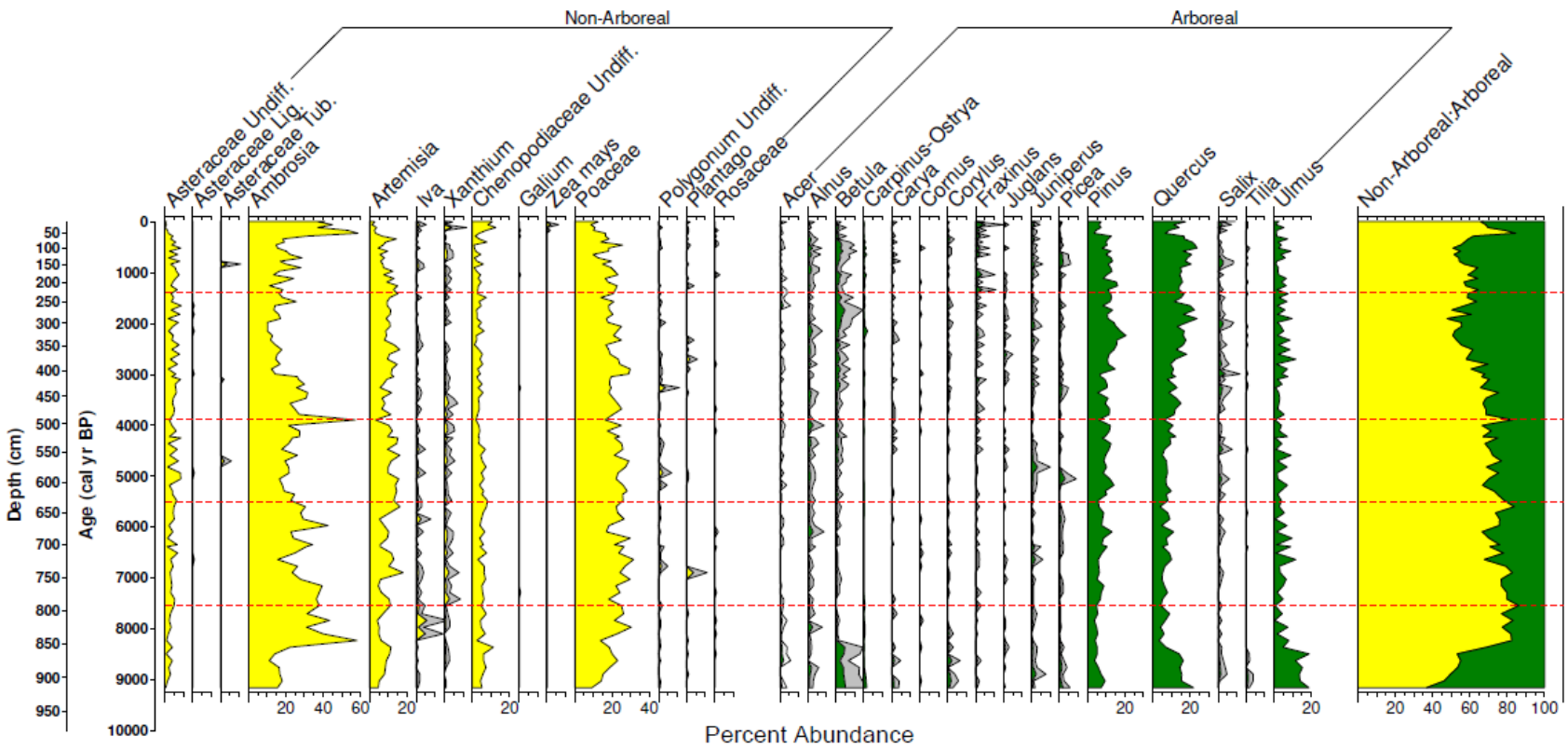

Figure 2.4: Pollen percentages of dominant terrestrial pollen taxa for Fox Lake, MN plotted against age and depth. Non-arboreal taxa are shown in yellow and arboreal taxa are shown in green. Dashed lines indicate zones defined from constrained hierarchical cluster analysis on magnetic susceptibility data (see Figure 2.3).

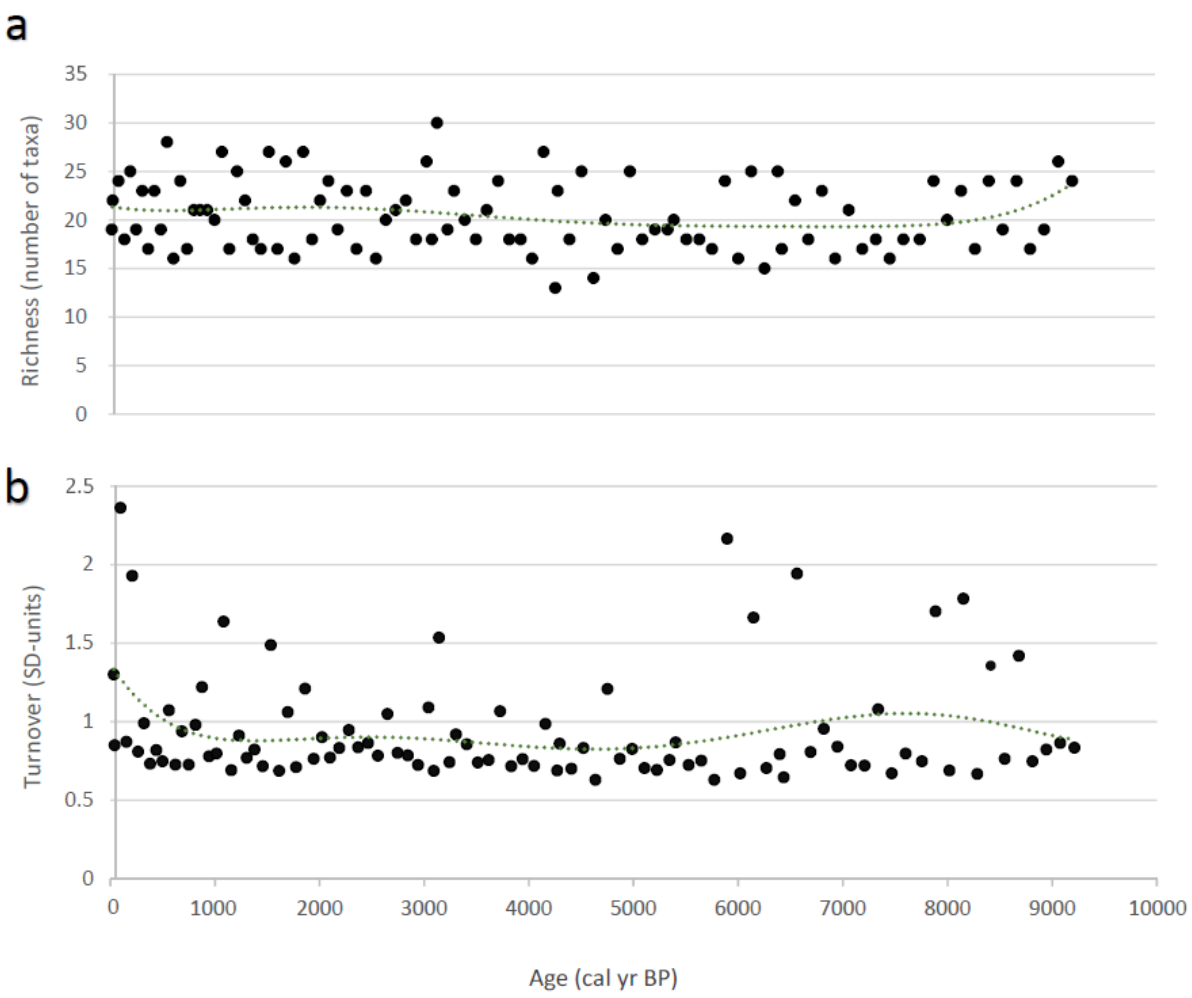

Figure 2.5: Pollen assemblage richness and turnover at Fox Lake, MN. Trendlines were defined by a 6th order polynomial fit. Panel (a) portrays taxonomic richness (number of taxa present in a sample) and panel (b) portrays turnover (standard deviation units) with age. Higher standard deviation values represent higher turnover of pollen taxa from one sample to the next sample in the chronology.

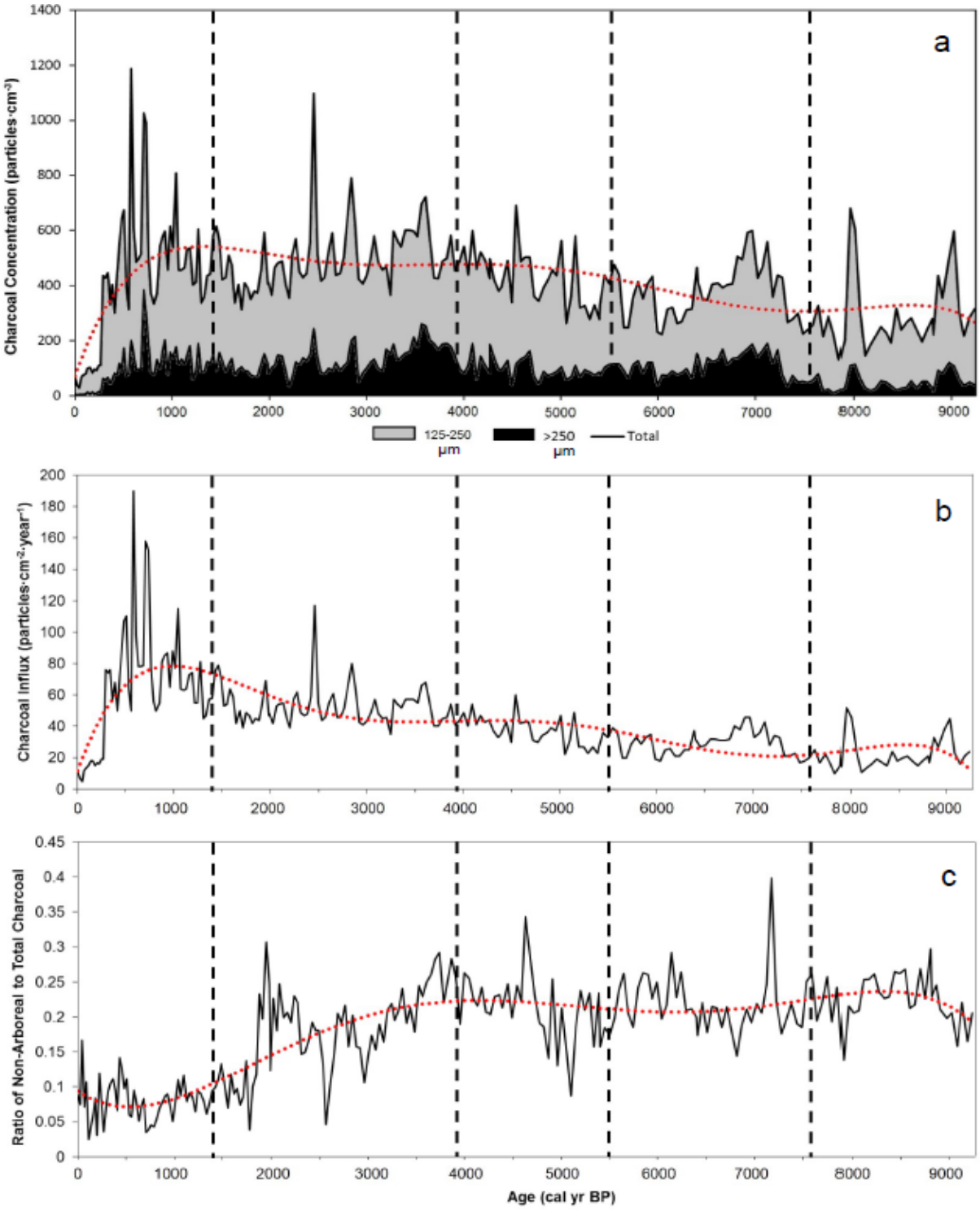

Figure 2.6: Charcoal data for Fox Lake, MN plotted against age (cal yr BP). Panel (a) portrays the total charcoal concentration (particles·cm-3), the charcoal concentration of particles larger than 250 µm (particles·cm-3), and the charcoal concentration of particles 125-250 µm in size (particles·cm-3). Panel (b) portrays the total charcoal influx (particles·cm-2·yr-1). Panel (c) portrays the ratio of non-arboreal to total charcoal particles. All trendlines were defined by a 6th order polynomial fit.

Chapter 3 - High dissimilarity within a multi-year annual record of pollen assemblages from a North American tallgrass prairie

Abstract

Grassland vegetation varies in composition across North America and has been historically influenced by multiple biotic and abiotic drivers, including fire, herbivory, and topography. Yet, the amount of temporal and spatial variability exhibited among grassland pollen assemblages, and the influence of these biotic and abiotic drivers on pollen assemblage composition and diversity has been relatively understudied. Here, we examine four years of modern pollen assemblages collected from a series of 28 traps at the Konza Prairie Biological Station in the Flint Hills of Kansas, U.S.A, with the aim of evaluating the influence of these drivers, as well as quantifying the amount of spatial and temporal variability in the pollen signatures of the tallgrass prairie biome. We include all terrestrial pollen taxa in our analyses while calculating four summative metrics of pollen diversity and composition—beta-diversity, Shannon index, non-arboreal pollen percentage, and *Ambrosia:Artemisia*—and find different roles of fire, herbivory, and topography variables in relation to these pollen metrics. In addition, we find significant annual differences in the means of three of these metrics, particularly the year 2013 which experienced high precipitation relative to the other three years of data. To quantify spatial and temporal dissimilarity among the samples over the four-year study, we calculate pairwise Squared-Chord Distances (SCD). The SCD values indicate higher compositional dissimilarity across the traps (0.38 mean) among all years than within a single trap from year-to-year (0.31 mean), suggesting that grassland vegetation can have different pollen signatures across finely-sampled space and time, and emphasizing the need for additional long-term annual monitoring of grassland pollen.

Introduction

Grasslands occupy 24% of Earth's land area and contribute to global food production through row-crop agriculture and grazing or pasture lands. Because grasslands experience high spatial and temporal variability in climate, they are predicted to be especially vulnerable to future climate change (IPCC 2014). Grasslands in North America are particularly at-risk because they are currently spatially restricted and regularly experience severe droughts such as the Dust Bowl of the 1930s (Cook et al. 2010). Other similar long-term drought events have occurred in this region throughout the Holocene (the past 11,500 years), changing the species composition and extent of this biome (Clark et al. 2001; Umbanhowar et al. 2006; Grimm et al. 2011). However, the precise timing of these changes and the factors influencing those changes at various spatial scales are still unknown. Therefore, both the composition and biodiversity of grasslands over time and the role that biotic and abiotic factors have played in structuring them remain unanswered questions. A long-term perspective is essential to capture the slow processes thought to be important in North American grasslands, such as megadroughts, grazing from large herbivores, and changes in fire regimes.

Pollen from lacustrine sediment cores records how vegetation responded to those processes on relevant timescales of several decades to millennia (Brown et al. 2005; Clark et al. 2001). While pollen from sediment cores can provide a unique source of information about past vegetation on a landscape, it has been difficult to obtain quantitative estimates of vegetation cover. The main reason for this problem is that pollen is not produced in proportion to plant abundance on the landscape (Sugita 1994). One way to overcome this limitation is by calibrating modern pollen assemblages with site features such as vegetation, climate, fire, herbivory, or topography. For example, much work has been done to calibrate pollen with vegetation by

calculating pollen productivity of select plant taxa in Europe (Brostrom et al. 2008; Mazier et al. 2008; Soepboer et al. 2007), and in the United States (Commerford et al. 2013; Sugita et al. 2006). In addition, calibrations of pollen with climate have been conducted in a variety of ecosystems, including grasslands (Minckley et al. 2008; Tonello and Prieto 2008; Gajewski et al. 2002).

Modern pollen samples are acquired in several ways, including surface sediments from lakes or ponds, moss polsters, or Tauber traps (Tauber 1974). Tauber traps have been successfully deployed over a variety of forested landscapes in Poland, Norway, Finland, Latvia, Czech Republic, Switzerland, Greece, and Bulgaria in multi-year studies of pollen production through the European Pollen Monitoring Programme (Giesecke et al. 2010). The goal of these studies has been to calibrate pollen deposition with vegetation cover, and examine annual and seasonal variability (Hicks 1985, 2001; Räsänen et al. 2004; Giesecke and Fontana 2008; Bjune 2014). Tauber traps are typically made of thick plastic, are cylindrical in shape, and are approximately 25 cm tall by 15 cm in diameter (Figure 3.1). An opening of 5 cm in diameter at the top of the trap allows pollen to enter and remain trapped for the duration of the sampling period.

Two recent examples from Europe demonstrate the significant value of these multi-year pollen records. In a birch-pine forest in Norway, nine Tauber traps were used to collect pollen annually from 2004 to 2012 (Bjune 2014). After eight years of sampling, there was higher interannual variability in pollen productivity than after only two years of sampling. These results suggested that multi-year, annual records of pollen deposition are necessary to understand the degree of variability in pollen representing a landscape over time. In a similar study in a birch forest in Finland, six years of pollen at four different Tauber traps were collected and compared

with corresponding years of meteorological data (Autio and Hicks 2004). Here, the deposition of *Pinus* (pine) pollen was positively correlated with July temperature. These findings demonstrated that climate conditions, particularly temperature, could be used to predict pollen production for the following year. These studies of annual pollen production reveal the need for caution in over-interpreting environmental conditions at the onset of changes in paleoenvironmental records as increases in individual pollen taxa could be responses to rapid shifts in climate (Minckley et al. 2012a).

While multi-year studies have been important for improving vegetation and climatic interpretations from pollen, to our knowledge there have been few similar studies in North America. One North American study examined annual modern grassland pollen records, but focused on spatial differences among grassland types and only collected pollen for one or two years (Hoyt 2000). Most importantly, little work has been done to calibrate factors aside from climate or vegetation, such as fire, herbivory, or topography. These factors are of major importance in grasslands (Knapp et al. 1999b; Craine and McLauchlan 2004; Grimm et al. 2011). Consequently, there is a clear need to understand the quantitative relationships among fire, herbivory, and topography and present day grassland composition. A detailed examination of how those factors influence pollen deposition on an annual basis is required to understand these relationships in the distant past.

Here, we present a four-year annual record of modern pollen assemblages from a tallgrass prairie in Kansas, U.S.A, with the aim of quantifying temporal and spatial variation in the context of biotic and abiotic drivers. We evaluate annual grassland pollen assemblages with several different fire, herbivory, and topography variables to achieve three main objectives: (1) assess the influence of these variables on the pollen assemblages; and (2) quantify the degree of

interannual variability among the pollen assemblages; and (3) determine whether the pollen assemblages exhibit higher spatial variation (between sample locations) or temporal variation (within sample locations). To do this, we calculate four summative metrics from each pollen assemblage to represent their composition and/or diversity, and then quantify the degree of explanation of each of these metrics by the environmental variables. We then statistically compare the differences in these metrics across the four years of sampling. Finally, we evaluate the degree of dissimilarity between pollen assemblages across the study area and through time by calculating squared-chord distance between each pollen assemblage and all other assemblages. By doing so, we provide greater insight into the factors that drive grassland pollen assemblage composition and diversity, as well as highlight the amount of variation that exists among grassland pollen assemblages across space and through time.

Materials and Methods

Study Area

Konza Prairie Biological Station (hereafter "Konza") is a 3,487-hectare preserve of native tallgrass prairie in the Flint Hills of northeastern Kansas (Figure 3.1). The Flint Hills contains the largest contiguous unplowed tract of prairie remaining in North America (Knapp et al. 1999b), and the parent material consists of alternating layers of limestone and mudstone. Konza is divided into watershed-level experimental units that were delineated in 1981, and each unit has a specified grazing and burning treatment. Each watershed is burned every 1, 2, 3, 4, or 20 years. A herd of approximately 300 native bison has resided on Konza since its introduction in 1987.

The preserve is floristically diverse, with 597 different plant species: 86 species of grasses, 409 species of forbs, and 59 woody species (Towne 2002). Konza was chosen for this study for a number of reasons: 1) It has never been plowed and so is the best present-day proxy

for grasslands prior to the onset of modern agriculture; 2) Its floristic diversity provides an ideal location for capturing differences in pollen representation among grassland plants; 3) The different burning and grazing treatments facilitate direct comparison between pollen assemblages in watersheds that are burned at different frequencies, in addition to grazed versus ungrazed areas; and 4) Its purpose as a long-term ecological research area enables a multi-year study where pollen traps can remain in-place for several years with minimal disruption.

Data Collection

Twenty-eight modified Tauber traps (Tauber 1974) were placed on Konza in October 2008. Traps were placed stratified-randomly to cover both grazed and ungrazed areas, different burning treatments, and upland and lowland areas. Traps were placed at least 500 m apart. The trap contents were collected in October 2009, 2010, 2011, 2012, 2013, and 2014 (at the end of the growing season). Each trap was rinsed in the field with deionized water and poured into an empty jug. In the lab, the contents were filtered through cellulose paper and soaked with glacial acetic acid to prevent the growth of mold or fungi. Each filter paper was processed and prepared for pollen analysis using standard techniques (Faegri & Iversen 1989) with a modification made for dissolving the filter paper based on the European Pollen Monitoring Programme protocol. Each pollen sample was mounted in silicone oil, examined under a light microscope, and counted to a minimum sum of 300 terrestrial grains. All pollen grains were identified to the finest possible taxonomic resolution, generally following McAndrews *et al.* (1973). This paper focuses specifically on the pollen data collected in 2011, 2012, 2013, and 2014. The pollen data from 2009 and 2010 are published in Gill *et al.* (2013).

To evaluate the effects of fire, grazing, and topography on the pollen assemblages, we measured several different environmental variables at each sample location. Most environmental

variables for each sample location were obtained from Leys *et al.* (2015), which examined macroscopic charcoal from this same set of traps for the same years (2011-2014). The fire metrics we included were mean fire return interval, fire return interval, fire frequency, time since last fire, regional area burned within the Flint Hills ecoregion, local area burned within Konza, and area burned within 500 m of the trap. Topography metrics we included from Leys *et al.* (2015) were elevation, presence of bare soil around the trap, presence of bison manure (as a qualitative proxy for presence/absence of bison), and presence of limestone rocks (within 500 meters of the trap). To supplement the above variables, we used bison density data calculated as amount of time spent by bison within 500 m of each trap via GPS collars and previously reported in Gill *et al.* (2013). We also calculated total precipitation and mean average, maximum, and minimum temperature for the months May through August for each year, based on data from the Konza Prairie weather station (KPBS 2015), to examine any covariance of these factors with the four years of pollen data. All three temperature variables were found to exhibit no significant annual differences for the four years covered in this study and so were not pursued further. Precipitation was included because of significant annual differences.

Data Analysis

Raw pollen counts were converted to percentages using a pollen sum that included all terrestrial upland taxa and analyzed in Tilia 2.0 (Grimm 1993). High variability in volume of water used to wash the traps and filter their contents precluded calculations of absolute pollen influx rate, although the protocol could be amended in future years to allow that calculation. One trap was excluded from the analyses because it contained no pollen in 2011 and 2012. To initially examine the degree to which the environmental variables explained the multivariate pollen samples, we conducted a canonical correspondence analysis (CCA) (Ter Braak 1986)

using Canoco 5 Software (Ter Braak and Smilauer 2012). The CCA suggested some influence of certain environmental variables on the multivariate pollen assemblages, but overall low explanation (highest eigenvalue = 0.06). Thus, we determined that a collective value of diversity or composition for each sample based on all of the pollen taxa would be more useful for directly assessing the influence of the environmental variables. We chose to summarize each pollen sample (each trap from each year) using four different metrics included in a regression analysis and compared across all four years. The four different metrics calculated were: 1) Shannon index, 2) beta-diversity, 3) non-arboreal pollen percentage, and 4) ratio of *Ambrosia:Artemisia* pollen. Shannon index was calculated using the standard equation for Shannon diversity (Figure 3.2), where p is the proportion of the sample belonging to pollen taxa i. Shannon index has been found to be a robust measure of vegetation diversity when used on pollen assemblages (Matthias et al. 2015). Beta-diversity was calculated via a detrended canonical correspondence analysis (DCCA), constrained by year. This metric computes the ratio between the sample diversity at a given trap for one year compared to the sample diversity at that same trap for the other three years. Non-arboreal pollen percentage was calculated by totaling the abundance proportions of all grass and forb pollen in each sample. *Ambrosia:Artemisia* was calculated as the ratio of *Ambrosia:Artemisia* pollen percentages in each sample, and has been suggested to be an indicator of grassland type (tallgrass versus shortgrass) (Morris 2013).

To assess which environmental variables influenced each of the four summative pollen metrics, individual multiple regressions were performed. All summative metrics and environmental variables were rescaled between 0 and 1 using the "scales" package in R (Wickham 2016). Each regression used one of the four summative metrics (Shannon index, beta-diversity, non-arboreal percentage, and *Ambrosia:Artemisia*) as the response variable, and all of

the previously mentioned environmental variables as the explanatory fixed-effect variables. Random effects for trap and year were also included in each regression model and tested for significance. For each response variable, this was done by creating a full model of all fixed effects (environmental variables) and random effects (for trap and year). Then, the random effects of trap and year were each removed individually from the full model, and the resulting model was statistically compared to the full model. The regression models were built using lme4 package (Bates *et al.* 2015) in R. Comparisons between the full models and the models with random effects removed were conducted using the stats package in R (R Core Team 2015). Please see Appendix A for specific code.

We also compared differences in the summative metrics across all four years of data. To do this, a Kruskal-Wallis ANOVA test was conducted on each of the four metrics across the four years, to determine whether the means for each year were significantly different overall (at $p<0.05$). A Kruskal-Wallis post-hoc pairwise comparison tested for significant differences between the mean of each year and each of the other three years (at $p<0.05$). Finally, an analysis of covariance (ANCOVA) was conducted to test the covariance of total growing season precipitation and year for each of the four summative metrics. The temperature variables mentioned earlier (minimum, average, and maximum temperature) were excluded from the analysis because they were not significantly different across the four years of data. All of these analyses were conducted in R statistical software (R Core Team 2015), using the stats package for the regression and ANCOVA analyses (R Core Team 2015), and the PGIRMESS package (Giraudoux 2014) for the ANOVAs and post-hoc comparisons. Please see Appendix A for specific code.

To evaluate the dissimilarity between each pollen sample, we calculated pairwise squared chord distances. The squared chord distance (SCD) metric (Overpeck *et al.* 1985) incorporates all pollen taxa in each sample and essentially computes the component distance between sample pairs, such that pairs with higher SCD values are more dissimilar, while pairs with lower SCD values are more similar. SCD has long been used in pollen studies to detect a matching modern pollen sample for a fossil pollen sample (Williams *et al.* 2009; Minckley *et al.* 2012b; McLauchlan *et al.* 2013). It has also been used to compare dissimilarity among pollen samples across a modern study area (Hoyt 2000; Gavin *et al.* 2005; Minckley *et al.* 2008), such as in this study. We calculated SCD in R Statistical Software (R Core Team 2015), using the Analogue package (Simpson 2015). Please see Appendix A for specific code.

Results

Pollen assemblages among traps and years

Percent abundance of pollen taxa varies significantly among the 27 Tauber traps at the Konza study area from 2011, 2012, 2013 and 2014 (Figure 3.3). The number of different pollen taxa from each trap/year ranges from 11 to 32, averaging 22 taxa. The six most abundant pollen taxa found in the traps on average are (in order from the highest): *Ambrosia* (31.1%), *Quercus* (18.9%), Poaceae (9.6%), Undifferentiated Asteraceae (8.9%), Cupressaceae (5.7%), and Amaranthaceae (4.1%). Four of these taxa are non-arboreal (*Ambrosia*, Poaceae, Undifferentiated Asteraceae and Amaranthaceae), and two of these taxa are arboreal (*Quercus* and Cupressaceae).

The identity of the most abundant pollen taxa varies locally from trap to trap, although certain traps exhibit more variation across the four years of data than other traps. At Trap 2 and Trap 8, *Quercus* is consistently the most abundant taxa for all four years of data. Conversely, at

Trap 1, 11, 12, 13, 21, and 25, *Ambrosia* is consistently the most abundant taxa for all four years. In addition, some of the less abundant (but still common) taxa also exhibit trends. *Xanthium* pollen is higher at Trap 10 than at any of the other traps for 2011, 2012, and 2013. *Artemisia* is highest in 2011, 2012, and 2013 at Trap 22 compared to all the other traps but is higher at Trap 17 in 2014. Thus, trap locations contribute to the types of pollen captured.

The role of environmental variables on pollen metrics

Overall, the four summative pollen metrics—beta-diversity, Shannon index, non-arboreal percentage (NAP%), and *Ambrosia:Artemisia*—are each partially influenced by different environmental variables (Table 3.1). Some environmental variables (fixed effects) significantly influence more than one of the summative metrics. For example, the area burned within the Flint Hills contributes to both beta-diversity and NAP%. Shannon index is influenced by bison density. Beta-diversity is influenced by the area burned within the Flint Hills and the area burned within Konza. NAP% is influenced by area burned within the Flint Hills and area burned within Konza. *Ambrosia:Artemisia* is influenced by the area burned within 500 meters of the trap. The random effects of trap location and year also vary in significance for the four summative metrics. Trap location significantly influences Shannon index, NAP%, and *Ambrosia:Artemisia*. Year significantly influences Shannon index only. Beta-diversity is not significantly influenced by trap location or year.

There are significant differences among the four years for each of the four summative pollen metrics (Shannon Index, beta-diversity, NAP%, and *Ambrosia:Artemisia*) demonstrated by the Kruskal-Wallis tests (Figure 3.4). However, the amount of variation depends at least to some degree on the metric being used. 2013 stands out as either the highest or lowest year for each of the four metrics. Shannon Index is lowest in 2013 (median 1.82). Beta-diversity is also

lowest in 2013 (median 0.84). Both the NAP% and *Ambrosia:Artemisia* are highest in 2013 (median 73.95 and 23.25, respectively). 2013 is significantly different (at $p<0.05$) from 2011 in all four metrics. However, it is not significantly different from 2012 in NAP% and beta-diversity, or from 2014 in Shannon Index. 2011 and 2014 were not significantly different from each other in any of the four metrics. In addition, *Ambrosia:Artemisia* did not show any significant differences among the four years of data. Total growing season precipitation significantly co-varies with year for explaining beta-diversity and NAP% ($p<0.05$), but not for explaining Shannon Index or *Ambrosia:Artemisia*. Precipitation was highest in 2013 (462 mm) and lowest in 2012 (301 mm).

Squared Chord Distance dissimilarity

Squared chord distance was examined between each sample and all other samples from all traps in all years as an estimation of overall dissimilarity between the multivariate assemblages. The spatial differences in the average dissimilarity between each sample and all other samples across Konza (Figure 3.5) are generally higher than the temporal differences for a single trap among the four years (Figure 3.6). Thus, within-trap dissimilarity (Figure 3.6) is lower than a sample's average dissimilarity to all other samples (across Konza from all four years) (Figure 3.5). The average dissimilarity between all samples is 0.38, while the within-trap average dissimilarity is 0.31. Within-trap dissimilarity is lowest from 2011-2012 (average 0.28) and highest from 2012-2013 (average 0.33). However, some traps have relatively low within-trap dissimilarity, while others have high within-trap dissimilarity (from year to year). For example, Trap 13 has the lowest within-trap dissimilarity (average 0.11), while Trap 15 has the highest (average 0.70). Minimum dissimilarity for a given sample (the lowest squared-chord distance

value of all pairwise comparisons for a given sample) ranges between 0.01 and 0.30 (Figure 3.7), and averages 0.11.

Discussion

Explanatory power of fire, grazing, and topography variables

The environmental variables known to influence grassland vegetation—fire frequency, bison density, and elevation—are somewhat reflected in pollen assemblages produced by grassland vegetation. Each of the four summative pollen metrics are influenced by different environmental variables, which is logical given that some of the calculated pollen metrics assess diversity while others focus on pollen composition (Table 3.1). Previous work in other regions has suggested that there is no single best metric for assessing pollen diversity and composition (Weng *et al.* 2007; Birks *et al.* 2016), and our results indicate that the same is true for grasslands in North America. However, some variables (e.g. area burned within Konza and area burned within the Flint Hills) significantly contribute to more than one pollen metric.

The negative influence of bison density on Shannon index is somewhat puzzling (Table 3.1), as previous work has suggested that bison grazing increases local plant diversity (Hartnett *et al.* 1996). This could be explained by over-representation of high pollen producers like *Ambrosia* and Amaranthaceae in the pollen assemblage, or, under-representation of low pollen producers like sunflowers (Asteraceae Undiff.) or Fabaceae family plants (*Amorpha sp*., *Baptisia sp*., or *Lespedeza sp*.) (Commerford *et al.* 2013). All are common forbs at Konza (Towne 2002). Furthermore, the presence of bison manure (used as a qualitative measure of bison presence/absence) had no influence. This suggests that bison herbivory does have an effect on grassland pollen assemblage diversity, but this signal can only be detected with quantitative herbivore abundance.

Area burned within 500 meters of the trap is the only environmental variable that contributed significantly to *Ambrosia:Artemisia* (negative relationship). Higher levels of *Ambrosia* pollen (or lower levels of *Artemisia*, leading to a high ratio) correspond with less area burned. This suggests that grassland fires, at least in a tallgrass prairie like at Konza, may help keep *Ambrosia* abundance or pollen productivity low. This could occur either by fires directly inhibiting *Ambrosia* growth (Abrams & Gibson 1991), or by promoting the growth of grasses and other forbs (including *Artemisia*) in place of *Ambrosia* (Knapp & Seastedt 1986). Additionally, a negative relationship between *Ambrosia* pollen and charcoal was found over the Holocene in the northern Great Plains (Grimm *et al.* 2011), suggesting that the *Ambrosia*-fire relationship is robust across different temporal scales.

Although beta-diversity is influenced by two broader-scale spatial variables—the area burned within the Flint Hills, and the area burned within Konza (Table 3.1)—this could be partially due to the nature of how the beta-diversity metric is calculated. Here, we calculated temporal beta-diversity, in which the value for each sample was the ratio between the sample diversity for one year compared to the sample diversity at that same trap for the other three years. Because the two abovementioned variables are equal across all traps for a given year, it is logical that they would have some influence on the temporal beta-diversity in this case. However, the lack of influence of the very local, spatial fire variable—area burned within 500 m—is more surprising. Both the area burned within Konza and the area burned within the Flint Hills operate at a broader spatial scale, indicating that temporal beta-diversity in our pollen samples is more influenced by annual changes in fires occurring at the local or regional scale than at the very local scale (within 500 m). The influence of regional burning could be manifested directly through fire driving vegetation composition and structure, or could suggest that an indirect

regional mechanism, such as prevailing wind direction or speed, is influencing pollen dispersal (Davis 2000). Additionally, the other four fire variables—the amount of time since the last fire, fire frequency, mean fire return interval, and fire return interval—had no influence. These variables describe temporal aspects of the fire histories at Konza. This finding is similar to that from Leys *et al.* (2015), who examined charcoal pieces from these same traps and found that the amount of charcoal was significantly influenced by the area burned within the Flint Hills and Konza, but not by any other fire variables.

Although there is little topographic relief (less than 100 meters) in the study area compared to mountain environments, elevation changes might affect pollen spectra. While elevation did not significantly influence any of the summative metrics at $p<0.05$, it was very close to contributing to NAP% ($p=0.057$, negative coefficient) and Shannon Index ($p=0.074$, positive coefficient), and so is worth mentioning. In a montane region in Norway, pollen assemblages from a set of traps spanning a larger elevational transect (~500 meters) were found to vary greatly in their composition, mostly due to differences in vegetation composition and structure (Birks & Bjune 2010; Bjune 2014). Although the Konza traps span a smaller elevational gradient, the influence of elevation on pollen assemblages here could also be due to systematic differences in vegetation at lower versus higher elevations, although the influence is not significant in the four-year record here. Yet, upland soils have been found to support greater vegetation species diversity than lowland soils at Konza (Gibson & Hulbert 1987). Additionally, the lower elevations at Konza contain riparian areas with a greater abundance of arboreal vegetation compared to the upland areas dominated by grass and forbs (Veach *et al.* 2014). Further, arboreal species tend to be relatively high pollen producers (Brostrom *et al.* 2008). Thus, the pollen signal of these woody species, particularly *Quercus macrocarpa* and *Quercus*

muehlenbergii at Konza, could be amplified in riparian areas where they are already more abundant on the landscape, muting the assemblage diversity assessed by the Shannon Index. It is important to reiterate that the influence of elevation is not statistically significant within the four year record of pollen data presented here. However, additional years of data from these traps could reveal or refute the influence of local elevation differences on these pollen assemblages.

Additionally, the random effects of trap location and year are significant in some of the summative metrics, and could be causing the environmental variables (fixed effects) to appear to less significant. The random effect of trap location is significant in Shannon Index, NAP%, and *Ambrosia:Artemisia* (Table 3.1). This significance indicates that temporal autocorrelation is likely occurring among the four years of pollen data within a given trap. This is not completely surprising, as our SCD values within a trap (Figure 3.6) were also found to be lower than the SCD values across all traps and years (Figure 3.5), indicating higher similarity among the pollen assemblages at a given trap. Vegetation composition is known for being the strongest driver of pollen assemblage composition. While we did not measure vegetation composition as a driver of pollen assemblages, its relationship has been quantified with pollen assemblages in various biomes. At Konza, vegetation varies less at a given trap from year-to-year and more from trap-to-trap, so it is logical that pollen assemblages would also vary less at a given trap from year-to-year. In addition, the random effect of year is also significant in Shannon Index, indicating spatial autocorrelation in Shannon index values (but not in NAP%, beta-diversity, or *Ambrosia:Artemisia* values) across traps within a given year. This suggests that an annual-scale driver not included in the regression analyses is influencing Shannon index.

Annual differences in pollen assemblage diversity

In lacustrine sediment cores, pollen sampling for vegetation reconstruction often does not follow a continuous scheme. Therefore, there is the potential for compositional changes in vegetation (inferred from pollen assemblages) to go undetected during the time between samples (Liu et al. 2012). Beta-diversity has been calculated on vegetation proxies from lacustrine sediment cores in various regions around the world (Birks 2006; Leys et al. 2014), including pollen from the Great Plains (Commerford et al. 2016), but not on annual modern pollen samples. Our ANOVA results demonstrate statistically significant differences in beta-diversity between some of the years from 2011-2014 (Figure 3.4). Yet, despite these differences, our annual averages for beta-diversity range only between 0.8 and 1.2 SD units. Comparatively, Holocene pollen assemblages from Fox Lake in the northern Great Plains had beta-diversity values that averaged around 0.8 SD units (4 SD units would imply full turnover), suggesting that grassland vegetation at that site exhibited little change in beta-diversity over much of the Holocene, despite recurring fire and drought (Commerford et al. 2016). Our beta-diversity values are similar, suggesting that the amount of change is comparable on an annual time scale.

The pollen data from 2013 are the most extreme of our four year record: lowest beta-diversity, lowest Shannon diversity, highest *Ambrosia:Artemisia*, and highest NAP% (Figure 3.4). This change in the average for all traps in 2013 seems to indicate a regional-scale driver. Higher precipitation in the 2013 growing season (462.1 mm from May to August, an increase of at least 35% over the other three years) is a likely cause. The mechanism could be either through a direct influence on pollen production of certain non-arboreal taxa (McLauchlan et al. 2011) or through increased inwash of pollen from overland flow (Birks and Bjune 2010; Bjune 2014). High summer precipitation has been associated with high levels of *Ambrosia* pollen, while high

spring precipitation has been associated with high levels of Poaceae pollen at other monitoring sites in the region (McLauchlan et al. 2011). Given that *Ambrosia* and Poaceae are the two most abundant non-arboreal pollen types in our four-year dataset, an increase in their production would certainly affect our summative metrics. *Ambrosia* and Poaceae abundances are highest in 2013 (compared to all other years) at the majority of the traps (Figure 3.3), providing further support for the increase being due to production. Higher flowering is a possible instigator of this increase in production (Hicks 2006). However, increased inwash of pollen from overland flow cannot be ruled out as another potential cause. Birks & Bjune (2010) identified inwash as a source of plant macroremains in traps in a Norwegian woodland, and Bjune (2014) also suggested it as a mechanism for pollen deposition. Given the topography of the limestone and mudstone hills at Konza, some of our traps at the lower elevations could be particularly susceptible to pollen deposition via inwash.

In long-term records of modern pollen, an anomalous year of pollen data (either summarized by a single metric or by individual key taxa) could be muted by the other years of data if averaged over the entire record. Alternatively, a single anomalous year might significantly influence the average if it is substantially different from the other years of data. The role of anomalous individual years could be especially relevant for fossil pollen records from non-laminated lacustrine sediment cores, where a 1-cm sample often spans a decade or more (depending on the location and the deposition rate) (Goring et al. 2012; Minckley et al. 2012a). Ultimately, modern multi-year records that match the time frame of deposition rates in lacustrine cores from the same region could highlight "tipping points" for how anomalous a single year needs to be to affect an average. The longest-running annual Tauber trap pollen records of which we are aware are in Europe, some of which span eight years or more (Bjune 2014; Hättestrand

2013; Pidek et al. 2013). In the Great Plains, pollen and sediment deposition rates in lakes are relatively rapid (*e.g.* 5 years cm^{-1}, Grimm *et al.* 2011) and so fewer years of pollen monitoring would be needed to match their temporal resolution. The medical community has monitored pollen taxa on the Great Plains for decades and has found a direct influence of temperature on pollen production of common allergenic taxa such as *Ambrosia* and *Juniperus* (Ziska et al. 2011; Levetin 2001). Although the collection devices used in those studies are specifically designed to trap airborne pollen rather than deposited pollen—and thus may not serve as a direct comparison to pollen deposited in lake sediment—these records could be sufficiently long to demonstrate the impact of a single anomalous year of pollen production on a multi-year average.

High dissimilarity among samples

The limited temporal resolution of non-laminated lacustrine sediment cores has been seen as a potential issue for accurately reconstructing vegetation from pollen assemblages throughout the Holocene (Hicks and Hyvärinen 1999), because it is impossible to achieve an annual-scale sampling resolution. However, even in the best case scenario it is likely that sedimentary pollen analysis will not achieve finer than sub-decadal resolution (Joosten and de Klerk 2007). Yet, the results of our squared-chord distance dissimilarity analysis indicate that pollen assemblage composition is more dissimilar across all traps and years (Figure 3.5), than it is between years at a single trap (Figure 3.6). The relatively lower within-trap dissimilarity values (year to year) (Figure 3.6) indicate that, though significant, annual-scale differences in pollen productivity or subtle annual changes in grassland vegetation composition may not have as much of an impact on pollen assemblage composition as spatial differences.

Our pollen samples from the Konza prairie have an overall average dissimilarity of 0.38 (the average of the SCD values between all pairs of samples), but an average minimum

dissimilarity of 0.11 (the average of the lowest SCD value for all samples). This difference between the overall average and the average minimum dissimilarity between samples indicates that most samples have a close compositional match, but also are quite dissimilar from many of the other samples in our dataset. Our results are similar to those from modern pollen samples from other grassland regions of North America and Africa. In Africa, modern grassland pollen samples were found to have an average minimum dissimilarity of 0.13, while savanna samples were slightly higher at 0.16 (Gajewski *et al.* 2002). Our Konza prairie samples exhibited slightly lower average minimum dissimilarity (0.11). In Oklahoma and north-central Texas, tallgrass prairie pollen samples from Tauber traps have also been found to be fairly similar to each other (0.10), but dissimilar to samples from short grass and mixed grass prairie in west Texas and New Mexico (0.40) (Hoyt 2000). Among our Konza prairie samples, the average dissimilarity between all samples is 0.38, which is more comparable to the 0.40 dissimilarity found between the different grassland types by Hoyt (2000). Our samples could be more dissimilar because our traps were intentionally placed to span a range of different burning and grazing treatments to examine the influence of those factors on the diversity and composition of the pollen assemblages. Hoyt (2000) aimed to identify pollen signatures among different grassland types (tallgrass, mixed grass, shortgrass) and therefore did not discuss any variation in burning and grazing, if any, among sample sites.

All of the traps in this study are located within a 3,487 hectare area that is predominantly grassland despite some local differences in the amount and type of nearby woody vegetation. Yet, the pollen assemblages from the 27 traps would not all be considered analogs for each other using the Modern Analog Technique with a suggested SCD threshold of 0.20 to 0.30 (Williams & Shuman 2008). The high variation in these modern pollen assemblages implies that defining a

pollen assemblage as “grassland” (particularly when examining fossil pollen assemblages) could be more difficult than previously thought. However, Tauber traps typically detect a very local vegetation signal given their relatively small 5-cm opening compared to lake surfaces, which have a much larger source area (Calcote 1995; Sugita 2007b). In a lake, the pollen from the entire source area would be mixed together (Sugita 2007a) and so the small source area associated with traps may be a reason for the high dissimilarity among our samples compared to samples from soils or lake sediments. Thus, the mean abundance values from all of the traps would likely be most useful when comparing our samples to grassland fossil pollen records in future work (as suggested by Bjune 2014).

Conclusion

Modern tallgrass prairie pollen assemblages are more similar temporally than spatially, as shown by SCD values across the four-year record. Our SCD values similar to SCD values for pollen samples from modern African grasslands, but higher compared to other modern grasslands in North America. The higher dissimilarity compared to other North American grasslands pollen samples could be due to our larger sample size, and the deliberate placement of the traps in this study to include a range of elevations, burning frequencies, and grazing intensities. In addition, annual differences in pollen composition and diversity are significant in three of the four summative metrics that we examined: beta-diversity, Shannon index, and non-arboreal pollen abundance (not significant in *Ambrosia:Artemisia*). Interannual variability in precipitation is significantly related to these differences. The 2013 growing season experienced significantly higher precipitation than 2011, 2012, and 2014, as well as the highest NAP%, lowest Shannon Index, and lowest beta-diversity of the four-year record. Variables of topography, fire, and grazing do have some effect on the diversity and composition of pollen

taxa among traps, although their individual significance varies depending on the metric. Further long-term modern pollen records from grasslands are essential in order to better establish the degree of variation in pollen production and deposition on an annual basis.

Acknowledgements

We gratefully acknowledge the numerous individuals, primarily students at Kansas State University, who helped collect samples from the field. We thank J. Mueller, S. McConaghy and R. Scharping for lab assistance, and TJ Gajda for pollen processing. We also thank K. Courtois for photographic assistance. We thank Simon Goring and an anonymous reviewer for providing helpful comments that improved an earlier version of this manuscript. Funding to maintain the fire and grazing treatments at the Konza Prairie LTER was NSF DEB-0823341. JC was funded by NSF BCS-0955225 to KM, a GK-12 fellowship (NSF DGE-0841414 to C. Ferguson), and an NSF Doctoral Dissertation Research Improvement Grant (NSF BCS-1558228 to KM and JC).

References

Abrams, M.D. and D. J. Gibson 1991: Effects of fire exclusion on tallgrass prairie and gallery forest communities in eastern Kansas. *Fire and the environment: ecological and cultural perspectives: Proceedings of an international symposium*, pp. 3–10. Knoxville, TN.

Autio, J. and S. Hicks 2004: Annual variations in pollen deposition and meteorological conditions on the fell Aakenustunturi in northern Finland: Potential for using fossil pollen as a climate proxy. *Grana*, **43**, 31–47.

Birks, H.J.B. 2006: Estimating the amount of compositional change in late-Quaternary pollen-stratigraphical data. *Vegetation History and Archaeobotany*, **16**, 197–202.

Birks, H.H. and A.E. Bjune 2010: Can we detect a west Norwegian tree line from modern samples of plant remains and pollen? Results from the DOORMAT project. *Vegetation History and Archaeobotany*, **19**, 325–340.

Bjune, A.E. 2014: After 8 years of annual pollen trapping across the tree line in western Norway: are the data still anomalous? *Vegetation History and Archaeobotany*, **23**, 299–308.

Brostrom, A., Nielsen, A.B., Gaillard, M.-J., Hjelle, K., Mazier, F., Binney, H., Bunting, M.J., Fyfe, R., Meltsov, V., Poska, A., Rasanen, S., Soepboer, W., von Stedingk, H., Suutari, H. & Sugita, S. 2008: Pollen productivity estimates of key European plant taxa for quantitative reconstruction of past vegetation: a review. *Vegetation History and Archaeobotany*, **17**, 461–478.

Brown, K.J., Clark, J.S., Grimm, E.C., Donovan, J.J., Mueller, P.G., Hansen, B.C.S. & Stefanova, I. 2005: Fire cycles in North American interior grasslands and their relation to prairie drought. *Proceedings of the National Academy of Sciences of the United States of*

America, **102**, 8865–70.

Calcote, R. 1995: Pollen source area and pollen productivity: evidence from forest hollows. *Journal of Ecology*, **83**, 591-602.

Clark, J.S., Grimm, E.C., Lynch, J. & Mueller, P.G. 2001: Effects of Holocene climate change on the C4 grassland/ woodland boundary in the Northern Plains, USA. *Ecology*, **82**, 620–636.

Commerford, J.L., Leys, B., Mueller, J.R. & McLauchlan, K.K. 2016: Great Plains vegetation dynamics in response to fire and climatic fluctuations during the Holocene at Fox Lake, Minnesota (USA). *The Holocene*, **26**, 302–313.

Commerford, J.L., McLauchlan, K.K. & Sugita, S. 2013: Calibrating vegetation cover and grassland pollen assemblages in the Flint Hills of Kansas, USA. *American Journal of Plant Sciences*, **4**, 1–10.

Cook, E.R., Seager, R., Heim Jr., R.R., Vose, R.S., Herweijer, C. & Woodhouse, C. 2010: Megadroughts in North America: placing IPCC projections of hydroclimatic change in a long-term palaeoclimate context. *Journal of Quaternary Science*, **25**, 48–61.

Craine, J.M. and K.K. McLauchlan 2004: The influence of biotic drivers on North American palaeorecords: alternatives to climate. *Holocene*, **14**, 787–791.

Davis, M.B. 2000: Palynology after Y2K - Understanding the Source Area of Pollen in Sediments. *Annual Review of Earth and Planetary Sciences*, **28**, 1–18.

Faegri, K. and J. Iversen 1989: *Textbook of pollen analysis*. Wiley, Chichester.

Gajewski, K., Lézine, A.M., Vincens, A., Delestan, A. & Sawada, M. 2002: Modern climate-vegetation-pollen relations in Africa and adjacent areas. *Quaternary Science Reviews*, **21**,

1611–1631.

Gavin, D.G., Brubaker, L.B., McLachlan, J.S. & Oswald, W. 2005: Correspondence of pollen assemblages with forest zones across steep environmental gradients, Olympic Peninsula, Washington, USA. *The Holocene*, **15**, 648–662.

Gavin, D.G., Oswald, W.W., Wahl, E.R. & Williams, J.W. 2003: A statistical approach to evaluating distance metrics and analog assignments for pollen records. *Quaternary Research*, **60**, 356–367.

Gibson, D.J. and L.C. Hulbert 1987: Effects of fire, topography and year-to-year climate variation on species composition in tallgrass prairie. *Vegetatio*, **72**, 175–185.

Giesecke, T. and S.L. Fontana 2008: Revisiting pollen accumulation rates from Swedish lake sediments. *Holocene*, **18**, 293–305.

Giesecke, T., Fontana, S.L., Knaap, W.O., Pardoe, H.S. & Pidek, I. 2010: From early pollen trapping experiments to the Pollen Monitoring Programme. *Vegetation History and Archaeobotany*, **19**, 247–258.

Gill, J.L., McLauchlan, K.K., Skibbe, A.M., Goring, S., Zirbel, C.R. & Williams, J.W. 2013: Linking abundances of the dung fungus Sporormiella to the density of bison: implications for assessing grazing by megaherbivores in palaeorecords. *Journal of Ecology*, **101**, 1125–1136.

Giraudoux, P. 2014: PGIRMESS: Data Analysis in Ecology.

Goring, S., Williams, J.W., Blois, J.L., Jackson, S.T., Paciorek, C.J., Booth, R.K., Marlon, J.R., Blaauw, M. & Christen, J.A. 2012: Deposition times in the northeastern United States during the Holocene: Establishing valid priors for Bayesian age models. *Quaternary*

Science Reviews, **48**, 54–60.

Grimm, E.C. 1993: TILIA: a pollen program for analysis and display.

Grimm, E.C., Donovan, J.J. & Brown, K.J. 2011: A high-resolution record of climate variability and landscape response from Kettle Lake, northern Great Plains, North America. *Quaternary Science Reviews*, **30**, 2626–2650.

Hartnett, D.C., Hickman, K.R. & Walter, L.E.F. 1996: Effects of bison grazing, fire, and topography on floristic diversity in tallgrass prairie. *Journal of Range Management*, **49**, 413–420.

Hättestrand, M. 2013: Eight years of annual pollen monitoring in northern Sweden, from the boreal forest to above the birch forest-line. *Grana*, **52**, 26–48.

Hicks, S. 1985: Modern Pollen Deposition Records from Kuusamo, Finland .1. Seasonal and Annual Variation. *Grana*, **24**, 167–184.

Hicks, S. 2001: The use of annual arboreal pollen deposition values for delimiting tree-lines in the landscape and exploring models of pollen dispersal. *Review of Palaeobotany and Palynology*, **17**, 1–29.

Hicks, S. 2006: When no pollen does not mean no trees. *Vegetation History and Archaeobotany*, **15**, 253–261.

Hicks, S. and H. Hyvärinen 1999: Pollen influx values measured in different sedimentary environments and their palaeoecological implications. *Grana*, **38**, 228–242.

Hoyt, C.A. 2000: Pollen signatures of the arid to humid grasslands of North America. *Journal of Biogeography*, **27**, 687–696.

Intergovernmental Panel on Climate Change 2014: *Climate Change 2014: Impacts, Adaptation,*

and Vulnerability. Part A: Global and Sectoral Aspects. Contribution of Working Group II to the Fifth Assessment Report of the Intergovernmental Panel on Climate Change [Field, C.B., V.R. Barros, D.J. Dokken, K.J. Cambridge University Press, Cambridge, United Kingdom and New York, NY, USA.

Joosten, H. and P. de Klerk 2007: In search of finiteness: the limits of fine-resolution palynology of Sphagnum peat. *The Holocene*, **17**, 1023–1031.

Knapp, A.K., Blair, J.M., Briggs, J.M., Collins, S.L., Hartnett, D.C., Johnson, L.C. & Towne, E.G. 1999: The keystone role of bison in north American tallgrass prairie - Bison increase habitat heterogeneity and alter a broad array of plant, community, and ecosystem processes (A.L.L. Angert SL Ostfeld,RS, Ed.). *Bioscience*, **49**, 39–50.

Knapp, A.K. and T.R. Seastedt 1986: Detritus accumulation limits productivity of tallgrass prairie. *Bioscience*, **36**, 662–668.

Konza Prairie Biological Station 2015: Meteorological data from the Konza Prairie headquarters weather station. **2015**. URL http://www.konza.ksu.edu/knz/pages/data/knzdata.aspx

Levetin, E. 2001: Effects of climate change on airborne pollen. *Journal of Allergy and Clinical Immunology*, **107**, S172.

Leys, B., Brewer, S.C., McConaghy, S., Mueller, J.R. & McLauchlan, K.K. 2015: Fire history reconstruction in grassland ecosystems: amount of charcoal reflects local area burned. *Environmental Research Letters*, **10**, 114009.

Leys, B., Finsinger, W. & Carcaillet, C. 2014: Historical range of fire frequency is not the Achilles' heel of the Corsican black pine ecosystem. *Journal of Ecology*, **102**, 381–395.

Liu, Y., Brewer, S.C., Booth, R.K., Minckley, T.A. & Jackson, S.T. 2012: Temporal density of

pollen sampling affects age determination of the mid-Holocene hemlock (Tsuga) decline. *Quaternary Science Reviews*, **45**, 54–59.

Matthias, I., Semmler, M.S.S. & Giesecke, T. 2015: Pollen diversity captures landscape structure and diversity. *Journal of Ecology*, **103**, 880–890.

Mazier, F., Brostrom, A., Gaillard, M.-J., Sugita, S., Vittoz, P. & Buttler, A. 2008: Pollen productivity estimates and relevant source area of pollen for selected plant taxa in a pasture woodland landscape of the Jura Mountains (Switzerland). *Vegetation History and Archaeobotany*, **17**, 479–495.

McAndrews, J.H., Berti, A.A. & Norris, G. 1973: *Key to the Quaternary Pollen and Spores of the Great Lakes Region*. Royal Ontario Museum, Toronto, Ontario.

McLauchlan, K.K., Barnes, C.S. & Craine, J.M. 2011: Interannual variability of pollen productivity and transport in mid-North America from 1997 to 2009. *Aerobiologia*, **27**, 181–189.

McLauchlan, K.K., Commerford, J.L. & Morris, C.J. 2013: Tallgrass prairie pollen assemblages in mid-continental North America. *Vegetation History and Archaeobotany*, **22**, 171–183.

Minckley, T.A., Bartlein, P.J., Whitlock, C., Shuman, B.N., Williams, J.W. & Davis, O.K. 2008: Associations among modern pollen, vegetation, and climate in western North America. *Quaternary Science Reviews*, **27**, 1962–1991.

Minckley, T.A., Booth, R.K. & Jackson, S.T. 2012a: Response of arboreal pollen abundance to late-Holocene drought events in the Upper Midwest, USA. *The Holocene*, **22**, 531–539.

Minckley, T.A., Shriver, R.K. & Shuman, B. 2012b: Resilience and regime change in a southern Rocky Mountain ecosystem during the past 17,000 years. *Ecological Monographs*, **82**, 49–

68.

Morris, C.J. 2013: *Analysis of modern pollen data from the prairies of central North America*. Kansas State University, Manhattan, KS.

Overpeck, J.T., Webb, T. & Prentice, I.C. 1985: Quantitative Interpretation of Fossil Pollen Spectra - Dissimilarity Coefficients and the Method of Modern Analogs. *Quaternary Research*, **23**, 87–108.

Pidek, I.A., Svitavská-Svobodová, H., Van der Knaap, W.O. & Magyari, E. 2013: Pollen percentage thresholds of Abies alba based on 13-year annual records of pollen deposition in modified Tauber traps: Perspectives of application to fossil situations. *Review of Palaeobotany and Palynology*, **195**, 26–36.

Räsänen, S., Hicks, S. & Odgaard, B.V. 2004: Pollen deposition in mosses and in a modified 'Tauber trap' from Hailuoto, Finland: what exactly do the mosses record? *Review of palaeobotany and palynology*, **129**, 103–116.

R Core Team 2013: R: A language and environment for statistical computing.

Simpson, G.L. 2015: Analogue: Analogue and Weighted Averaging Methods for Paleoecology (J. Oksanen, Ed.).

Soepboer, W., Sugita, S., Lotter, A.F., van Leeuwem, J.F.N. & van der Knaap, W.O. 2007: Pollen productivity estimates for quantitative reconstruction of vegetation cover on the Swiss Plateau. *The Holocene*, **17**, 65–77.

Sugita, S. 1994: Pollen representation of vegetation in quaternary sediments: theory and method in patchy vegetation. *Journal of Ecology*, **82**, 881–897.

Sugita, S. 2007a: Theory of quantitative reconstruction of pollen I: Pollen from large lakes

REVEALS regional vegetation composition. *The Holocene*, **17**, 229–241.

Sugita, S. 2007b: Theory of quantitative reconstruction of pollen II: all you need is LOVE. *The Holocene*, **17**.

Sugita, S., Parshall, T. & Calcote, R. 2006: Detecting differences in vegetation among paired sites using pollen records. *Holocene*, **16**, 1123–1135.

Tauber, H. 1974: Static Nonoverload Pollen Collector. *New Phytologist*, **73**, 359–369.

Ter Braak, C.J.F. 1986: Canonical Correspondence Analysis a New Eigenvector Technique for Multivariate Direct Gradient Analysis. *Ecology (Washington D C)*, **67**, 1167–1179.

Ter Braak, C.J.F. & P. Smilauer 2012: *Canoco reference manual and user's guide: software for ordination, version 5.0*. Microcomputer Power, Ithaca, NY.

Tonello, M.S. and A.R. Prieto 2008: Modern vegetation-pollen-climate relationships for the Pampa grasslands of Argentina. *Journal of Biogeography*, **35**, 926–938.

Towne, E.G. 2002: Vascular plants of Konza Prairie Biological Station: An annotated checklist of species in a Kansas tallgrass prairie. *Sida*, **20**, 269–294.

Umbanhowar, C.E., Camill, P., Geiss, C.E. & Teed, R. 2006: Asymmetric vegetation responses to mid-Holocene aridity at the prairie–forest ecotone in south-central Minnesota. *Quaternary Research*, **66**, 53–66.

Veach, A.M., Dodds, W.A. & Skibbe, A. 2014: Fire and grazing influences on rates of riparian woody plant expansion along grassland streams. *PLoS ONE*, **9**, e106922.

Weng, C., Hooghiemstra, H. & Duivenvoorden, J.F. 2007: Response of pollen diversity to the climate-driven altitudinal shift of vegetation in the Colombian Andes. *Philosophical Transactions of the Royal Society B: Biological Sciences*, **362**, 253–262.

Williams, J.W. & Shuman, B. 2008: Obtaining accurate and precise environmental reconstructions from the modern analog technique and North American surface pollen dataset. *Quaternary Science Reviews*, **27**, 669–687.

Williams, J.W., Shuman, B. & Bartlein, P.J. 2009: Rapid responses of the prairie-forest ecotone to early Holocene aridity in mid-continental North America. *Global and Planetary Change*, **66**, 195–207.

Ziska, L., Knowlton, K., Rogers, C., Dalan, D., Tierney, N., Elder, M.A., Filley, W., Shropshire, J., Ford, L.B., Hedberg, C., Fleetwood, P., Hovanky, K.T., Kavanaugh, T., Fulford, G., Vrtis, R.F., Patz, J. a, Portnoy, J., Coates, F., Bielory, L. & Frenz, D. 2011: Recent warming by latitude associated with increased length of ragweed pollen season in central North America. *Proceedings of the National Academy of Sciences of the United States of America*, **108**, 4248–4251.

Table 3.1: Multiple regression results of the four summative metrics listed at top (beta-diversity, Shannon index, non-arboreal pollen percentage, and *Ambrosia:Artemisia*), explained by the topography, grazing, and fire variables listed at the left. Random effects of trap location and year were assessed for significance at p<0.05. Coefficients of the variables that significantly contribute to each summative metric are listed. *Indicates the fixed effect variable is significant at p<0.05. **Indicates the fixed effect variable is significant at p<0.01. ***Indicates the fixed effect variable is significant at p<0.001.

		Summative pollen metrics			
		Beta-diversity	**Shannon**	**NAP%**	***Ambrosia:Artemisia***
Fixed effects	**Elevation**	-	-	-	-
	Bare Soil	-	-	-	-
	Limestone Rocks	-	-	-	-
	Bison Manure	-	-	-	-
	Bison Density	-	-0.25*	-	-
	Area Burned 500 m	-	-	-	-0.14*
	Area Burned Flint Hills	0.45***	-	-0.13**	-
	Fire Return Interval	-	-	-	-
	Mean Fire Return Inter.	-	-	-	-
	Fire Frequency	-	-	-	-
	Time Since Last Fire	-	-	-	-
	Area Burned Konza	-0.29***	-	0.16***	-
Random effects	**Trap**	Not significant	Significant (p<0.001)	Significant (p<0.001)	Significant (p<0.001)
	Year	Not significant	Significant (p<0.05)	Not significant	Not significant

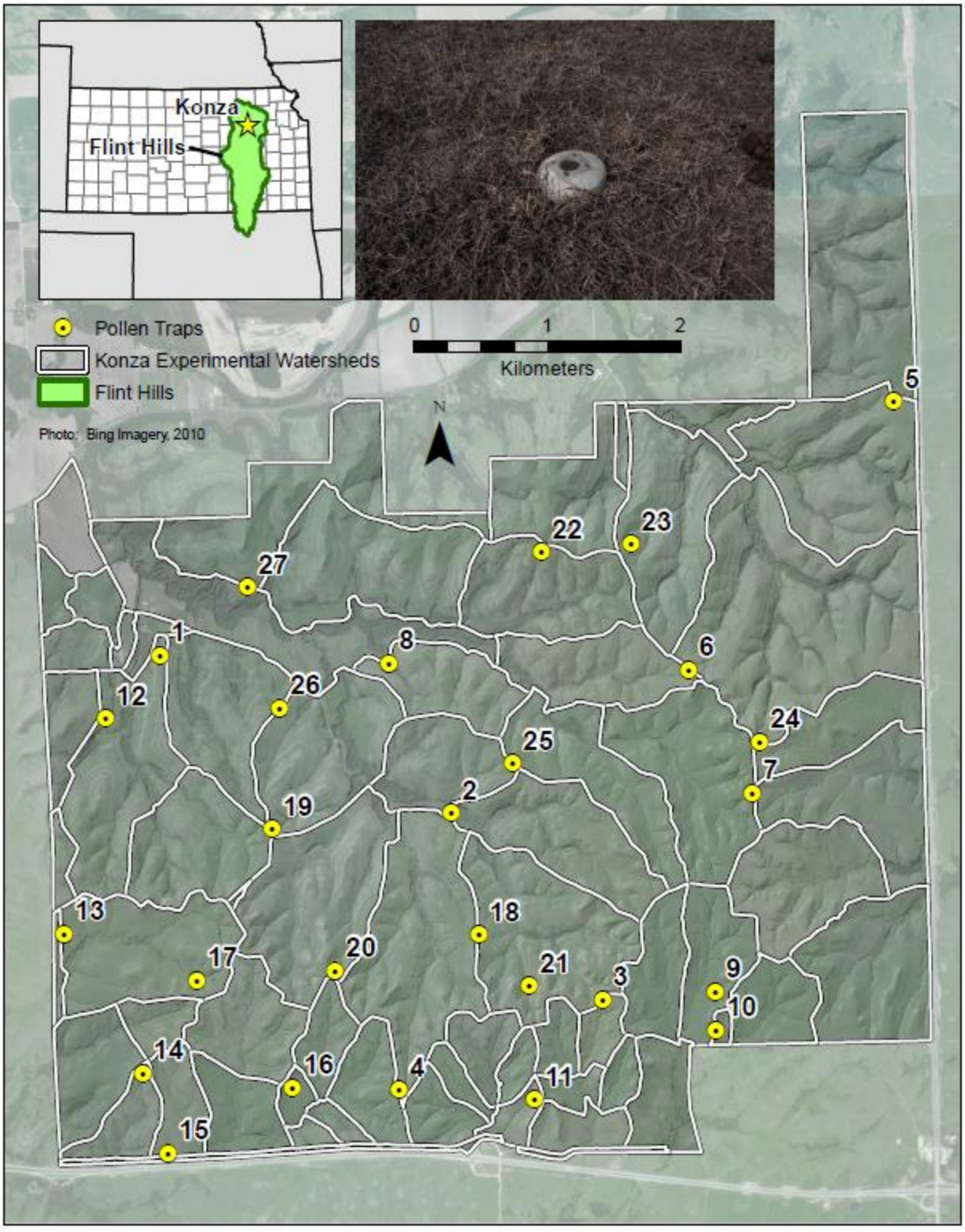

Figure 3.1: Trap locations within the Konza Prairie Biological Station. Konza is located within the Flint Hills ecoregion (inset map). A typical trap is pictured in the photo. Trap ID numbers are shown on the map.

$$H' = -\sum_{i=1}^{R} p_i \ln p_i$$

Figure 3.2: Shannon Index equation.

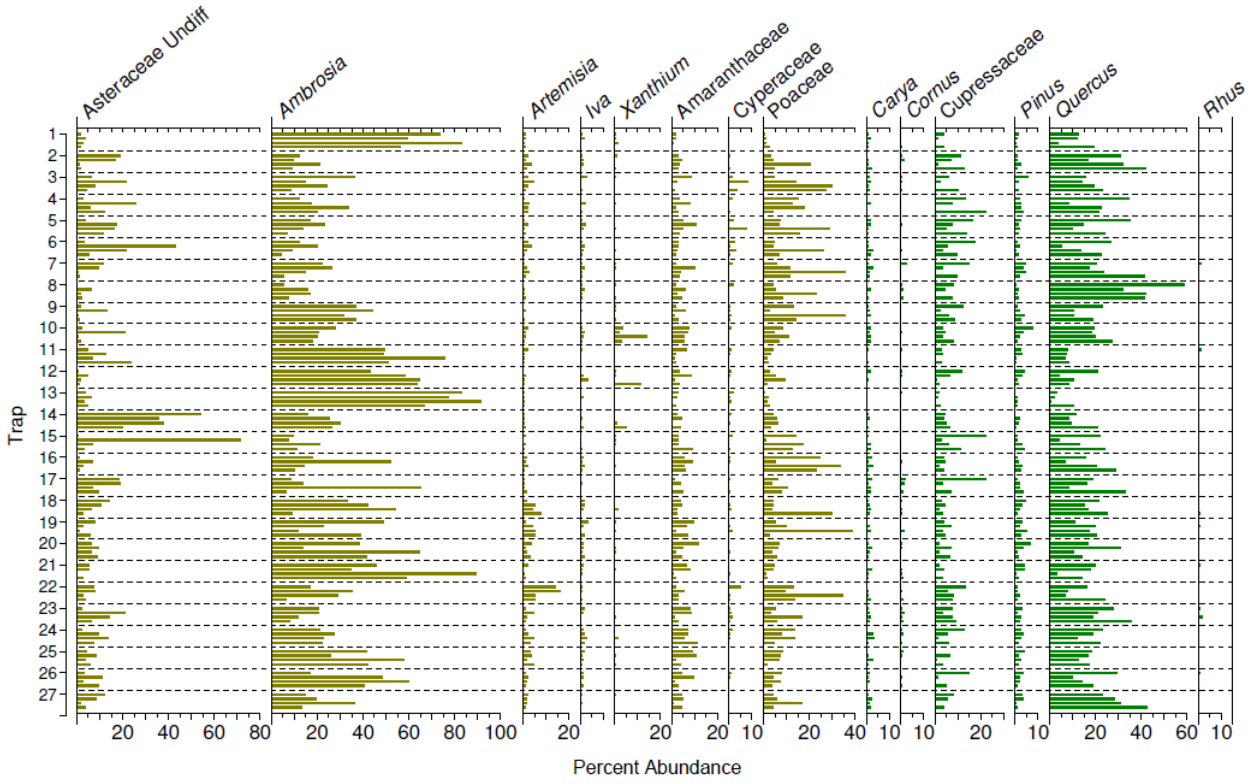

Figure 3.3: Pollen abundance (%) for the 6 most abundant taxa and other key taxa. Non-arboreal taxa are shown in brown and arboreal taxa are shown in green. For each trap, each bar signifies one collection year, beginning with 2011 at the top and 2014 at the bottom.

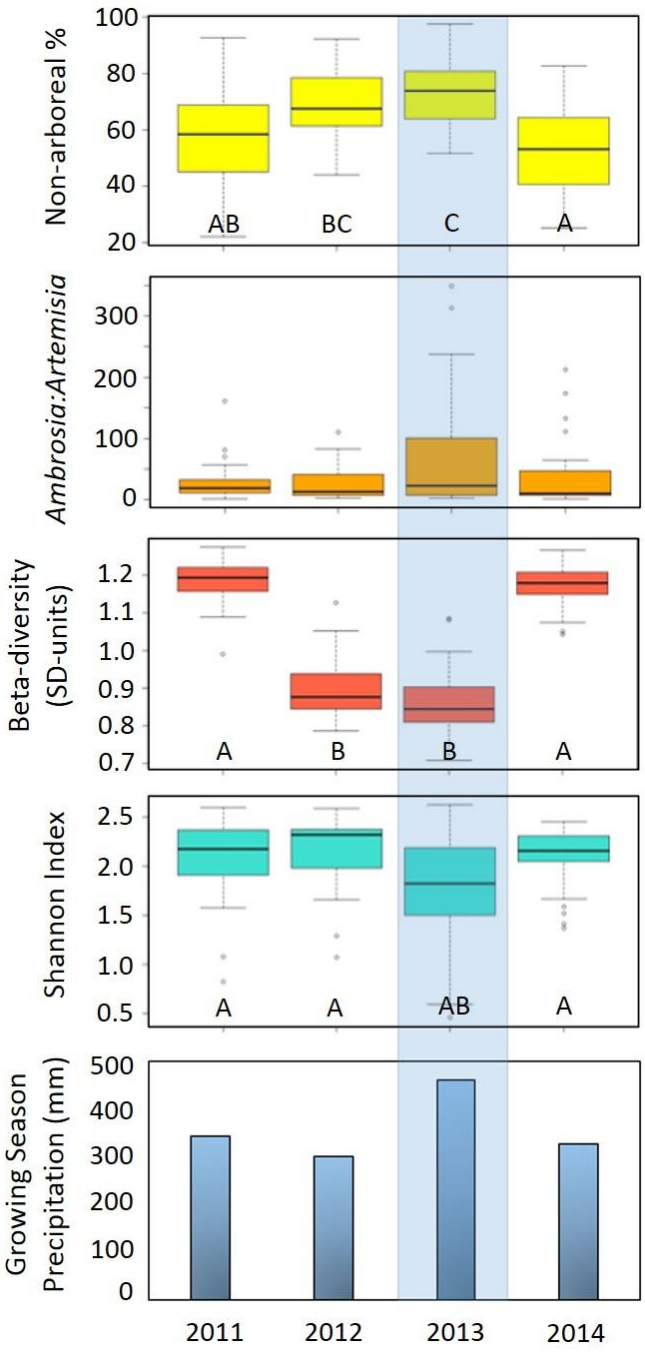

Figure 3.4: Kruskal-Wallis ANOVA results by year of the four summative metrics, compared to growing season precipitation. Letters (A, B, C, etc.) indicate groupings from the Kruskal-Wallis pairwise comparisons. *Ambrosia:Artemisia* showed no significant difference among the four years of data and have no letters. The blue shading signifies the high precipitation in the 2013 growing season. From top to bottom: Non-arboreal percentage, *Ambrosia:Artemisia*, Beta-diversity (SD-units), Shannon index, and growing season precipitation (mm).

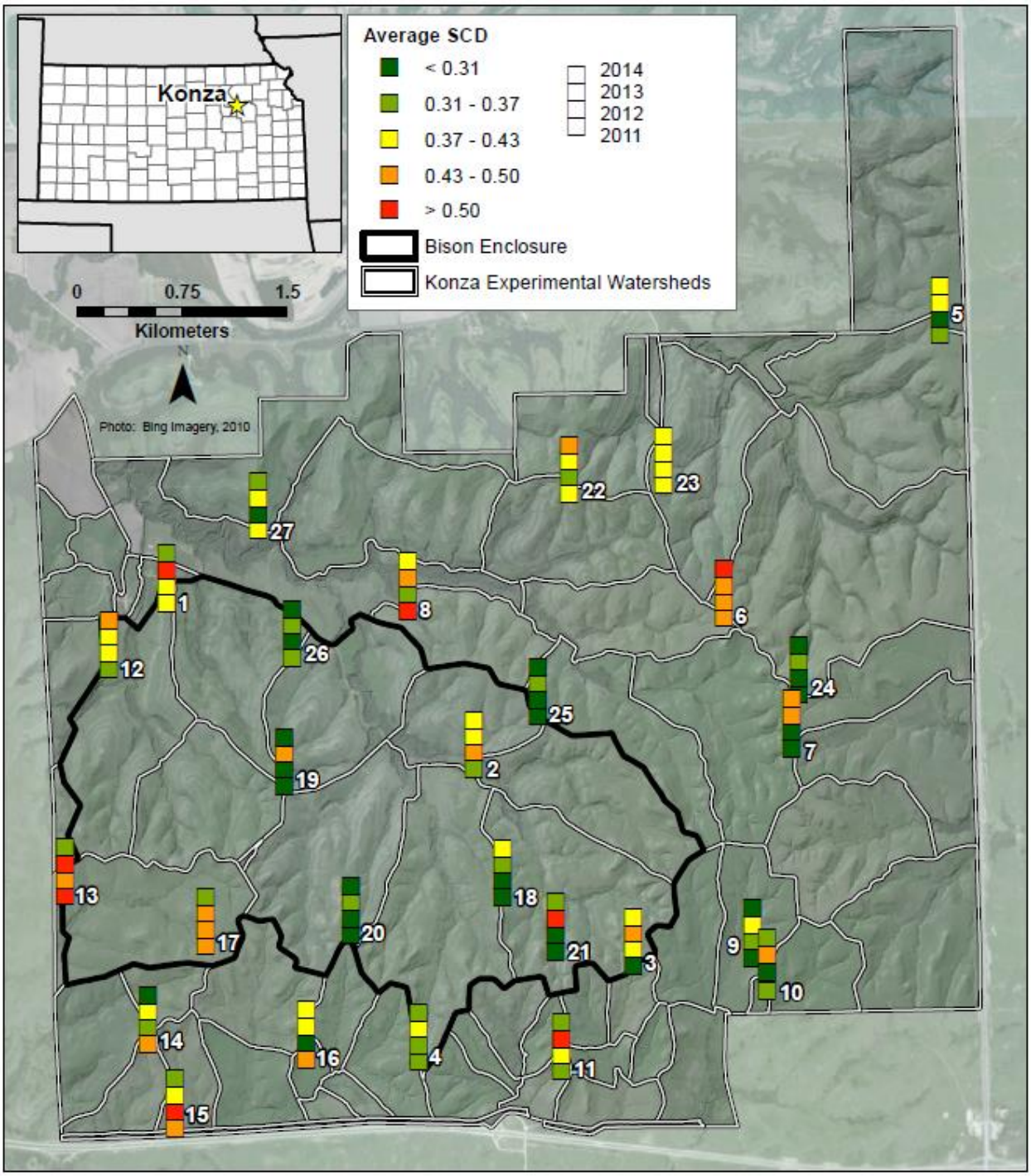

Figure 3.5: Average Squared-Chord Distance dissimilarity between a trap sample and all other samples (from all traps and all years). Green values represent lower average dissimilarity and red values represent higher average dissimilarity.

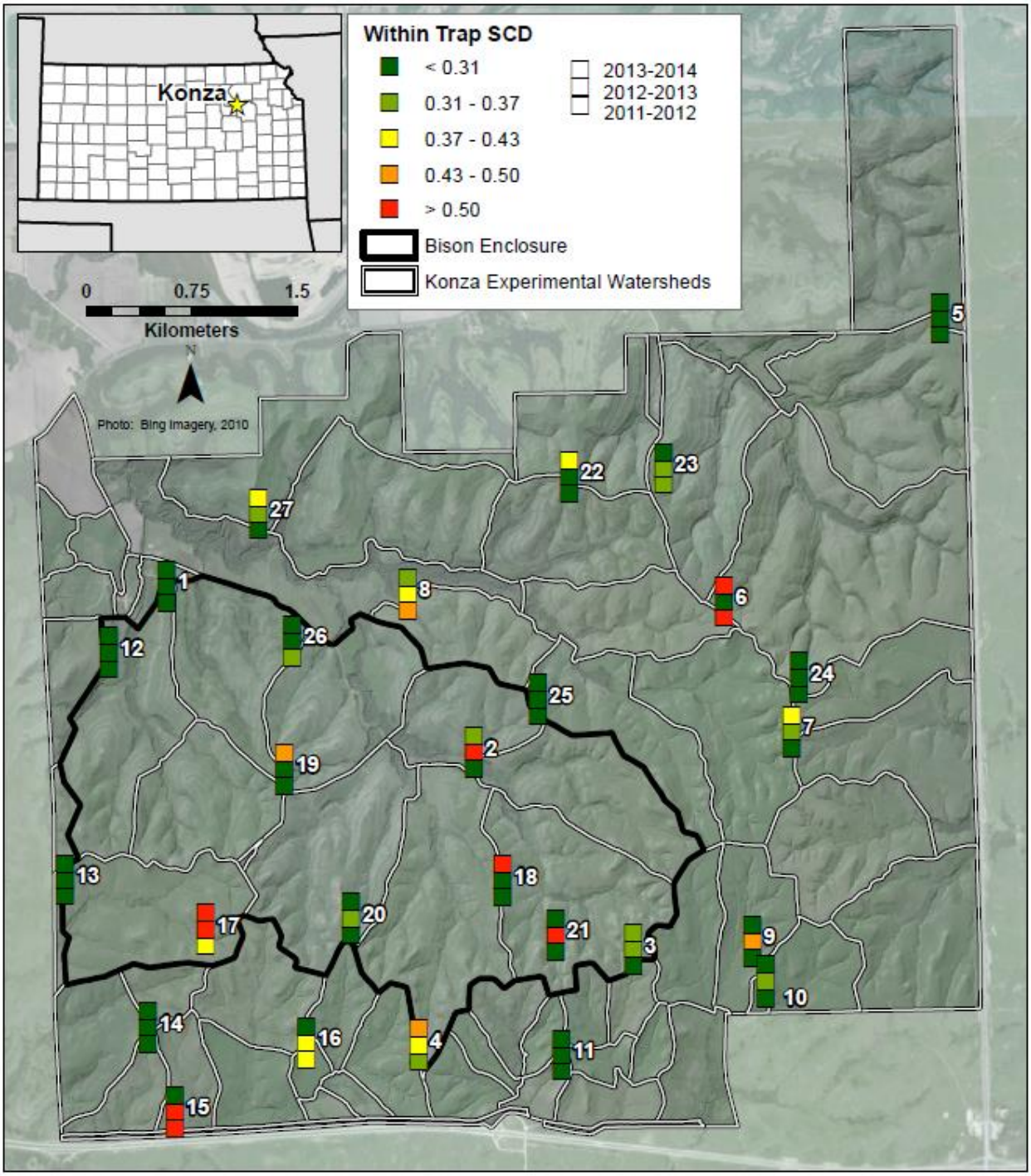

Figure 3.6: Within trap Squared-Chord Distance dissimilarity from 2011-2012, 2012-2013, and 2013-2014. Green values represent lower average dissimilarity and red values represent higher average dissimilarity.

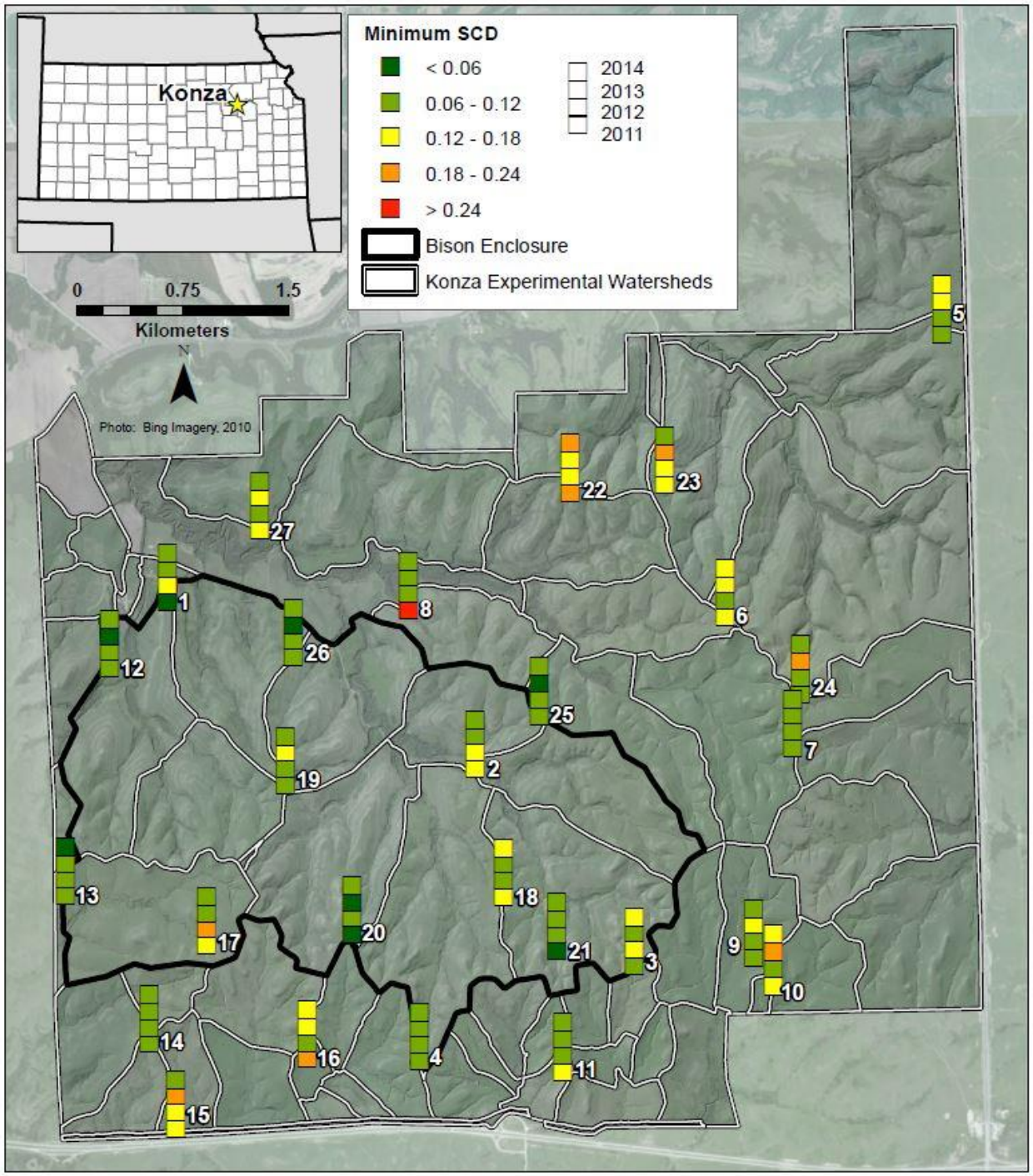

Figure 3.7: Minimum Squared-Chord Distance dissimilarity between a trap sample and all other samples (from all traps and all years). Green values represent lower minimum dissimilarity and red values represent higher minimum dissimilarity. Please note that the color breaks in the legend are different from the breaks used on Figure 3.5 and Figure 3.6.

Chapter 4 - Mid-Holocene aridity quantified from pollen in the Great Plains of North America

Abstract

The Great Plains experienced extreme fluctuations in precipitation and temperature throughout the Holocene, but these fluctuations have been difficult to quantify systematically across the region. Fossil pollen has long been used as a proxy for reconstructing climate changes, but its power is limited if a region is devoid of modern pollen samples to facilitate comparison with known climate conditions. Here, we present a set of pollen-climate transfer functions developed using weighted-averaging partial least squares to reconstruct mean annual precipitation (MAP), mean annual temperature (MAT), and mean temperature of the warmest month (July) (MJT). At the foundation of these transfer functions is a new set of 141 modern pollen samples that specifically cover the climate space of the Great Plains. Our functions quantify a robust relationship between pollen assemblages and climate in this region ($r = 0.928$, 0.891, and 0.897 for MAP, MAT, and MJT, respectively). We applied these functions to three previously established pollen records taken from lacustrine sites in the region—Fox Lake, Minnesota; Moon Lake, North Dakota; and Colo Marsh, Iowa—to reconstruct precipitation and climate at these sites throughout the Holocene. We found that the lowest precipitation levels occurred at 5,000 yr BP at all three sites, but were not coupled with high temperatures, indicating that low precipitation was the driving force behind the aridity of the mid-Holocene in this region.

Introduction

Grasslands in North America experienced frequent fluctuations in climate over the duration of the Holocene. Yet, quantifying the magnitude and timing of these changes has remained difficult because of their time-transgressive nature and the lack of direct proxy data capable of measuring these events in comparable way across sites. Pollen from lacustrine sediment records is commonly used as an indirect indicator of climate, but its power has been limited by the quality and quantity of calibrations linking modern pollen with known modern climate variables. This gap is exacerbated by the fact that disturbances such as severe megadroughts (Cook *et al.* 2010, 2014) and fire (Umbanhowar *et al.* 2006) were frequently changing the composition and spatial extent of this vegetation community (Grimm *et al.* 2011; Schmieder *et al.* 2011) making accurate quantifications of climate during those times even more critical. Many of the megadroughts lasted for decades or even millennia (Michels *et al.* 2007), emphasizing the need for a long-term perspective to fully assess their magnitude.

Given the strong and direct influence that climate has on vegetation composition, much effort has been directed toward developing numerical techniques that can infer past climate from pollen deposited in lacustrine sediment cores. The modern analog technique (Overpeck *et al.* 1985; Williams and Shuman 2008), has been successful in quantitatively matching modern pollen assemblages from known climate conditions with fossil pollen assemblages to infer climate conditions in the past. However, analogs or near-analogs do not always exist for a given fossil pollen assemblage (Jackson and Williams 2004). The transfer function approach (Bartlein *et al.* 1984; ter Braak and Juggins 1993; Birks 1995) also relies on modern pollen data, but develops a function based on the quantities of each pollen taxa in relation to a known climate variable. In this way, it does not require a direct match or analog. However, it does assume that

species within a pollen taxa are functionally similar—an assumption that often does not hold true across biomes because the taxonomic resolution of pollen is usually to the family or genus level. Thus, models quantifying the pollen-climate relationship should be developed at the regional level (Williams and Shuman 2008).

The quantitative techniques mentioned above have been used to successfully reconstruct climate in various regions of the world, including Arctic Siberia (Klemm *et al.* 2013), northern China (Li *et al.* 2007; Xu *et al.* 2010), Europe (Mauri *et al.* 2015; Seppa *et al.* 2004), Africa (Cheddadi *et al.* 1998; Bonnefille and Chalie 2000), and North America (Williams and Shuman 2008; Viau and Gajewski 2009; Viau *et al.* 2012; Wahl *et al.* 2012). In North America, all of the reconstructions have either focused on forested regions, or included all biomes without any distinctive consideration for grasslands. In addition, despite the large number of modern pollen samples included in the continental-scale calibrations (Williams and Shuman 2008; Viau *et al.* 2012), only 9% of them, at most, were from grasslands. Many pollen records from lacustrine cores in the upper-Midwest have indicated substantial periods of grassland vegetation during the Holocene (Baker *et al.* 1990; Laird *et al.* 1996; Nelson and Hu 2008; Umbanhowar *et al.* 2009; Grimm *et al.* 2011; Commerford *et al.* 2016). In order to accurately reconstruct the climate from pollen during the grassland periods at these sites, grassland surface samples must be well-represented in the datasets used in the calibrations. Furthermore, to reconstruct both temperature and precipitation accurately, these samples must collectively cover the broadest possible temperature and precipitation conditions experienced by present-day grasslands.

Here, we present pollen-climate transfer functions for three climate variables—mean annual temperature, mean July temperature, and mean annual precipitation—developed with a new set of modern pollen data from the surficial sediments of 141 ponds across the Great Plains

region of North America. Our two main objectives with these functions are to: (1) quantify the magnitude and timing of climatic fluctuations at three sites in the northern Great Plains during the Holocene and (2) facilitate objective quantitative reconstructions of precipitation and temperature from pollen from other sites in the region. We used weighted-averaging partial least squares (WAPLS) (ter Braak and Juggins 1993), and validated each model using leave-one-out cross-validation. We also validated each model manually by dividing our samples into training and test sites: once randomly, and once by testing sites with extreme precipitation and temperature values. Finally, we applied the models to fossil pollen data from three sites in the region to reconstruct the mean annual temperature, mean July temperature, and mean annual precipitation at the three sites throughout the Holocene. By doing so, we quantified and characterized the periods of extreme climate change in this grassland region known for experiencing dynamic climate changes. We also demonstrated that temperature and precipitation have a direct and significant influence on North American grassland pollen assemblages—a relationship that can facilitate direct comparison of Holocene climate change at additional grassland sites in the region.

Geographical Setting

The Great Plains region of central North America is approximately 1.3 million km^2 in size and dominated by tallgrass, mixed grass, and shortgrass prairie (Figure 4.1). The tallgrass vegetation contains abundant warm season grasses such as *Andropogon gerardii* (big bluestem) and *Sorghastrum nutans* (indian grass) as well as a variety of forbs in the Asteraceae (sunflower) and Fabaceae (legume) families. The shortgrass vegetation contains warm season grasses such as *Bouteloua dactyloides* (buffalo grass), *Bouteloua gracilis* (blue grama), and *Bouteloua hirsute*

(hairy grama) in the south, and more abundant cool season grasses such as *Pascopyrum smithii* (western wheatgrass) and *Koeleria macrantha* (june grass) in the north. Drought-tolerant forbs such as *Artemisia fridiga* (prairie sagewort) also dominate the shortgrass prairies. The mixed-grass prairies contain an assortment species from both of the adjacent tallgrass and shortgrass prairies, and the mid-size warm season grass *Schizachyrium scoparium* (little bluestem) is commonly found.

Although much of the native grassland vegetation in the Great Plains has been converted to agriculture, the gradient in grassland type generally follows climate. There is a strong east-west gradient in precipitation, with higher amounts in the east (high mean annual precipitation: 1207 mm) and lower amounts in the west (low mean annual precipitation: 186 mm). Conversely, the mean annual temperature gradient follows north-south, with cooler temperatures in the north (coolest value: 0.4°C), and warmer temperatures in the south (warmest value: 21.3°C).

Data and Methods

Surface pollen sampling

Surficial sediment samples were collected from 141 ponds less than 5 ha in surface area. Both natural and human-made ponds were sampled, reflecting the natural differences in topography and geology across the Great Plains. In the southern portion of the region—eastern Colorado, Kansas, Nebraska, Oklahoma, and Texas—human-made ponds comprised 90% of the ponds sampled. In the northern portion of the region—Montana, North Dakota, and South Dakota—natural and human-made ponds were nearly evenly sampled. The sample locations cover a mean annual temperature range of 4.09 – 16.23 °C, and a mean annual precipitation range of 302.42 – 1029.96 mm (Figure 4.2). The 24 samples in the southeast portion of tallgrass

prairie were reported in a previous study (Commerford *et al.* 2013). Sediment was collected from the near deepest point of each pond using an Eckman dredge or Hongve sampler, and the top 2 cm were retained, which represent approximately 5-10 years of sediment deposition (Grimm 2016, personal communication) Pollen was extracted from each sample using standard acetolysis techniques (Faegri and Iversen 1989). Each pollen sample was mounted in silicone oil and counted under a light microscope to a minimum of 300 terrestrial grains at the finest possible taxonomic resolution, generally following McAndrews *et al.* (1973). The raw counts were converted to percentages; a total of 87 pollen taxa were included in the subsequent modeling process.

Climate data acquisition

Four climate rasters were acquired from PRISM Climate Group's 30-Year Normals gridded dataset: mean annual precipitation, mean annual temperature, mean July temperature (hottest month), and mean January temperature (coldest month) (PRISM 2016). This dataset has an 800-m spatial resolution, spans the period from 1981-2010, and covers the conterminous United States. The values of the four climate variables were extracted at each pollen sample location in GIS.

Numerical analysis

To explore the general patterns of variation in pollen assemblages among the sites, a detrended correspondence analysis (DCA) (Hill and Gauch 1980) was conducted using square root transformations, detrending by segments, and downweighting of rare taxa. DCA axes 1 and 2 had gradients with lengths of 1.72 and 1.17 and accounted for 23.65% of the variation in the pollen data. This indicated that either a linear response model or unimodal response model would be suitable for our data. We opted to use a unimodal response model because previous work has

shown that unimodal models can provide a better transfer function even when gradients are less than 2 SD units (ter Braak 1995; Birks 1995; Bigler and Hall 2002).

To identify the climate variables that account for the most variation in the pollen assemblages, we conducted a detrended canonical correspondence analysis (DCCA). The variable inflation factors (VIFs) from this analysis indicated high autocorrelation among the three temperature variables with VIFs > 20. Because autocorrelation can weaken the predictive power of transfer function models (Telford and Birks 2005), it was necessary for us to remove one of the temperature variables. We chose to eliminate mean January temperature instead of mean July temperature or mean annual temperature because July is within the growing season for most plant species in the Great Plains, and mean annual temperature is holistic and comprises the temperature from all months. We performed the DCCA again using only mean annual precipitation, mean annual temperature, and mean July temperature, and checked the VIF values. The VIFs for all three variables were all lower than 10, indicating that each has a unique influence on the pollen assemblages. All ordinations were carried out in Canoco 5 software (ter Braak and Smilauer 2012).

Model development and validation

To generate numerical transfer functions between the pollen assemblages and each of the three climate variables, we used weighted-averaging regression and partial least squares calibration (WAPLS) (ter Braak and Juggins 1993). The multivariate pollen data (as percent abundances) were the explanatory variables, and each of the three climate variables were the response variables. This technique accounts for the unimodal response of pollen data while using the residuals to reduce bias and improve performance. We identified the optimal number of components included in the functions through leave-one-out jackknifing (ter Braak 1995),

following Li *et al.* (2007). For each climate variable, we selected the best function as the one with the greatest R^2 with a p-value less than 0.05. All functions were created in R statistical software (R Core Team 2013), using the rioja package (Juggins 2015).

We validated each model three ways, generally following Li *et al.* (2007). First, we internally cross-validated each model using the leave-one-out method, which trains the model using all but one sample, and makes a prediction for the one sample that was not included. This process repeats *n* times, until all samples have been tested. This was conducted using the crossval function in the rioja package (Juggins 2015). Second, we randomly tested each model by dividing the 141 pollen samples into a training set of 126 random samples and a test set of the remaining 15 samples. We used the 126 random samples to train the model, and predicted the climate value for each of the 15 test samples. We plotted the predicted climate values against the actual climate values (from PRISM) for each of the 15 sites, and calculated the correlation coefficient. Third, we tested each model by dividing the 141 pollen samples into new sets of 126 training samples and 15 test samples, but deliberately selected the 15 test samples to include at least two extreme values from each climate variable (two extremes from mean annual precipitation, two from mean annual temperature, and two from mean July temperature). We also selected one more sample that was extreme in two-dimensional climate space (low in precipitation, but high in annual temperature) (Figure 4.2). The remaining samples were selected randomly until 15 samples were reached. Then, following the same process used for the random sets discussed above, we trained the models with the set of 126 training samples, predicted the values for the 15 test sites, and plotted the predicted versus actual climate values.

Paleoclimate reconstructions

The three transfer functions (one each for Mean Annual Precipitation, Mean Annual Temperature, and Mean July Temperature) were applied to pollen assemblage data from sediment cores from three sites in the Great Plains region. The three sites selected—Moon Lake, Fox Lake, and Colo Marsh—are situated along a 650-km transect that extends from northwest to southeast. These sites were selected because they contain the best available pollen chronologies that cover most of the Holocene and collectively span a precipitation and temperature gradient that is said to have shifted spatially at different times throughout the Holocene (Williams *et al.* 2009). Original chronologies were retained as they meet modern standards based on AMS radiocarbon and ^{210}Pb methodologies. Fox Lake pollen data were from Commerford *et al.* (2016). Moon Lake pollen data (Laird *et al.* 1996) and Colo Marsh pollen data (Baker *et al.* 1990) were acquired from the Neotoma Paleoecology Database.

Results

Model performance

The models for mean annual precipitation (MAP), mean annual temperature (MAT), and mean July temperature (MJT) each performed well using the leave-one-out cross-validation method (Figure 4.3). The estimated MAP and actual MAP are strongly correlated ($r = 0.928$, $p = 0.002$). For the temperature variables—MAT and MJT—the estimated and actual values are also strongly correlated ($r = 0.891$ at $p = 0.001$ and $r = 0.897$ at $p = 0.005$, respectively), although slightly lower than for precipitation. The root mean square error (RMSE), R^2, bias estimates, and p-values for the first five components for each modeled climate variable are listed in Table 1. For

all three climate variables, two components were the optimal number of components to include in each model (selected by the lowest RMSE value where $p < 0.05$) (Table 1).

The three models also performed well in manual validation (Figure 4.4). The mean annual precipitation model performed slightly better when validated on extreme values ($r = 0.952$), compared to random values ($r = 0.937$), or cross-validation ($r = 0.928$). Mean July temperature also performed best with the extreme method of validation ($r = 0.969$), compared to random values ($r = 0.927$), or cross-validation ($r = 0.897$). Mean annual temperature performed better using extreme validation ($r = 0.966$) compared to cross-validation ($r = 0.891$), but worse in random validation ($r = 0.834$).

Paleoclimate reconstructions

Mean Annual Precipitation

The precipitation reconstructions for Colo Marsh, Moon Lake, and Fox Lake exhibit similar temporal trends with respect to relative high and low values, but major differences in absolute values (Figure 4.5). The greatest amount of annual precipitation (800 mm or greater) occurs around 8000 yr BP at all three sites. At Colo Marsh, this moist period is only exhibited in one sample (possibly due to lower temporal sampling resolution), while at Moon Lake it is manifested in approximately 2000 years of sharp fluctuations that repeatedly reach greater than 800 mm. In contrast, Fox Lake experiences this level of moisture around 8000 yr BP, but also at other times during the Holocene: at 9000 yr BP, 4000 yr BP, and present day.

At all three sites, the driest time of the record occurs between 6000 and 4000 yr BP. During this time, precipitation at Colo Marsh and Moon Lake falls below 400 mm, but at Fox Lake it barely falls below 600 mm. At Fox Lake, precipitation remains greater than 600 mm for most of its 9,200-year record, while at Moon Lake it remains lower than 600 mm for the entire

latter half of its record (from 6000 yr to present). Regardless, the 6000-4000 yr BP period is still a time of relatively low precipitation at Fox Lake, despite the fact that it received more precipitation than Colo Marsh or Moon Lake.

Mean Annual Temperature and Mean July Temperature

At each site, mean annual temperature and mean July temperature exhibit fluctuations of similar magnitude (Figure 4.5) throughout the records. One exception is Colo Marsh at the onset of the Holocene. There, mean July temperature increases more than mean annual temperature (4°C versus 1°C, respectively) during the period from 12,000 to 10,000 yr BP. However, between 9,000 and 8,000 yr BP, mean annual temperature abruptly increases from 2°C to 10°C. At Moon Lake, mean July temperature and mean annual temperature behave similarly to each other, but exhibit a different trend overall than at Colo Marsh. At Moon Lake, temperature (both mean annual temperature and mean July temperature) increases abruptly at 12,000 yr BP, but is followed by a period of level temperatures for about 2,000 years before temperatures increase abruptly again. The Fox Lake record extends from 9,200 years to present, and thus is not sufficiently long to capture the early Holocene period.

From 9,000 to 7,000 yr BP, all three sites experience similar temperature—approximately 8°C-10°C mean annual temperature, and 22°C-24°C mean July temperature (Figure 4.5). This changes at 7,000 yr BP, when temperatures at Moon Lake decrease relative to the other two sites and remain cooler until present. At approximately 4,000 to 3,500 yr BP, both Moon Lake and Fox Lake experience an increase in temperature relative to immediately preceding and following times. Similar warming is exhibited earlier at Colo Marsh—around 6,000 to 5,500 yr BP.

Discussion

Model performance

The pollen-climate transfer functions developed here perform as well as functions developed in biomes elsewhere in the world. Our root mean square errors of prediction (RMSEP) (MAP = 67 mm, MAT = 1.47°C, MJT = 1.14°C) (Table 4.1) are better than those from Northern China (MAP = 69 mm, MAT = 1.97°C, MWarmest = 2.44°C) (Li *et al.* 2007), and worse than Siberia for MAP (40 mm), but better for MJT (1.67°C) (Klemm *et al.* 2013). However, if a set of modern samples covers a smaller climate space, RMSEP may naturally be smaller. This could partially be the reason for Siberia's MAP being smaller than our MAP RMSEP. Our modern sample locations cover a large range in temperature (4°C-16°C) and precipitation (300 mm – 1000 mm), but particularly in precipitation (Figure 4.2). Furthermore, our high R^2 values indicate that our three models have robust predictive power (Table 4.1).

Although all three models are robust, MAP performs slightly better than MAT or MJT in cross-validation (Figure 4.3) and in prediction of temperature at randomly selected test sites (Figure 4.4). This seems to suggest that the relationship between pollen and precipitation is more direct than the relationship between pollen and temperature in this region—or at least more discernible in the pollen signatures. In the Great Plains, the structural vegetation transition from tallgrass prairie in the east to shortgrass prairie in the west is directly driven by changes in precipitation, with greater precipitation in the east supporting greater biomass production (Lane *et al.* 2000). Temperature, which exhibits a north-south gradient, has little to no influence on that structural transition, as both prairie types are sustained at warm and cool temperatures, albeit with different taxonomic compositions (Hayden 1998). Nonetheless, the relationship between

temperature (both MAT and MJT) and pollen is still strong, verifying significant compositional change in the pollen assemblages between the warmer and cooler sites.

In addition to temperature-driven changes in herbaceous vegetation composition along the north-south gradient, there could be important differences in the abundance and types of arboreal pollen present in the assemblages. Arboreal pollen types were found to be key indicators of prairie types in the southern Great Plains (McLauchlan *et al.* 2013). In China, *Betula* and *Pinus* pollen abundances have been shown to be crucial in differentiating among woodland, steppe, and grassland-woodland (Liu *et al.* 1999). Although the Great Plains region is a grassland, it has traditionally supported a variety of trees—particularly in riparian areas or areas of locally high effective soil moisture (West and Ruark 2004). Yet, these trees (e.g., *Pinus ponderosa, Juniperus virginiana, Quercus macrocarpa, Populus deltoides, Cornus drummondii, Maclura pomifera*) vary in abundance and type from north to south. More work is needed to assess the significance of these arboreal taxa in grassland pollen assemblages, as their abundances could be key indicators of climate or grassland vegetation type.

The temperature models are better at predicting temperatures for surface sample sites found in extreme climate space than for randomly selected sites. In this study, a single particular site in the Black Hills of South Dakota skews the models' overall performance (Figure 4.4). This site has an actual MAT of 4°C, but the model predicts it to be less than 0°C. This suggests that there may be a wide range of pollen "signatures" at the cold end of our temperature space, given that this site is one of the coolest of our modern sample set. This could be remedied by sampling the cooler temperature areas in greater detail to get a fuller representation of grassland pollen assemblages found there.

Aside from the sample mentioned above, nine other samples are from the Black Hills region of western South Dakota. The Black Hills is a 21,820 km^2 woodland region within the shortgrass prairie portion of Great Plains, and locally dominated by ponderosa pine (*Pinus ponderosa).* As such, it experiences cooler temperatures and greater precipitation than the surrounding grassland. We considered excluding these sites from our models, because locally they are not within grassland vegetation. However, they capture important natural variation in vegetation and climate found at the regional scale, so excluding them would provide an unrealistic representation of the Great Plains region as a whole. Additionally, these surface samples capture the structure and function of a woodland biome closely related to nearby grasslands—something that is important to include when reconstructing climate throughout the Holocene from lacustrine cores in the region. The climate space represented by these sites facilitates more accurate reconstruction of cooler time periods.

To our knowledge, the modern pollen sample set used in this study represents the most comprehensive climate conditions from the Great Plains, with a broad range in precipitation and temperature covering a variety of grassland types. However, some gaps remain. In particular, the modern climate space between 600-800 mm annual precipitation and 10-12°C mean annual temperature is not well-represented by our dataset (Figure 4.2). It is possible that the relative lack of modern pollen samples from this climate space limits our models' ability to reconstruct precipitation and temperature within that range, although one strength of the WAPLS transfer function is its capacity to predict climate outside the climate space covered by the modern samples. Sampling this space would be quite difficult, because it is geographically located in eastern Nebraska where a majority of the original grassland is now cultivated. As a result, fewer ponds exist relative to the northern Great Plains, which have abundant natural basins created by

glaciers, or the Great Plains of Kansas where ranching activities have prompted the creation of human-made ponds for watering cattle. Nonetheless, it is important that future efforts be directed toward obtaining modern pollen samples from this climate space—either from the few available ponds or marshes, or through the placement of traps—in order to facilitate accurate reconstruction of that space during the past.

Paleoclimate reconstructions

Mid-Holocene climate anomaly

At all three sites—Colo Marsh, Fox Lake, and Moon Lake—the lowest precipitation occurred around 5,000 yr BP. However, it was only coupled with high temperatures at Colo Marsh (Figure 4.5). This supports the idea that the aridity of the mid-Holocene climate anomaly was driven by low precipitation rather than high temperatures. High aridity in the mid-Holocene has been noted at other sites in the Great Plains, including in the Nebraska Sand Hills (Schmieder *et al.* 2013) where it occurred earlier—between 10,000 and 6,000 yr BP. Moisture began to increase in the Nebraska Sand Hills around 6,000 BP. Although precipitation at the three sites we examined also exhibited a brief period of high precipitation at 6,000 yr BP, it was not sustained, and precipitation drastically decreased to the lowest levels of the records by 5,000 yr BP.

Other work in the region has indicated that the arid mid-Holocene was punctuated by periods of increased moisture. At Kettle Lake, North Dakota, 400 km northwest of Moon Lake, high *Ambrosia* pollen during the multi-decadal droughts of the mid-Holocene (inferred from quartz and aragonite data) suggested annual periods of greater precipitation (Grimm *et al.* 2011). Our reconstruction of Moon Lake precipitation may be showing something similar. At Moon Lake, precipitation fluctuated repeatedly between 500 mm and 800 mm from 9,000 yr BP to

7,500 yr BP, while temperature fluctuated at least 4°C in both MAT and MJT during that same time (Figure 4.5). These fluctuations are not present in the Fox Lake or Colo Marsh records, potentially because of the lower temporal sampling resolution of those records.

Our reconstruction of Moon Lake precipitation also corresponds strongly with previously established levels of diatom-inferred salinity (Laird *et al.* 1996). The diatom record specifically demonstrates that salinity was greatest at Moon Lake between 7,300 to 4,700 yr BP, indicating drier conditions overall (Laird *et al.* 1996). Our pollen-based reconstructions (Figure 4.5) show that precipitation was lowest between 7,000 and 4,700 yr BP, with a brief increase at approximately 5,800 yr BP. This 5,800 yr BP increase in precipitation is not noted in the diatom record (Laird *et al.* 1996), which likely indicates that precipitation was not sufficiently high to cause Moon Lake to transition from a closed system to an open system. Additionally, high precipitation was also coupled with high temperatures at this time (Figure 4.5), potentially counteracting the increase in precipitation, and leading to minimal change in lake level or salinity. Yet, there was a change in the pollen assemblage composition, confirming the sensitivity of pollen assemblages to some driver at this time—most likely precipitation.

Even at its lowest precipitation levels, Fox Lake still receives more reconstructed precipitation than either Colo Marsh or Moon Lake. Fox Lake also exhibits a smaller range in precipitation throughout its record than the other two sites exhibit within the same time period (300 mm range compared to nearly 500 mm range). At present, Colo Marsh receives the highest modern MAP of the three sites with 908 mm compared with 775 mm at Fox Lake and 532 cm at Moon Lake. Our paleoclimate reconstructions indicate that these relative precipitation conditions between Fox Lake and Colo Marsh may have developed within recent centuries. However, their

collective greater precipitation conditions compared to Moon Lake may have been in place for millennia.

Previous work at Fox Lake found vegetation diversity to be resilient throughout the Holocene, including the mid-Holocene (Commerford *et al.* 2016). The high precipitation levels and relatively low range in precipitation noted here in our reconstruction of Fox Lake are likely a key reason for that resilient diversity. In addition, the temperature record at Fox Lake varies less than the other two sites, thus allowing for consistent effective moisture. Numerous diversity metrics have been found to increase significantly with increased precipitation in grasslands in Mongolia (Zhang *et al.* 2014). While pollen diversity is not always a direct reflection of plant diversity (Goring *et al.* 2013), most studies comparing modern pollen richness with modern plant richness have revealed strong, positive relationships (Birks *et al.* 2016).

Temporal climate asymmetry

It is clear from the Colo Marsh record that early Holocene warming (from 12,000 to 8,000 yr BP) was expressed more through warmer July temperatures than through warmer annual temperatures. That dynamic shifted between 8,500 and 8,000 yr BP, when MAT increased abruptly after increasing only slightly during the past 4,000 yrs compared to MJT. The timing of this change is consistent with the 8,200 yr BP event noted in the Greenland ice cores (Alley and Ágústsdóttir 2005) and in other lacustrine records of North America (Shuman *et al.* 2002), when the Laurentide ice sheet collapsed and climate shifted from being ice-sheet-and-insolation controlled to being mainly insolation controlled. To our knowledge, this difference between summer and annual temperatures leading up to the 8,200 yr BP event has not previously been discernible in climate reconstructions in the Great Plains, including other pollen-based reconstructions. Many sites further west on the Great Plains did not even experience the 8,200 yr

BP event, based on their lacustrine records. For example, Kettle Lake, North Dakota (Grimm *et al.* 2011) experienced a similar shift at 9,250 yr BP, but it was of smaller magnitude than the 8,200 yr BP event noted at other sites . At Moon Lake, the sharpest change in precipitation and temperature occurred around 8,500 yr BP but was of longer duration and preceded numerous rapid fluctuations (Figure 4.5).

Previous work in this region has described the vegetation transitions into the mid-Holocene and out of the mid-Holocene as being asymmetric, with an abrupt shift toward aridity between the early and mid-Holocene, and a gradual increase in moisture entering the late Holocene (Umbanhowar *et al.* 2006; Nelson and Hu 2008). In pollen records, this asymmetry has mainly been manifested as an abrupt decrease in woody taxa entering the mid-Holocene, and a gradual increase in woody taxa entering the late Holocene (Baker *et al.* 1992; Umbanhowar *et al.* 2006; Commerford *et al.* 2016). However, the precipitation and temperature reconstructions presented here indicate that climatically, these transitions were more complicated. While Colo Marsh experienced a gradual increase in precipitation throughout much of the late Holocene, Moon Lake did not. In fact, precipitation at Moon Lake decreased substantially at 3,000 yr BP and remained low until present (within the last 100 years). Temperature followed a similar temporal pattern and remained cool until present, possibly helping effective moisture remain higher despite low precipitation. Further, at Fox Lake, precipitation decreased to peak aridity levels twice before beginning to increase steadily at approximately 1800 yr BP. Overall, although the gradual increase in woody pollen taxa at these sites seems to indicate a gradual transition between mid- and late-Holocene, the climate reconstructions based on the overall pollen assemblages suggests a more complicated transition. This disjoint stresses the need to

fully evaluate the presence and abundance of woody pollen taxa in pollen assemblages that are predominantly herbaceous.

Conclusions

Here, we have presented transfer functions for three climate variables (mean annual precipitation, mean annual temperature, and mean July temperature) based on a new set of modern pollen samples from the Great Plains of North America. All three functions perform well in cross-validation and in manual validation using random testing sites and testing sites from extreme climate space. By applying these functions to fossil pollen from sediment cores from Fox Lake (Minnesota), Moon Lake (North Dakota), and Colo Marsh (Iowa), we have reconstructed Holocene temperature and precipitation in the northern Great Plains region. While the three sites show similar temporal fluctuations in temperature and precipitation, the magnitude of these fluctuations varied. Fox Lake and Colo Marsh remained warmer than Moon Lake for most of the Holocene, and generally received more precipitation. The driest time of the Holocene occurred around 5,000 yr BP at all three sites.

A gradual increase in woody vegetation entering the late-Holocene has been exhibited in vegetation reconstructions from pollen at these sites (and others in the region, e.g., Umbanhowar *et al.* 2006); however, the climate reconstructions that we present here demonstrate that precipitation did not increase in the same manner. At Fox Lake, precipitation decreased to near lowest levels (600 mm) at 3,000 yr BP and 1,000 yr BP before increasing toward present. At Moon Lake, precipitation decreased to near lowest levels (400 mm) at 2,000 yr BP and remained low until recent centuries. Nonetheless, woody pollen taxa increased in all records throughout the Holocene, suggesting that their increase may not have been solely climate-driven.

Alternatively, local scale differences in fire, human activity, herbivory, or other factors could have caused vegetation to respond differently at each site despite similar climate. Future efforts must be directed toward evaluating the role of woody vegetation in North American grasslands throughout the Holocene and specifically assessing its presence in grassland pollen records.

Acknowledgements

We gratefully acknowledge the numerous landowners who allowed access to their property. Without them, we would not have been able to obtain many of the modern pollen samples. We thank Simon Goring for helpful discussion. JC and CM were funded by NSF BCS-0955225 to KM and GK-12 fellowships (NSF DGE-0841414 to C. Ferguson). JC was also funded by a Doctoral Dissertation Research Improvement grant (NSF DGE-1558228 to KM and JC).

References

Alley, R. B., and A. M. Ágústsdóttir, 2005: The 8k event: cause and consequences of a major Holocene abrupt climate change. *Quat. Sci. Rev.*, **24**, 1123–1149.

Baker, R. G., C. A. Chumbley, P. M. Witinok, and H. K. Kim, 1990: Holocene vegetational changes in eastern Iowa. *J. Iowa Acad. Sci.*, **97**, 167–177.

Baker, R. G., L. J. Maher, C. A. Chumbley, and K. L. Vanzant, 1992: Patterns of Holocene Environmental-Change in the Midwestern United-States. *Quat. Res.*, **37**, 379–389.

Bartlein, P. J., T. Webb, and E. Fleri, 1984: Holocene Climatic-Change in the Northern Midwest - Pollen-Derived Estimates. *Quat. Res.*, **22**, 361–374.

Bigler, C., and R. I. Hall, Diatoms as indicators of climatic and limnological change in Swedish Lapland: a 100-lake calibration set and its validation for paleoecological reconstructions. *J. Paleolimnol.*, **27**, 97–115.

Birks, H. J. B., 1995: No Title. *Statistical modeling of Quaternary science data.*, D. Edwards, D. Maddy, and J.S. Brew, Eds., Quaternary Research Association, 161–254.

Birks, H. J. B., V. A. Felde, A. E. Bjune, J.-A. Grytnes, H. Seppä, and T. Giesecke, 2016: Does pollen-assemblage richness reflect floristic richness? A review of recent developments and future challenges. *Rev. Palaeobot. Palynol.*, doi:10.1016/j.revpalbo.2015.12.011.

Bonnefille, R., and F. Chalie, 2000: Pollen-inferred precipitation time-series from equatorial mountains, Africa, the last 40 kyr BP. *Glob. Planet. Change*, **26**, 25–50.

ter Braak, C. J. F., 1995: Non-linear methods for multivariate statistical calibration and their use in palaeoecology: a comparison of inverse (k-nearest neighbours, partial least squares and weighted averaging partial least squares) and classical approaches. *Chemom. Intell. Lab. Syst.*, **28**, 165–180.

ter Braak, C. J. F., and S. Juggins, 1993: Weighted averaging partial least squares regression (WA-PLS): an improved method for reconstructing environmental variables from species assemblages. *Hydrobiologia*, **269**, 485–502.

ter Braak, C. J. F., and P. Smilauer, 2012: *Canoco reference manual and user's guide: software for ordination, version 5.0*. Microcomputer Power, Ithaca, NY.

Cheddadi, R., H. Lamb, J. Guiot, and S. van der Kaars, 1998: Holocene climatic change in Morocco: a quantitative reconstruction from pollen data. *Clim. Dyn.*, **14**, 883–890.

Commerford, J. L., K. K. McLauchlan, and S. Sugita, 2013: Calibrating vegetation cover and grassland pollen assemblages in the Flint Hills of Kansas, USA. *Am. J. Plant Sci.*, **4**, 1–10.

Commerford, J. L., B. Leys, J. R. Mueller, and K. K. McLauchlan, 2016: Great Plains vegetation dynamics in response to fire and climatic fluctuations during the Holocene at Fox Lake, Minnesota (USA). *The Holocene*, **26**, 302–313.

Cook, B. I., J. E. Smerdon, R. Seager, and E. R. Cook, 2014: Pan-Continental Droughts in North America over the Last Millennium. *J. Clim.*, **27**, 383–397.

Cook, E. R., R. Seager, R. R. Heim Jr., R. S. Vose, C. Herweijer, and C. Woodhouse, 2010: Megadroughts in North America: placing IPCC projections of hydroclimatic change in a long-term palaeoclimate context. *J. Quat. Sci.*, **25**, 48–61.

Faegri, K., and J. Iversen, 1989: *Textbook of pollen analysis*. Wiley, Chichester.

Goring, S., T. Lacourse, M. G. Pellatt, and R. W. Mathewes, 2013: Pollen assemblage richness does not reflect regional plant species richness: a cautionary tale. *J. Ecol.*, **101**, 1137–1145.

Grimm, E. C., 2016: Personal Communication.

Grimm, E. C., J. J. Donovan, and K. J. Brown, 2011: A high-resolution record of climate variability and landscape response from Kettle Lake, northern Great Plains, North America.

Quat. Sci. Rev., **30**, 2626–2650.

Hayden, B. P., and others, 1998: Regional climate and the distribution of tallgrass prairie. *Grassl. Dyn. long-term Ecol. Res. tallgrass prairie. Oxford Univ. Press. New York*, 19–34.

Hill, M. O., and H. Gauch, 1980: Detrended correspondence analysis: an improved ordination technique. *Plant Ecol.*, **42**, 47–58.

Jackson, S. T., and J. W. Williams, 2004: Modern analogs in Quaternary paleoecology: Here today, gone yesterday, gone tomorrow? *Annu. Rev. Earth Planet. Sci.*, **32**, 495–537.

Juggins, S., 2015: Rioja: Analysis of Quaternary Science Data. https://cran.r-project.org/web/packages/rioja/rioja.pdf.

Klemm, J., U. Herzschuh, M. F. J. Pisaric, R. J. Telford, B. Heim, and L. A. Pestryakova, 2013: A pollen-climate transfer function from the tundra and taiga vegetation in Arctic Siberia and its applicability to a Holocene record. *Palaeogeogr. Palaeoclimatol. Palaeoecol.*, **386**, 702–713.

Laird, K. R., S. C. Fritz, E. C. Grimm, and P. G. Mueller, 1996: Century scale paleoclimatic reconstruction from Moon Lake, a closed-basin lake in the northern Great Plains. *Limnol. Oceanogr.*, **41**, 890–902.

Lane, D., D. Coffin, and W. Lauenroth, 2000: Changes in grassland canopy structure across a precipitation gradient. *J. Veg. Sci.*, **11**, 359–368.

Li, Y., Q. Xu, J. Liu, X. Yang, and T. Nakagawa, 2007: A transfer-function model developed from an extensive surface-pollen data set in northern China and its potential for paleoclimate reconstructions. *The Holocene*, **17**, 897–905.

Liu, H., H. Cui, R. Pott, and M. Speier, 1999: The surface pollen of the woodland–steppe ecotone in southeastern Inner Mongolia, China. *Rev. Palaeobot. Palynol.*, **105**, 237–250.

Mauri, A., B. A. S. Davis, P. M. Collins, and J. O. Kaplan, 2015: The climate of Europe during the Holocene: A gridded pollen-based reconstruction and its multi-proxy evaluation. *Quat. Sci. Rev.*, **112**, 109–127.

McAndrews, J. H., A. A. Berti, and G. Norris, 1973: *Key to the Quaternary Pollen and Spores of the Great Lakes Region*. Royal Ontario Museum, Toronto, Ontario,.

McLauchlan, K. K., J. L. Commerford, and C. J. Morris, 2013: Tallgrass prairie pollen assemblages in mid-continental North America. *Veg. Hist. Archaeobot.*, **22**, 171–183.

Michels, A., K. R. Laird, S. E. Wilson, D. Thomson, P. R. Leavitt, R. J. Oglesby, and B. F. Cumming, 2007: Multidecadal to millenial-scale shifts in drought conditions on the Canadian prairies over the past six millenia: implications for future drought assessment. *Glob. Chang. Biol.*, **13**, 1295–1307.

Nelson, D. M., and F. S. Hu, 2008: Patterns and drivers of Holocene vegetational change near the prairie-forest ecotone in Minnesota: revisiting McAndrews' transect. *New Phytol.*, **179**, 449–459.

Overpeck, J. T., T. Webb, and I. C. Prentice, 1985: Quantitative Interpretation of Fossil Pollen Spectra - Dissimilarity Coefficients and the Method of Modern Analogs. *Quat. Res.*, **23**, 87-108.

PRISM Climate Group, 2016: 30-Year normals of precipitation and temperature. http://prism.oregonstate.edu (Accessed April 4, 2016).

R Core Team, 2013: R: A language and environment for statistical computing. http://www.r-project.org/.

Schmieder, J., and Coauthors, 2011: A regional-scale climate reconstruction of the last 4000 years from lakes in the Nebraska Sand Hills, USA. *Quat. Sci. Rev.*, **30**, 1797–1812.

Schmieder, J., S. C. Fritz, E. C. Grimm, K. C. Jacobs, K. J. Brown, J. B. Swinehart, and S. C. Porter, 2013: Holocene variability in hydrology, vegetation, fire, and eolian activity in the Nebraska Sand Hills, USA. *Holocene*, **23**, 515–527.

Seppa, H., H. J. B. Birks, A. Odland, A. Poska, and S. Veski, 2004: A modern pollen-climate calibration set from northern Europe: Developing and testing a tool for palaeoclimatological reconstructions. *J. Biogeogr.*, **31**, 251–267.

Shuman, B., P. Bartlein, N. Logar, P. Newby, and T. Webb, 2002: Parallel climate and vegetation responses to the early Holocene collapse of the Laurentide Ice Sheet. *Quat. Sci. Rev.*, **21**, 1793–1805.

Telford, R. J., and H. J. B. Birks, 2005: The secret assumption of transfer functions: Problems with spatial autocorrelation in evaluating model performance. *Quat. Sci. Rev.*, **24**, 2173–2179.

Umbanhowar, C. E., P. Camill, C. E. Geiss, and R. Teed, 2006: Asymmetric vegetation responses to mid-Holocene aridity at the prairie–forest ecotone in south-central Minnesota. *Quat. Res.*, **66**, 53–66.

Umbanhowar, C. E., and Coauthors, 2009: Regional fire history based on charcoal analysis of sediments from nine lakes in western Mongolia. *Holocene*, **19**, 611–624.

Viau, A. E., and K. Gajewski, 2009: Reconstructing Millennial-Scale, Regional Paleoclimates of Boreal Canada during the Holocene. *J. Clim.*, **22**, 316–326,328–330.

Viau, A. E., M. Ladd, and K. Gajewski, 2012: The climate of North America during the past 2000years reconstructed from pollen data. *Glob. Planet. Change*, **84-85**, 75–83.

Wahl, E. R., H. F. Diaz, and C. Ohlwein, 2012: A pollen-based reconstruction of summer temperature in central North America and implications for circulation patterns during

medieval times. *Glob. Planet. Change*, **84-85**, 66–74.

West, E., and G. Ruark, 2004: Historical evidence of riparian forests in the Great Plains and how that knowledge can aid with restoration and management. *J. Soil Water Conserv.*, **59**, 104A – 110A.

Williams, J. W., and B. Shuman, 2008: Obtaining accurate and precise environmental reconstructions from the modern analog technique and North American surface pollen dataset. *Quat. Sci. Rev.*, **27**, 669–687.

Williams, J. W., B. Shuman, and P. J. Bartlein, 2009: Rapid responses of the prairie-forest ecotone to early Holocene aridity in mid-continental North America. *Glob. Planet. Change*, **66**, 195–207.

Xu, Q., J. Xiao, Y. Li, F. Tian, and T. Nakagawa, 2010: Pollen-based quantitative reconstruction of Holocene climate changes in the Daihai lake area, Inner Mongolia, China. *J. Clim.*, **23**, 2856–2868.

Zhang, Q., and Coauthors, 2014: Alpha, beta and gamma diversity differ in response to precipitation in the Inner Mongolia Grassland. *PLoS One*, **9**, doi:10.1371/journal.pone.0093518.

Table 4.1: Prediction error estimates for each transfer function calculated by leave-one-out cross-validation. Root mean square errors of prediction (RMSEP), adjusted R^2 between predicted and actual values (R^2), average bias (Avg-Bias) and maximum bias (Max-bias) of parameter estimates are listed. P-values are listed for the first five components of each function.

Variable	Component	RMSEP	R^2	Avg-Bias	Max-Bias	*p*
Mean Annual Precipitation (mm) (MAP)	Comp01	80.45	0.80	0.29	109.71	0.001
	Comp02	67.49	0.86	0.30	95.20	0.002
	Comp03	62.65	0.88	-0.92	102.72	0.058
	Comp04	61.14	0.89	-2.52	104.42	0.212
	Comp05	63.38	0.88	-0.94	109.75	0.903
Mean Annual Temperature (°C) (MAT)	Comp01	1.77	0.70	0.02	2.19	0.001
	Comp02	1.47	0.79	0.06	1.67	0.001
	Comp03	1.42	0.81	0.06	1.11	0.389
	Comp04	1.44	0.81	0.09	1.06	0.632
	Comp05	1.44	0.81	0.09	0.93	0.433
Mean July Temperature (°C) (warmest month) (MJT)	Comp01	1.27	0.76	0.01	1.65	0.001
	Comp02	1.14	0.80	0.03	2.16	0.005
	Comp03	1.13	0.81	0.05	1.74	0.431
	Comp04	1.17	0.80	0.07	1.44	0.84
	Comp05	1.14	0.82	0.04	1.43	0.215

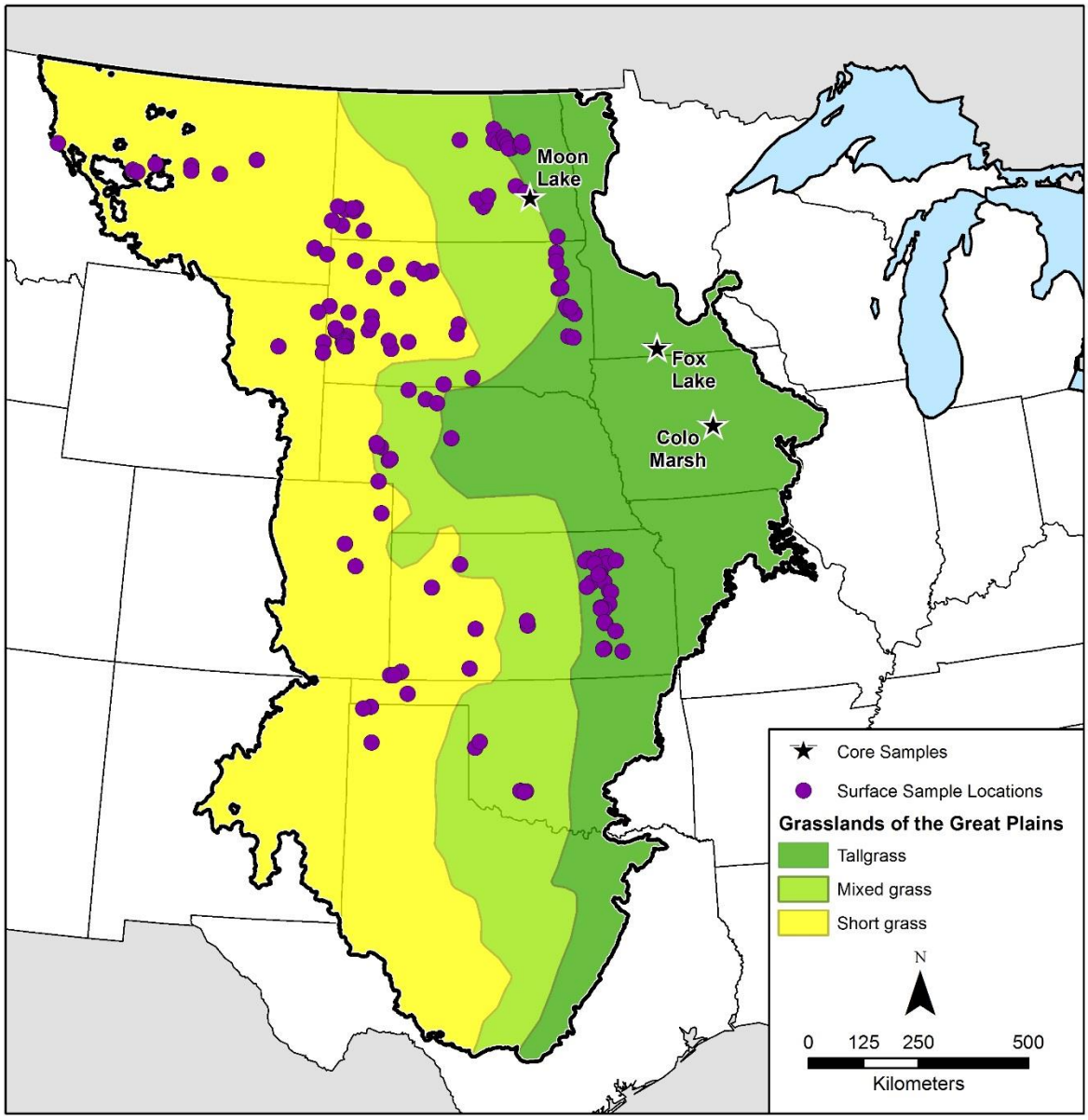

Figure 4.1: Pollen surface samples used to create the transfer functions (purple) and fossil pollen samples to which the functions were applied (black). Great Plains grassland distributions generally follow Illinois State Museum.

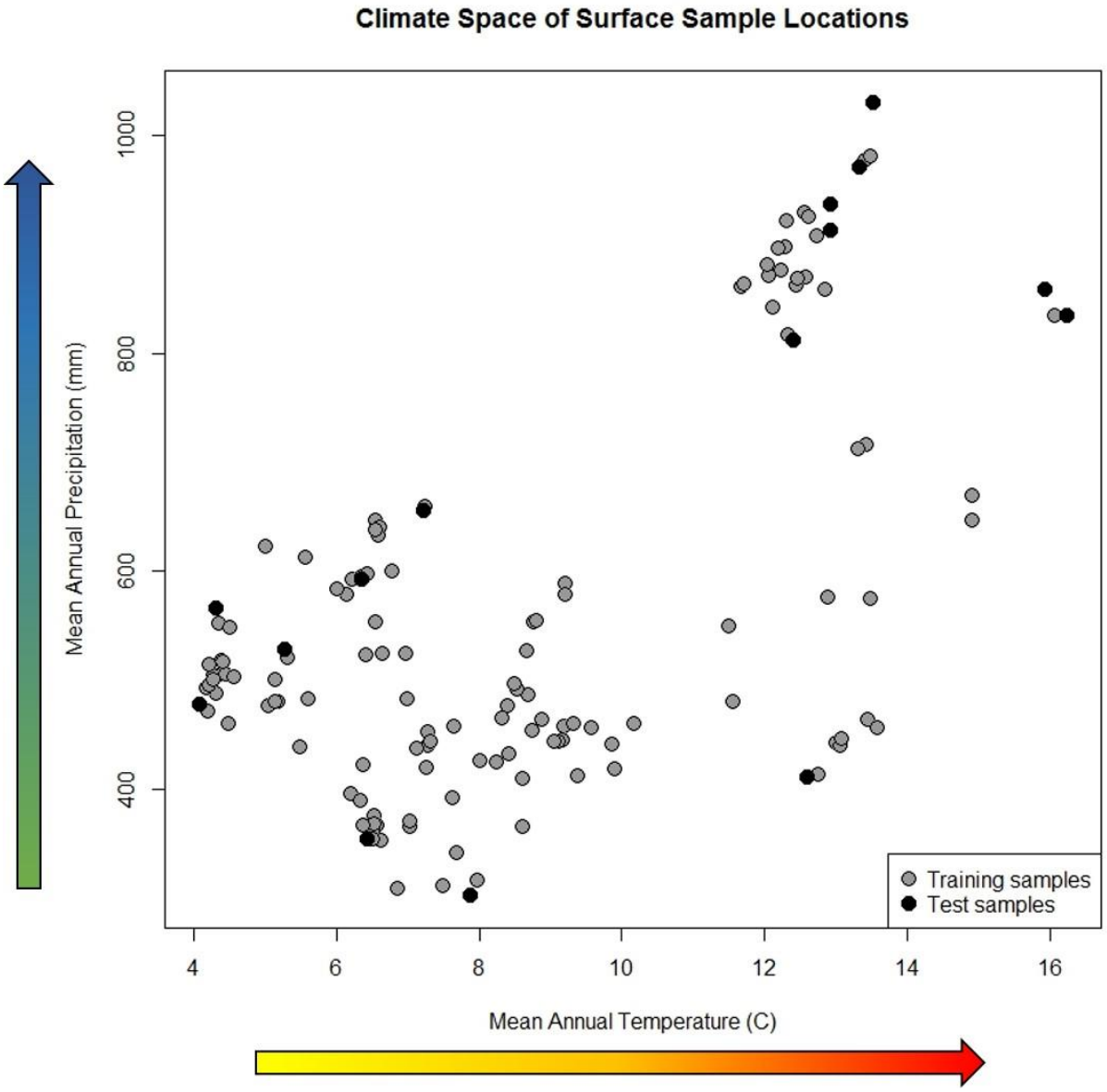

Figure 4.2: Mean Annual Precipitation (mm) and Mean Annual Temperature (°C) of the 141 pollen surface samples. Black dots are the test samples and gray dots are the training samples used in manual validation of extreme climate space sites.

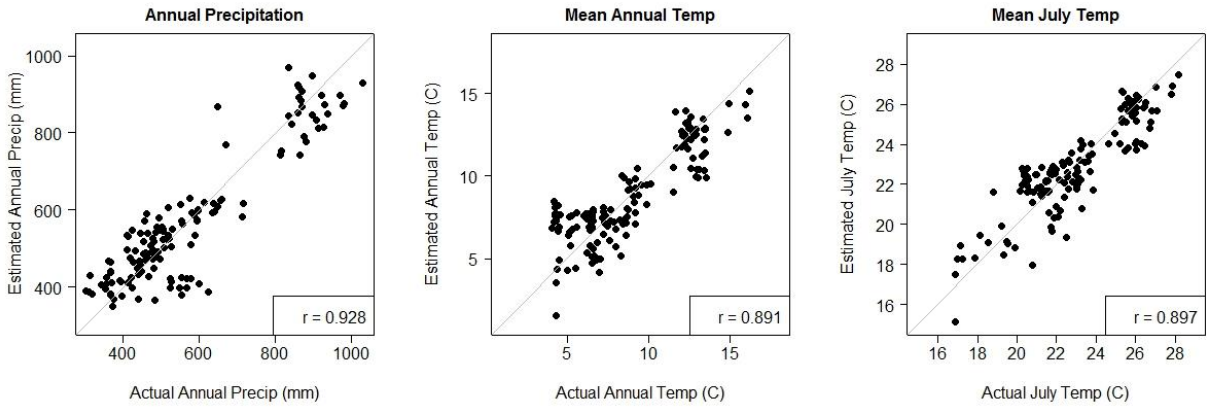

Figure 4.3: Cross-validation of Mean Annual Precipitation, Mean Annual Temperature, and Mean July Temperature functions using leave-one-out jackknifing. Actual values are on the x-axis and estimated values (predicted by the functions) are on the y-axis.

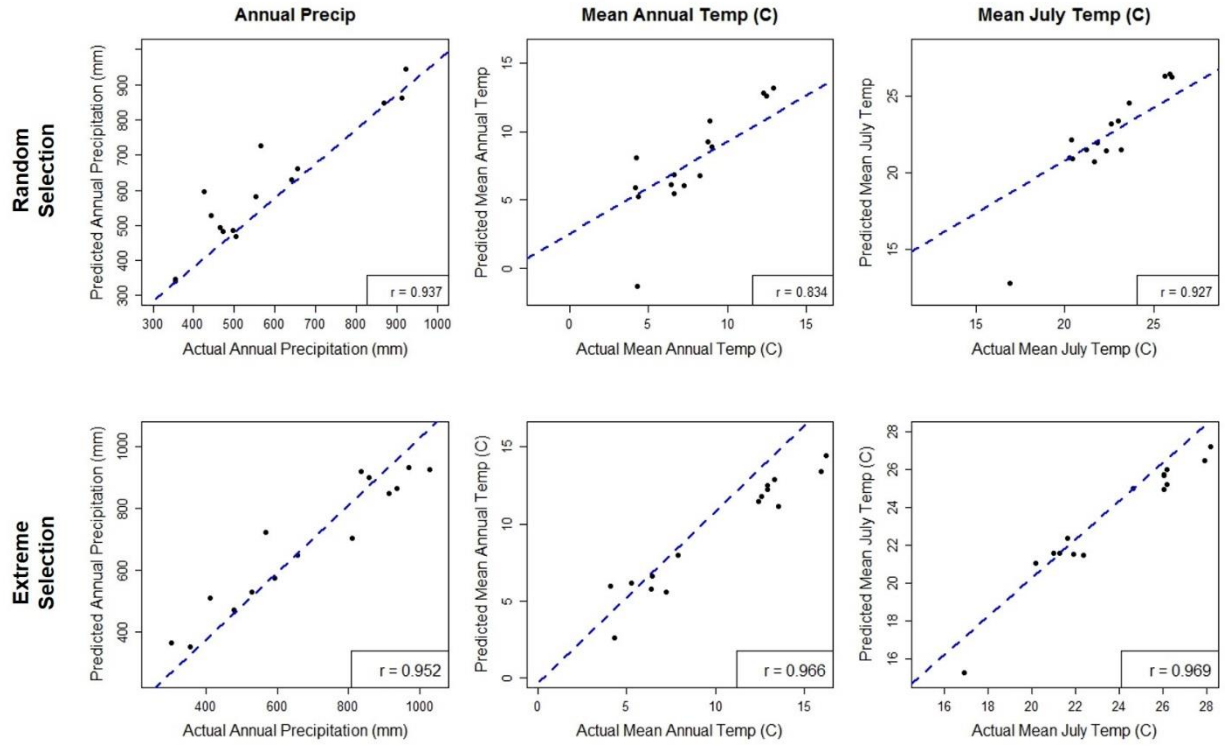

Figure 4.4: Manual validation of Mean Annual Precipitation, Mean Annual Temperature, and Mean July Temperature functions. The top panel shows the results of validation using 126 randomly selected sites to train the functions, applied to the remaining 15 sites. The bottom panel shows the results of validation using deliberately selected test sites to include extreme values of each of the three climate parameters. Actual values are on the x-axis and estimated values (predicted by the functions) are on the y-axis.

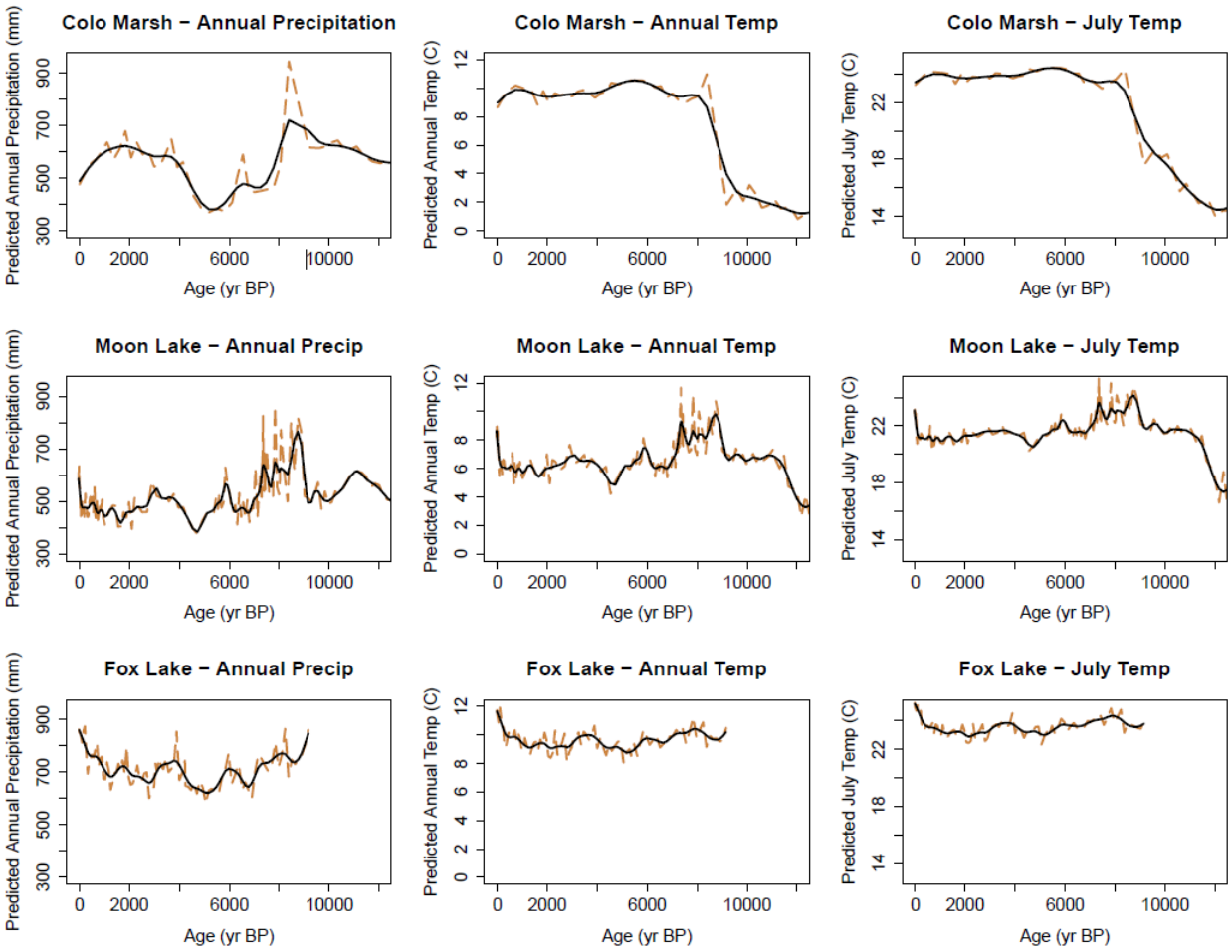

Figure 4.5: Pollen-based climate reconstructions of Colo Marsh, Iowa (top row), Moon Lake, North Dakota (middle row), and Fox Lake, Minnesota (bottom row) using the transfer functions developed in this study. Age (yr BP) is on the x-axis and predicted climate values are on the y-axis. Dashed orange lines are the raw reconstructed values and black lines are smoothed values fitted with a spline (smoothing parameter of 0.5).

Chapter 5 - Conclusion

This dissertation sought to investigate changes in North American grassland vegetation within the context of climate, fire, herbivory, and topography—key drivers of grassland structure and function. Like many ecosystems, North American grasslands face an uncertain future because of impending climate change. This uncertainty is amplified in grasslands because they are currently spatially restricted. Because the drivers of grassland vegetation operate at inherently different spatial and temporal scales, a comprehensive understanding of grassland response to drivers must span space and time. The three chapters presented here investigate North American grassland ecosystems throughout the Holocene with respect to their composition and diversity, and evaluate how grasslands and their drivers are represented in pollen, a key proxy for interpreting vegetation in the past. This work takes a novel approach to connect the fields of paleoecology and geography by using biogeography as a framework to integrate modern and fossil pollen data for interpreting current and past grassland ecosystem function. This work is also unique because it examines modern grasslands through pollen assemblages across broad and fine spatial and temporal scales (Figure 5.1).

Chapter 2, *Great Plains vegetation dynamics in response to fire and climatic fluctuations during the Holocene at Fox Lake, Minnesota (USA)* reconstructs vegetation composition and diversity, fire activity and fuel sources, and erosion activity throughout the Holocene using pollen, charcoal, magnetic susceptibility, and elemental concentration data from a lacustrine sediment core. Erosion activity increases as vegetation transitions from woodland to grassland in the late Holocene. Fire activity remains constant throughout the Holocene and woody fuel sources dominate, despite the indications from the pollen record that this site was a grassland. Vegetation diversity—in terms of richness and turnover—also remains constant. A quantitative

reconstruction of climate at this site would help give more context to the apparent resilience of vegetation.

Chapter 3, *High dissimilarity within a multi-year annual record of pollen assemblages from a North American tallgrass prairie,* evaluates the influence of fire, grazing, and topography on four summative metrics of pollen assemblage composition and diversity (non-arboreal pollen percentage, Shannon index, beta-diversity, and *Ambrosia:Artemisia* ratio) from a set of 28 traps sampled annually for four years. It also quantifies compositional dissimilarity between traps, and within a given trap across the four year period. Fire, grazing, and topography have some influence on the summative metrics, but their influence varies. Significant annual differences are noted in three of the summative metrics: non-arboreal pollen percentage, Shannon index, and beta-diversity, but not in *Ambrosia:Artemisia* ratio. Compositional dissimilarity is higher across all the traps than at a single trap across the four years. It is also higher than in forested biomes, suggesting that defining a pollen assemblage as "grassland" may be more difficult than previously thought.

Chapter 4, Mid-Holocene aridity quantified from pollen in the Great Plains of North America, quantifies the relationship between modern pollen assemblages and climate in North American grasslands. Transfer functions are presented for mean annual precipitation, mean annual temperature, and mean July temperature. The three functions perform very well in cross-validation using leave-one-out jackknifing ($r = 0.89$ or greater), and in manual validation. The functions are then applied to pollen data from three lacustrine cores: Fox Lake, MN; Colo Marsh, IA; and Moon Lake, ND to reconstruct Holocene climate. The lowest precipitation occurred at 5,000 yr BP at all three sites. Temperature varied among the three sites, but remained generally high at Colo Marsh and Fox Lake throughout the last 8,000 yr BP compared to Moon Lake.

Collectively, the findings of these chapters are a major step forward for understanding North American grassland biogeography during the Holocene. Paleorecords allow us to understand how vegetation responded to past climate changes, which can provide a context for predicting vegetation response to future climate changes. This dissertation demonstrates that grassland vegetation diversity—as inferred through consistent pollen richness and low turnover at Fox Lake—was resilient to the climate changes of the Holocene. The resilience of vegetation at Fox Lake offers hope for the grassland biome in light of future climate change scenarios that predict decreased effective moisture (IPCC 2014). However, the cause of this resilience remains in question because the Great Plains regionally experienced numerous decadal to millennial-scale megadroughts. Was Fox Lake vegetation resilient to megadroughts because climate conditions were truly less dry compared to other sites in the region, or did local site factors cause the vegetation at Fox Lake to be more resilient in the face of megadroughts? The precipitation and temperature reconstructions presented in Chapter 4 help provide some climatic context, but are also based on pollen data; thus, this question is a limitation of this work. This question could be answered in future research by reconstructing precipitation and temperature at more sites to interpolate regional (Great Plains-wide) trends over time, or by examining additional independent proxies for climate in the Fox Lake record.

This work also highlights the importance of spatial and temporal scale in interpreting paleoecological data. The pollen assemblages examined from the Tauber traps at the Konza prairie represent the finest spatial and temporal resolution possible for pollen assemblage data. Thus, they are not directly comparable to pollen assemblages from lacustrine basins, which collect pollen from a broader area and do not facilitate annual-scale sampling. However, the small spatial area represented by the Tauber traps actually facilitate quantification of the

influence of fire activity, grazing, and topography on pollen assemblage composition and diversity. It would be difficult to effectively measure these drivers across a larger spatial area, which might not include the variation in fire and grazing treatments needed to effectively assess functional relationships. Additionally, each pollen assemblage from Konza represents exactly one year, which allowed assessment of interannual differences in precipitation for their influence on pollen assemblage composition and diversity.

Another theme that emerges from this research is the need to fully examine what arboreal pollen signifies in grasslands. Often, grassland periods are often roughly pinpointed in lacustrine records by high abundances of non-arboreal pollen and relatively lower abundances of arboreal pollen. This dissertation demonstrates that arboreal pollen can comprise a significant proportion of grassland pollen assemblages at all spatial and temporal scales. For example, the periods with the highest abundance of non-arboreal pollen at Fox Lake still had arboreal pollen that comprised approximately 20% of the overall assemblage (Chapter 2). Additionally, arboreal pollen was present in large amounts at Konza (between 25% and 50% of the assemblage, on average), and this amount varied significantly from year to year in conjunction with precipitation (Chapter 3). Across the Great Plains, arboreal pollen varied both in abundance and type, corresponding with differences in precipitation and temperature (Chapter 4). Thus, it is important to include arboreal pollen in analyses when searching for quantitative modern analogs or building transfer functions with climate. The amount and type of arboreal vegetation in grasslands is indeed sensitive to changes in climate, and this sensitivity is exhibited in pollen assemblages. Given that arboreal vegetation plays a functionally different role within grassland ecosystems than within forested ecosystems, it would be helpful to characterize this in pollen assemblages to help distinguish between grassland types. Ratios of key non-arboreal pollen taxa have been shown to distinguish

between grassland types (e.g. Morris 2013; Zhao *et al.* 2012). Arboreal pollen should be examined to identify key abundance thresholds between grassland types.

Through this research, I have identified several next steps to better understand changes in North American grassland ecosystems throughout the Holocene. First, pollen diversity should be examined across multiple lacustrine cores in the Great Plains region to determine if there is any regional signal in vegetation response to the climatic changes of the Holocene. To be most informative, this diversity should be assessed using multiple metrics, including turnover, richness, and Shannon index. Similarly, arboreal pollen should be characterized and quantified across the region to determine whether threshold abundances of certain taxa are indicative of a specific climate or grassland type. Second, precipitation and temperature need to be reconstructed at more sites across the region. This goal can be effectively and feasibly met using the transfer functions presented here in Chapter 4 and the many lacustrine pollen records currently stored in the Neotoma paleoecology database. However, the lack of natural lacustrine basins in the non-glaciated parts of the Great Plains is a deterrent to this goal. Non-lacustrine paleorecords, such as paleosols, may help overcome this limitation in parts of the region that lack natural lacustrine basins. Paleosols could also serve as another independent source for reconstructing climate, in order to avoid circular conclusions about vegetation-climate dynamics that could occur from relying on pollen data alone to reconstruct climate. Third, erosion dynamics need to be clarified at Fox Lake and at other sites in the region. The magnetic susceptibility signal alone cannot explain whether sediment was deposited via alluvial or eolian transport. However, this could be explained by coupling with magnetic susceptibility data with grain size analysis. These questions are all challenging and crucial questions to answer in order

to move toward achieving a fuller understanding of North American grassland dynamics during the Holocene.

References

IPCC, 2014: *Climate Change 2014: Impacts, Adaptation, and Vulnerability. Part A: Global and Sectoral Aspects. Contribution of Working Group II to the Fifth Assessment Report of the Intergovernmental Panel on Climate Change [Field, C.B., V.R. Barros, D.J. Dokken, K.J.* Cambridge University Press, Cambridge, United Kingdom and New York, NY, USA.

Morris, C. J., 2013: Analysis of modern pollen data from the prairies of central North America. Kansas State University, http://hdl.handle.net/2097/15749.

Zhao, Y., H. Liu, F. Li, X. Huang, J. Sun, W. Zhao, U. Herzschuh, and Y. Tang, 2012: Application and limitations of the Artemisia/Chenopodiaceae pollen ratio in arid and semi-arid China. The Holocene, ***22***, 1385–1392.

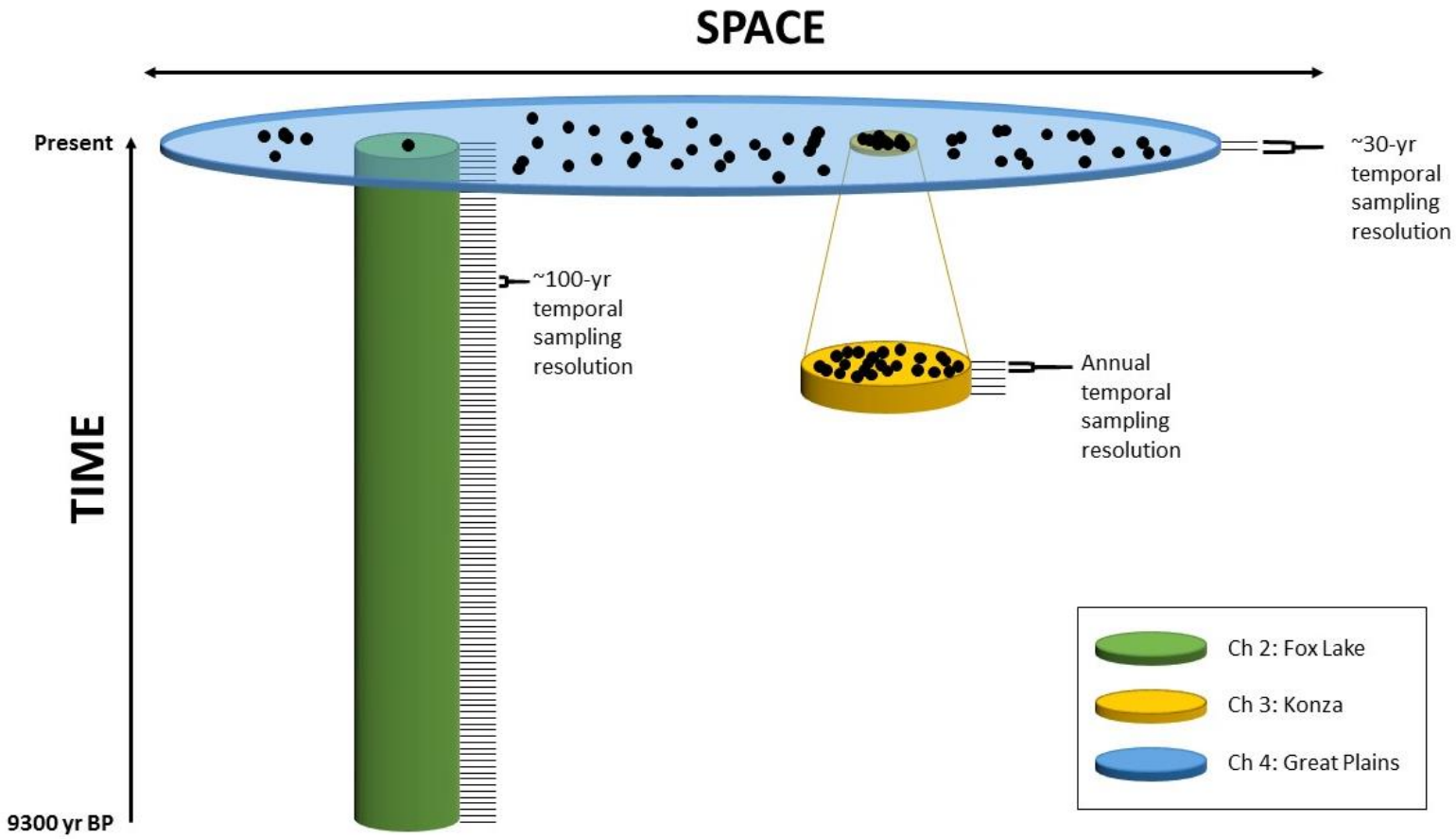

Figure 5.1: Spatial and temporal extents and sampling resolutions covered by this dissertation.

Appendix A - R Code

```
#############                KONZA PRAIRIE CHAPTER (CHAPTER 3)                ##########

###############################################################################################

############    MULTIPLE REGRESSIONS WITH FIXED AND RANDOM EFFECTS   ##########

###############################################################################################

konza = read.csv("Konza_Pollen.csv", header = TRUE)

head(konza)

install.packages("scales")

install.packages("lmerTest")

library("lme4")

library("scales")

library("lmerTest")

Year = konza$year

Year = factor(Year)

Trap = konza$trap

Trap = factor(Trap)
```

```
##Re-scale all variables from 0 to 1
konza$Elevation.rescaled <- rescale(konza$Elevation)
konza$BareSoil.rescaled <- rescale(konza$BareSoil)
konza$BisonManure.rescaled <- rescale(konza$BisonManure)
konza$LimestoneRocks.rescaled <- rescale(konza$LimestoneRocks)
konza$Bison_Density.rescaled <- rescale(konza$Bison_Density)
konza$LocalBurn.rescaled <- rescale(konza$LocalBurn)
konza$Konza.burn.rescaled <- rescale(konza$Konza.burn)
konza$RegionalBurn.rescaled <- rescale(konza$RegionalBurn)
konza$FRI.rescaled <- rescale(konza$FRI)
konza$meanFRI.rescaled <- rescale(konza$meanFRI)
konza$FireFrequency.rescaled <- rescale(konza$FireFrequency)
konza$TimeSinceLastFire.rescaled <- rescale(konza$TimeSinceLastFire)
konza$ShannonWeiner.rescaled <- rescale(konza$ShannonWeiner)
konza$Amb_Art.rescaled <- rescale(konza$Amb_Art)
konza$NAP.rescaled <- rescale(konza$NAP)
konza$PollenTurnover.rescaled <- rescale(konza$PollenTurnover)
```

```
##Non-arboreal pollen percentage (NAP%) regression

##Build full model using all fixed and random effects

fit_NAP_alleffects <- lmer(NAP.rescaled ~  Elevation.rescaled + BareSoil.rescaled + BisonManure.rescaled +
LimestoneRocks.rescaled + Bison_Density.rescaled + LocalBurn.rescaled + Konza.burn.rescaled + RegionalBurn.rescaled +
FRI.rescaled + meanFRI.rescaled + FireFrequency.rescaled + TimeSinceLastFire.rescaled + (1|Year) + (1|Trap), data=konza,
REML=FALSE)

##Same model as alleffects model, but with year effect removed

fit_NAP_fixed_and_trap_effects <- lmer(NAP.rescaled ~  Elevation.rescaled + BareSoil.rescaled + BisonManure.rescaled +
LimestoneRocks.rescaled + Bison_Density.rescaled + LocalBurn.rescaled + Konza.burn.rescaled + RegionalBurn.rescaled +
FRI.rescaled + meanFRI.rescaled + FireFrequency.rescaled + TimeSinceLastFire.rescaled + (1|Trap), data=konza, REML=FALSE)

##Same model as alleffects model, but with trap effect removed

fit_NAP_fixed_and_year_effects <- lmer(NAP.rescaled ~  Elevation.rescaled + BareSoil.rescaled + BisonManure.rescaled +
LimestoneRocks.rescaled + Bison_Density.rescaled + LocalBurn.rescaled + Konza.burn.rescaled + RegionalBurn.rescaled +
FRI.rescaled + meanFRI.rescaled + FireFrequency.rescaled + TimeSinceLastFire.rescaled + (1|Year), data=konza, REML=FALSE)

##Check for significance of each of the random effects (trap and year)

anova(fit_NAP_alleffects,fit_NAP_fixed_and_trap_effects)
```

```
anova(fit_NAP_alleffects,fit_NAP_fixed_and_year_effects)
##Above two lines show that controlling for year in NAP data does not make any difference.
##So, use this summary
summary(fit_NAP_fixed_and_trap_effects)

##Temporal Beta-diversity regression
##Build full model using all fixed and random effects
fit_PollenTurnover_alleffects <- lmer(PollenTurnover.rescaled ~  Elevation.rescaled + BareSoil.rescaled + BisonManure.rescaled + LimestoneRocks.rescaled + Bison_Density.rescaled + LocalBurn.rescaled + Konza.burn.rescaled + RegionalBurn.rescaled + FRI.rescaled + meanFRI.rescaled + FireFrequency.rescaled + TimeSinceLastFire.rescaled + (1|Year) + (1|Trap), data=konza, REML=FALSE)
##Same model as alleffects model, but with year effect removed
fit_PollenTurnover_fixed_and_trap_effects <- lmer(PollenTurnover.rescaled ~  Elevation.rescaled + BareSoil.rescaled + BisonManure.rescaled + LimestoneRocks.rescaled + Bison_Density.rescaled + LocalBurn.rescaled + Konza.burn.rescaled + RegionalBurn.rescaled + FRI.rescaled + meanFRI.rescaled + FireFrequency.rescaled + TimeSinceLastFire.rescaled + (1|Trap), data=konza, REML=FALSE)
##Same model as alleffects model, but with trap effect removed
```

```
fit_PollenTurnover_fixed_and_year_effects <- lmer(PollenTurnover.rescaled ~  Elevation.rescaled + BareSoil.rescaled +
BisonManure.rescaled + LimestoneRocks.rescaled + Bison_Density.rescaled + LocalBurn.rescaled + Konza.burn.rescaled +
RegionalBurn.rescaled + FRI.rescaled + meanFRI.rescaled + FireFrequency.rescaled + TimeSinceLastFire.rescaled + (1|Year),
data=konza, REML=FALSE)

##Check for significance of each of the random effects (trap and year)

anova(fit_PollenTurnover_alleffects,fit_PollenTurnover_fixed_and_trap_effects)

anova(fit_PollenTurnover_alleffects,fit_PollenTurnover_fixed_and_year_effects)

##Above two lines show that controlling for year and trap makes no difference (for beta-diversity).

##So, use this summary

fit_PollenTurnover_fixedeffects <- lm(PollenTurnover.rescaled ~  Elevation.rescaled + BareSoil.rescaled +
BisonManure.rescaled + LimestoneRocks.rescaled + Bison_Density.rescaled + LocalBurn.rescaled + Konza.burn.rescaled +
RegionalBurn.rescaled + FRI.rescaled + meanFRI.rescaled + FireFrequency.rescaled + TimeSinceLastFire.rescaled, data=konza)



##Shannon index regression

##Commentary is the same as above, except with Shannon index in place of NAP or pollenturnover
```

```
fit_ShannonWeiner_alleffects <- lmer(ShannonWeiner.rescaled ~  Elevation.rescaled + BareSoil.rescaled +
BisonManure.rescaled + LimestoneRocks.rescaled + Bison_Density.rescaled + LocalBurn.rescaled + Konza.burn.rescaled +
RegionalBurn.rescaled + FRI.rescaled + meanFRI.rescaled + FireFrequency.rescaled + TimeSinceLastFire.rescaled + (1|Year) +
(1|Trap), data=konza, REML=FALSE)

fit_ShannonWeiner_fixed_and_trap_effects <- lmer(ShannonWeiner.rescaled ~  Elevation.rescaled + BareSoil.rescaled +
BisonManure.rescaled + LimestoneRocks.rescaled + Bison_Density.rescaled + LocalBurn.rescaled + Konza.burn.rescaled +
RegionalBurn.rescaled + FRI.rescaled + meanFRI.rescaled + FireFrequency.rescaled + TimeSinceLastFire.rescaled + (1|Trap),
data=konza, REML=FALSE)

fit_ShannonWeiner_fixed_and_year_effects <- lmer(ShannonWeiner.rescaled ~  Elevation.rescaled + BareSoil.rescaled +
BisonManure.rescaled + LimestoneRocks.rescaled + Bison_Density.rescaled + LocalBurn.rescaled + Konza.burn.rescaled +
RegionalBurn.rescaled + FRI.rescaled + meanFRI.rescaled + FireFrequency.rescaled + TimeSinceLastFire.rescaled + (1|Year),
data=konza, REML=FALSE)

anova(fit_ShannonWeiner_alleffects,fit_ShannonWeiner_fixed_and_trap_effects)

anova(fit_ShannonWeiner_alleffects,fit_ShannonWeiner_fixed_and_year_effects)

##Controlling for both year and trap makes a difference for Shannon Index.

####So, use this summary

summary(fit_ShannonWeiner_alleffects)
```

```
##Ambrosia:Artemisia regression
fit_Amb_Art_alleffects <- lmer(Amb_Art.rescaled ~ Elevation.rescaled + BareSoil.rescaled + BisonManure.rescaled + LimestoneRocks.rescaled + Bison_Density.rescaled + LocalBurn.rescaled + Konza.burn.rescaled + RegionalBurn.rescaled + FRI.rescaled + meanFRI.rescaled + FireFrequency.rescaled + TimeSinceLastFire.rescaled + (1|Year) + (1|Trap), data=konza, REML=FALSE)
fit_Amb_Art_fixed_and_trap_effects <- lmer(Amb_Art.rescaled ~ Elevation.rescaled + BareSoil.rescaled + BisonManure.rescaled + LimestoneRocks.rescaled + Bison_Density.rescaled + LocalBurn.rescaled + Konza.burn.rescaled + RegionalBurn.rescaled + FRI.rescaled + meanFRI.rescaled + FireFrequency.rescaled + TimeSinceLastFire.rescaled + (1|Trap), data=konza, REML=FALSE)
fit_Amb_Art_fixed_and_year_effects <- lmer(Amb_Art.rescaled ~ Elevation.rescaled + BareSoil.rescaled + BisonManure.rescaled + LimestoneRocks.rescaled + Bison_Density.rescaled + LocalBurn.rescaled + Konza.burn.rescaled + RegionalBurn.rescaled + FRI.rescaled + meanFRI.rescaled + FireFrequency.rescaled + TimeSinceLastFire.rescaled + (1|Year), data=konza, REML=FALSE)
anova(fit_Amb_Art_alleffects,fit_Amb_Art_fixed_and_trap_effects)
anova(fit_Amb_Art_alleffects,fit_Amb_Art_fixed_and_year_effects)
##Controlling for year makes no significant difference, but controlling for trap does.
```

```
## So, use this summary
summary(fit_Amb_Art_fixed_and_trap_effects)

#############################################################################
###########                    ANOVA AND ANCOVAS                    ###########
#############################################################################

##First, test for normality.
shapiro.test(konza$ShannonWeiner)
shapiro.test(konza$PollenTurnover)
shapiro.test(konza$NAP)
shapiro.test(konza$Amb_Art)
##NAP is normally distributed, so could use regular "aov" function, but will use kruskal for consistency

install.packages("pgirmess")
library("pgirmess")
kruskal.test(ShannonWeiner ~ year, data=konza)
```

```
kruskal.test(PollenTurnover ~ year, data=konza)

kruskal.test(NAP ~ year, data=konza)

kruskal.test(Amb_Art ~ year, data=konza)

##Shannon, Beta-diversity (pollenturnover), and NAP all show significant differences (p<0.05), so do pairwise comparisons.

##Amb_Art does not, so will not do post-hoc pairwise comparisons.


kruskalmc(ShannonWeiner ~ year, data=konza)

kruskalmc(PollenTurnover ~ year, data=konza)

kruskalmc(NAP ~ year, data=konza)


####ANCOVAS TO CHECK FOR SIGNIFICANT VARIATION IN SUMMATIVE METRICS WITH GROWING SEASON PRECIP

ancova_Shannon <- aov(ShannonWeiner ~ Precip*year, data=konza)

summary(ancova_Shannon)


ancova_BetaDiversity <- aov(PollenTurnover ~ Precip*year, data=konza)

summary(ancova_BetaDiversity)
```

```
ancova_NAP <- aov(NAP ~ Precip*year, data=konza)
summary(ancova_NAP)

ancova_Amb_Art <- aov(Amb_Art ~ Precip*year, data=konza)
summary(ancova_Amb_Art)

################################################################################
###########      SQUARED-CHORD DISTANCE CALCULATIONS          ############
################################################################################

library('analogue')
konzatable <-read.csv("Konza_Pollen_Counts_for_SCD_proportions_noheaders.csv", header=FALSE)
konzadata = as.matrix(konzatable)
squaredchord <- distance(konzadata, method="SQchord")
head(squaredchord)
write.table(squaredchord, "Konza_squaredchord.txt", sep="\t")
```

```
########################   GREAT PLAINS CHAPTER  (CHAPTER 4) ##############################
##### STEP 1 – CREATE TRANSFER FUNCTIONS FROM POLLEN SURFACE SAMPLES ################
library("rioja")
setwd("C://Users//jcomm//Desktop//R_GreatPlains")
pollen <- read.csv("FH_Grimm_Morris.csv", header=TRUE, row.names = 1)
climate <- read.csv("Climate_Variables.csv", header=TRUE, row.names = 1)
precip<-climate$Ann_Precip
julytemp<-climate$July_MeanT
temp<-climate$Ann_MeanT

##Fit precip and temp models for GP pollen using all 141 samples and crossvalidate.
fit<-WAPLS(pollen, precip)
fit.cv<-crossval(fit, cv.method="loo")
rand.t.test(fit.cv)
par(mfrow=c(1,3), oma=c(0,4,0,0))
plot(fit.cv, pch=16, cex=1.5, xlab = "Actual Annual Precip (mm)", ylab = "Estimated Annual Precip (mm)", main="Annual
Precipitation")
```

```
legend("bottomright", "r = 0.928")


fit_temp<-WAPLS(pollen, temp)
fit_temp.cv<-crossval(fit_temp, cv.method="loo")
rand.t.test(fit_temp.cv)
plot(fit_temp.cv, pch=16, cex=1.5, xlim=c(1,18), ylim=c(1,18), xlab = "Actual Annual Temp (C)", ylab = "Estimated Annual Temp (C)", main="Mean Annual Temp")
legend("bottomright", "r = 0.891")


fit_julytemp<-WAPLS(pollen, julytemp)
fit_julytemp.cv<-crossval(fit_julytemp, cv.method="loo")
rand.t.test(fit_julytemp.cv)
plot(fit_julytemp.cv, pch=16, cex=1.5, xlim=c(15,29), ylim=c(15,29), xlab = "Actual July Temp (C)", ylab = "Estimated July Temp (C)", main="Mean July Temp")
legend("bottomright", "r = 0.897")
```

```
#Fit precip model for GP pollen using RANDOM training set and test with remaining samples.
pollen <- read.csv("FH_Grimm_Morris_Training.csv", header=TRUE, row.names = 1)
climate <- read.csv("Climate_Variables_Training.csv", header=TRUE, row.names = 1)
core <- read.csv("FH_Grimm_Morris_Test.csv", header=TRUE, row.names = 1)
climate_test <- read.csv("Climate_Variables_Test.csv", header=TRUE, row.names = 1)
precip<-climate$Ann_Precip
precip_actual <-climate_test$Ann_Precip
julytemp<-climate$July_MeanT
julytemp_actual <-climate_test$July_MeanT
temp<-climate$Ann_MeanT
temp_actual<-climate_test$Ann_MeanT

fit<-WAPLS(pollen, precip)
fit.cv<-crossval(fit, cv.method="loo")
plot(fit.cv, pch=16, cex=1.5, xlab = "Inferred Annual Precip (mm)", ylab = "Estimated Annual Precip (mm)")
rand.t.test(fit.cv)
```

```
pred <-predict(fit, core, npls=3)
pred

fit_temp<-WAPLS(pollen, temp)
fit_temp.cv<-crossval(fit_temp, cv.method="loo")
rand.t.test(fit_temp.cv)
pred_temp <-predict(fit_temp, core, npls=3)
pred_temp

fit_julytemp<-WAPLS(pollen, julytemp)
fit_julytemp.cv<-crossval(fit_julytemp, cv.method="loo")
rand.t.test(fit_temp.cv)
pred_julytemp <- predict(fit_julytemp, core, npls=3)
pred_julytemp

#Plot the predicted versus actual temp and precip
par(mfrow=c(2,3), oma=c(0,4,0,0))
```

```
plot(precip_actual, pred$fit[, 3], type="p", pch=19, ylim=c(300,1000), xlim=c(300,1000), ylab="Predicted Annual Precipitation (mm)", xlab="Actual Annual Precipitation (mm)", main="Annual Precip", cex.main=1.75)
abline(lm(precip_actual~pred$fit[, 3]), col="blue", lty=2, lwd=2)
cor(precip_actual, pred$fit[, 3])
legend("bottomright", "r = 0.937")

plot(temp_actual, pred_temp$fit[, 3], type="p", pch=19, ylim=c(-2,16), xlim=c(-2,16), ylab="Predicted Mean Annual Temp", xlab="Actual Mean Annual Temp", main="Mean Annual Temp", cex.main=1.75)
abline(lm(temp_actual~pred_temp$fit[, 3]), col="blue", lty=2, lwd=2)
cor(temp_actual, pred_temp$fit[, 3])
legend("bottomright", "r = 0.834")

plot(julytemp_actual, pred_julytemp$fit[, 3], type="p", xlim=c(12,28), ylim=c(12,28), pch=19, ylab="Predicted Mean July Temp", xlab="Actual Mean July Temp", main="Mean July Temp", cex.main=1.75)
abline(lm(julytemp_actual~pred_julytemp$fit[, 3]), col="blue", lty=2, lwd=2)
cor(julytemp_actual, pred_julytemp$fit[, 3])
legend("bottomright", "r = 0.927")
```

```
#predict the Fox Core using the Extreme Training set
setwd("C://Users//jcomm//Desktop//R_GreatPlains//Extreme_2D_Climate_Space")
pollen <- read.csv("FH_Grimm_Morris_Extreme_Training.csv", header=TRUE, row.names = 1)
climate <- read.csv("Climate_Variables_Extreme_Training.csv", header=TRUE, row.names = 1)
core <- read.csv("FH_Grimm_Morris_Extreme_Test.csv", header=TRUE, row.names = 1)
climate_test <- read.csv("Climate_Variables_Extreme_Test.csv", header=TRUE, row.names = 1)
precip<-climate$Ann_Precip
precip_actual <-climate_test$Ann_Precip
julytemp<-climate$July_MeanT
julytemp_actual <-climate_test$July_MeanT
temp<-climate$Ann_MeanT
temp_actual<-climate_test$Ann_MeanT

#Fit the model to the pollen data and known climate variable (precip in this case),
#using weighted averaging partial least squares
fit<-WAPLS(pollen, precip)
```

```
fit.cv<-crossval(fit, cv.method="loo")

rand.t.test(fit.cv)

pred <-predict(fit, core, npls=3)

pred


fit_temp<-WAPLS(pollen, temp)

fit_temp.cv<-crossval(fit_temp, cv.method="loo")

rand.t.test(fit_temp.cv)

pred_temp <-predict(fit_temp, core, npls=2)

pred_temp


fit_julytemp<-WAPLS(pollen, julytemp)

fit_julytemp.cv<-crossval(fit_julytemp, cv.method="loo")

rand.t.test(fit_temp.cv)

pred_julytemp <- predict(fit_julytemp, core, npls=2)

pred_julytemp
```

```
#Plot the predicted versus actual temp and precip
plot(precip_actual, pred$fit[, 3], type="p", pch=19, ylim=c(250,1050), xlim=c(250,1050), ylab="Predicted Annual Precipitation (mm)", xlab="Actual Annual Precipitation (mm)")
abline(lm(precip_actual~pred$fit[, 3]), col="blue", lty=2, lwd=2)
cor(precip_actual, pred$fit[, 3])
legend("bottomright", "r = 0.952")

plot(temp_actual, pred_temp$fit[, 2], type="p", pch=19, ylim=c(0,16), xlim=c(0,16), ylab="Predicted Mean Annual Temp", xlab="Actual Mean Annual Temp")
abline(lm(temp_actual~pred_temp$fit[, 2]), col="blue", lty=2, lwd=2)
cor(temp_actual, pred_temp$fit[, 2])
legend("bottomright", "r = 0.966")

plot(julytemp_actual, pred_julytemp$fit[, 2], type="p", xlim=c(15,28), ylim=c(15,28), pch=19, ylab="Predicted Mean July Temp", xlab="Actual Mean July Temp")
abline(lm(julytemp_actual~pred_julytemp$fit[, 2]), col="blue", lty=2, lwd=2)
cor(julytemp_actual, pred_julytemp$fit[, 2])
```

```
legend("bottomright", "r = 0.969")

##############################################################################################
########### STEP 2 – APPLY TRANSFER FUNCTIONS TO POLLEN FROM CORES ########################
##############################################################################################
library("rioja")
setwd("C://Users//jcomm//Desktop//R_GreatPlains//")

#Read in the files and variables
pollen <- read.csv("FH_Grimm_Morris.csv", header=TRUE, row.names = 1)
climate <- read.csv("Climate_Variables.csv", header=TRUE, row.names = 1)
precip<-climate$Ann_Precip
julytemp<-climate$July_MeanT
temp<-climate$Ann_MeanT
colo_core <- read.csv("Colo_Marsh_Pollen.csv", header=TRUE, row.names = 1)
colo_depth <- as.numeric(rownames(colo_core))
moon_core <- read.csv("Moon_Lake_Pollen.csv", header=TRUE, row.names = 1)
```

```
moon_depth <- as.numeric(rownames(moon_core))
fox_core <- read.csv("Fox_Pollen.csv", header=TRUE, row.names = 1)
fox_depth <- as.numeric(rownames(fox_core))



#Fit the model to the pollen data (full set) and known climate variable (precip in this case),
#using weighted averaging partial least squares
fit<-WAPLS(pollen, precip)
fit.cv<-crossval(fit, cv.method="loo")
plot(fit.cv, xlab = "Actual Annual Precip (mm)", ylab = "Estimated Annual Precip (mm)")
rand.t.test(fit.cv)
colo_pred <-predict(fit, colo_core, npls=2)
colo_pred
moon_pred <-predict(fit, moon_core, npls=2)
moon_pred
fox_pred <-predict(fit, fox_core, npls=2)
```

```
fox_pred


fit_temp<-WAPLS(pollen, temp)
fit_temp.cv<-crossval(fit_temp, cv.method="loo")
plot(fit_temp.cv, xlab = "Actual Annual Temp (C)", ylab = "Estimated Annual Temp (C)")
rand.t.test(fit_temp.cv)
colo_pred_temp <-predict(fit_temp, colo_core, npls=2)
colo_pred_temp
moon_pred_temp <-predict(fit_temp, moon_core, npls=2)
moon_pred_temp
fox_pred_temp <- predict(fit_temp, fox_core, npls=2)
fox_pred_temp


fit_julytemp<-WAPLS(pollen, julytemp)
fit_julytemp.cv<-crossval(fit_julytemp, cv.method="loo")
plot(fit_julytemp.cv, xlab = "Actual July Temp (C)", ylab = "Estimated July Temp (C)")
rand.t.test(fit_temp.cv)
```

```
colo_pred_julytemp <- predict(fit_julytemp, colo_core, npls=2)
colo_pred_julytemp
moon_pred_julytemp <- predict(fit_julytemp, moon_core, npls=2)
moon_pred_julytemp
fox_pred_julytemp <- predict(fit_julytemp, fox_core, npls=2)
fox_pred_julytemp

#Plot the predicted Colo Marsh precip against age
par(mfrow=c(3,3))
plot(colo_depth, colo_pred$fit[, 2], type="l", pch=19, col="tan3", lwd=2, lty=5, ylim=c(300,950), xlim=c(-30,12000),
ylab="Predicted Annual Precipitation (mm)", xlab="Age (yr BP)", main="Colo Marsh - Annual Precipitation")
colo_smoothed<-smooth.spline(colo_depth, colo_pred$fit[, 2], spar=0.5)
lines(colo_smoothed, lty=1, lwd=2)

#Plot the predicted Colo Marsh temp against age
plot(colo_depth, colo_pred_temp$fit[, 2], type="l", pch=19, col="tan3", lwd=2, lty=5, ylim=c(0,12), xlim=c(-30,12000),
ylab="Predicted Annual Temp (C)", xlab="Age (yr BP)", main="Colo Marsh - Annual Temp")
```

```
colo_temp_smoothed<-smooth.spline(colo_depth, colo_pred_temp$fit[, 2], spar=0.5)
lines(colo_temp_smoothed, lty=1, lwd=2)

#Plot the predicted Colo Marsh Julytemp against age
plot(colo_depth, colo_pred_julytemp$fit[, 2], type="l", pch=19, col="tan3", lwd=2, lty=5, ylim=c(13,25), xlim=c(-30,12000),
ylab="Predicted July Temp (C)", xlab="Age (yr BP)", main="Colo Marsh - July Temp")
smoothed<-smooth.spline(colo_depth, colo_pred_julytemp$fit[, 2], spar=0.5)
lines(smoothed, lty=1, lwd=2)

#Plot the predicted Moon Lake precip against age
plot(moon_depth, moon_pred$fit[, 2], type="l", pch=19, col="tan3", lwd=2, lty=5, ylim=c(300,950), xlim=c(-30,12000),
ylab="Predicted Annual Precipitation (mm)", xlab="Age (yr BP)", main="Moon Lake - Annual Precip")
smoothed<-smooth.spline(moon_depth, moon_pred$fit[, 2], spar=0.5)
lines(smoothed, lty=1, lwd=2)

#Plot the predicted Moon Lake temp against age
```

```
plot(moon_depth, moon_pred_temp$fit[, 2], type="l", pch=19, col="tan3", lwd=2, lty=5, ylim=c(0,12), xlim=c(-30,12000), ylab="Predicted Annual Temp (C)", xlab="Age (yr BP)", main="Moon Lake - Annual Temp")
smoothed<-smooth.spline(moon_depth, moon_pred_temp$fit[, 2], spar=0.5)
lines(smoothed, lty=1, lwd=2)

#Plot the predicted Moon Lake Julytemp against age
plot(moon_depth, moon_pred_julytemp$fit[, 2], type="l", pch=19, col="tan3", lwd=2, lty=5, ylim=c(13,25), xlim=c(-30,12000), ylab="Predicted July Temp (C)", xlab="Age (yr BP)", main="Moon Lake - July Temp")
smoothed<-smooth.spline(moon_depth, moon_pred_julytemp$fit[, 2], spar=0.5)
lines(smoothed, lty=1, lwd=2)

#Plot the predicted Fox Lake precip against age
plot(fox_depth, fox_pred$fit[, 2], type="l", pch=19, col="tan3", lwd=2, lty=5, ylab="Predicted Annual Precipitation (mm)", xlim=c(-30,12000), ylim=c(300,950), xlab="Age (yr BP)", main="Fox Lake - Annual Precip")
smoothed<-smooth.spline(fox_depth, fox_pred$fit[, 2], spar=0.5)
lines(smoothed, lty=1, lwd=2)
```

```
#Plot the predicted Fox Lake temp against age
plot(fox_depth, fox_pred_temp$fit[, 2], type="l", pch=19, col="tan3", lwd=2, lty=5, ylab="Predicted Annual Temp (C)",
xlim=c(-30,12000), ylim=c(0,12), xlab="Age (yr BP)", main="Fox Lake - Annual Temp")
smoothed<-smooth.spline(fox_depth, fox_pred_temp$fit[, 2], spar=0.5)
lines(smoothed, lty=1, lwd=2)

#Plot the predicted Fox Lake Julytemp against age
plot(fox_depth, fox_pred_julytemp$fit[, 2], type="l", pch=19, col="tan3", lwd=2, lty=5, ylab="Predicted July Temp (C)",
xlab="Age (yr BP)", xlim=c(-30,12000), ylim=c(13,25), main="Fox Lake - July Temp")
smoothed<-smooth.spline(fox_depth, fox_pred_julytemp$fit[, 2], spar=0.5)
lines(smoothed, lty=1, lwd=2)
```